ENHANCED BACKSCATTERING FROM ROUGH SURFACES

Principal Investigator: J C Dainty
Contractor: Imperial College
Contract Number: DAJA45-87-C-0039

Final Report

July 1987 — July 1990
(Report Date: 18th October 1991)

"The research reported in this document has been made possible through the support and sponsorship of the US Government through its European Research Office of the US Army. The report is intended only for the internal management use of the Contractor and the US Government."

SECURITY CLASSIFICATION OF THIS PAGE

REPORT DOCUMENTATION PAGE

Form Approved OMB No. 0704-0188

1a. REPORT SECURITY CLASSIFICATION UNCLASSIFIED	1b. RESTRICTIVE MARKINGS NONE
2a. SECURITY CLASSIFICATION AUTHORITY	3. DISTRIBUTION/AVAILABILITY OF REPORT UNLIMITED
2b. DECLASSIFICATION/DOWNGRADING SCHEDULE	
4. PERFORMING ORGANIZATION REPORT NUMBER(S)	5. MONITORING ORGANIZATION REPORT NUMBER(S)
6a. NAME OF PERFORMING ORGANIZATION Imperial College, London 6b. OFFICE SYMBOL (If applicable)	7a. NAME OF MONITORING ORGANIZATION US Army Research, Development and Standardisation Group
6c. ADDRESS (City, State, and ZIP Code) Blackett Laboratory Prince Consort Rd., London SW7 2BZ, U.K.	7b. ADDRESS (City, State, and ZIP Code) 223 Old Marylebone Road London NW1 5TH, U.K.
8a. NAME OF FUNDING/SPONSORING ORGANIZATION as 7(a) 8b. OFFICE SYMBOL (If applicable)	9. PROCUREMENT INSTRUMENT IDENTIFICATION NUMBER DAJA45-87-C-0039
8c. ADDRESS (City, State, and ZIP Code) as 7(b)	10. SOURCE OF FUNDING NUMBERS PROGRAM ELEMENT NO. / PROJECT NO. / TASK NO / WORK UNIT ACCESSION NO.

11. TITLE (Include Security Classification)
ENHANCED BACKSCATTERING FROM ROUGH SURFACES

12. PERSONAL AUTHOR(S)
J.C. Dainty

13a. TYPE OF REPORT	13b. TIME COVERED	14. DATE OF REPORT (Year, Month, Day)	15. PAGE COUNT
FINAL	FROM 7/87 TO 7/90	1991 October 18	

16. SUPPLEMENTARY NOTATION

17. COSATI CODES			18. SUBJECT TERMS (Continue on reverse if necessary and identify by block number)
FIELD	GROUP	SUB-GROUP	

19. ABSTRACT (Continue on reverse if necessary and identify by block number)

This report summarises research carried out on Enhanced Backscattering at Imperial College between July 1987 and July 1990. It consists of an Executive Summary, copies of 8 refereed publications and an Appendix comprising a draft copy of the PhD Thesis of A.J. Sant

20. DISTRIBUTION/AVAILABILITY OF ABSTRACT	21. ABSTRACT SECURITY CLASSIFICATION
☒ UNCLASSIFIED/UNLIMITED ☐ SAME AS RPT. ☐ DTIC USERS	UNCLASSIFIED
22a. NAME OF RESPONSIBLE INDIVIDUAL	22b. TELEPHONE (Include Area Code) / 22c. OFFICE SYMBOL

D Form 1473, JUN 86 *Previous editions are obsolete.* SECURITY CLASSIFICATION OF THIS PAGE

CONTENTS

Appendix (separate document)

Thesis, A J Sant "Enhanced Backscattering of Light from Randomly Rough Surfaces"

1 Executive Summary

The aim of this section is to provide an overall summary of the research carried out with the full or partial support of the contract. Although formal support was only provided for one PhD research student, A J Sant, in practice other students, notably M-J Kim, N C Bruce and D N Qu all benefitted indirectly from ERO support and contributed to the project.

Background

To set the research in context, it is worthwhile reviewing the work of ourselves and others prior to mid-1987, concentrating on enhanced backscattering from randomly rough surfaces. There is, of course, a vast literature on the scattering of electromagnetic waves by randomly rough surfaces. Prior to 1987, the vast majority of theoretical studies were performed using analytical methods and it was therefore necessary to make approximations in order to get any kind of answer at all for the scattering cross-section (ensemble average intensity). In fact the great majority of treatments assumed either a *perturbation* situation (for which the rms surface height σ typically has to be less than $\lambda/100$, where λ is the wavelength) or one where single scattering and the Kirchhoff approximation applied (i.e. surfaces for which $\sigma/\tau<<1$, where τ is the correlation length of the surface roughness) — this is also called "Beckmann theory" or the "physical optics" approach. The first prediction of enhanced backscattering was made by McGurn et al[1], using an analytical approach in the perturbation situation; for one-dimensional silver surfaces with $\sigma \approx \lambda/100$ and $\tau \approx \lambda/5$, they showed that a peak of intensity occurs in the backscatter direction for p-polarisation but not for s-polarisation. (In p-polarisation, the electric vector lies in the plane of incidence, whereas for s-polarisation the electric vector is perpendicular to the plane of incidence: p-polarisation is also referred to as TM and as V, whereas s-polarisation is also called TE or H.) The polarisation dependence suggests that surface plasmons play a crucial role for scattering by surfaces of these parameters. Carefully controlled experiments to verify this theory have still to be made but Gu et al[2] have observed the effect for a (relatively uncharacterised) surface.

Perturbation theory is valid only for relatively smooth surfaces and the only analytical approach capable of dealing with rougher surfaces, $\sigma \approx \lambda$, is physical optics. This does not predict enhanced backscattering (see, e.g., the book by Beckmann and Spizzichino[3]). In experiments carried out in 1986, inspired by reports of enhanced backscattering in dense volume media by three groups[4–6], Mendez and O'Donnell[7,8] showed experimentally that surfaces which show multiple scattering also can exhibit enhanced backscattering[§].

The work of Méndez and O'Donnell has proved to mark a watershed in progress in scattering from randomly rough surfaces, for three reasons. First, particular attention was paid to fabricating the surfaces with reasonably well-defined statistical properties; the light scattering measurements were therefore from (more-or-less) well characterised surfaces. Second, the scattering cross-sections were remarkable for that fact that they were in complete disagreement with existing theoretical predictions, not only in the backscatter direction but in all other directions as well. Third, the importance of multiple scattering could not be ignored. Prior to their experiments, enhanced backscattering due to scattering from high-sloped surfaces had not been predicted by a single theoretical calculation — after publication of the results, almost every calculation showed the effect!

Work in rough surface scattering at Imperial College commenced in 1985, with support from the UK Science and Engineering Research Council. During the first year, the scattering equipment was designed and constructed and with it Méndez and O'Donnell obtained their first

[§] It is worth pointing out, for the historical record, that the original paper by Mendez and O'Donnell (ref 7) was rejected by Physical Review Letters as "not of interest to readers of PRL", despite its close connection to the work on dense volume media which was, and still is, almost exclusively reported in PRL and PR.

enhanced backscattering results in mid-1986. On completion of their post-doctoral terms, Méndez and O'Donnell took up permanent positions at CICESE, Mexico and Georgia Tech, USA. ARO support for this research started in mid-1987.

Progress during period July '87 to July '90

One dimensional surfaces - experimental results for conducting surfaces

The experimental results reported in Refs[7] and [8] were for two dimensional, isotropic, surfaces. However, the prospects for theoretical or numerical work on two dimensional surfaces were not good and since a major aim of this project was to link experiment and theory, it was decided early on to manufacture and make measurements on one dimensional surfaces, i.e. random gratings. The surfaces were made by exposing photoresist to laser speckle patterns produced by slit-like apertures; during the course of the work, replication techniques were developed (see [R2]). As with previous work, all surfaces have had a Gaussian probability density function of surface height, with rms roughness σ, and a Gaussian correlation function of 1/e width equal to τ. (It is possible with this technique to make surfaces with a probability density function that is approximately a chi^2 with 2N degrees of freedom, where N is the number of independent speckle patterns superposed in the exposure of the photo-resist.) Another advantage of one dimensional surfaces is that they can be characterised with much greater confidence than two dimensional surfaces: this is because a sharper, chisel-shaped stylus can be used in a mechanical surface profiling instrument. A Talystep profiler was purchased in 1988 for this project using University funds and has significantly improved the reliability of surface characterisation. The details of surface fabrication, replication and measurement are given in Chapter 3 of the Appendix.

The emphasis has been on producing a few, reliable measurements of the angular scattering by one dimensional rough surfaces at up to four wavelengths (λ = 0.63, 1.15, 3.39 and 10.6 μm), for comparison with numerical calculations. Publications [R3] and [R8] give "definitive" measurements of the s-s and p-p scattering cross-sections. In [R8], the surface has an rms roughness $\sigma = 1.22 \pm 0.02\mu$m and a correlation length $\tau = 3.17 \pm 0.07\mu$m: particular attention should be given to Figures 3 and 4 in [R8], which show the angular scatter for p- and s-polarisation at three angles of incidence for a gold-coated surface at the four wavelengths. These results are available on floppy disc (PC or MAC) to any interested person. It should be noted that the scattering cross-sections for p- and s-polarisation are essentially the same at shorter wavelengths (with interesting differences in the side-lobes of the enhanced backscattering peak) but are significantly different at longer wavelengths, with the p-polarisation showing the tendency to enhanced backscattering. This is consistent with the fact that, in the surface plasmon regime ($\sigma << \lambda$), only the p-polarisation couples into the plasmons.

We have compared our measurements to numerical calculations. These have been done more-or-less independently by Nieto-Vesperinas[9,10], Maradudin[11,12] and Maystre[13] for the kind of surface parameters used in the experiments. Using the method described by Nieto-Vesperinas[9], we have developed programs for calculating the scattering cross-section for surfaces that are (i) perfect conductors, (ii) non-absorbing dielectrics and (iii) arbitrary materials (the storage requirements and computer times for (ii) twice those for (i), are (iii) involves another doubling.) In [R3] and [R8] we compare some perfect conductor calculations with experimental results: there is good overall agreement at near-normal angles of incidence but the agreement is less good for higher angles of incidence (>20°), particularly at higher scattering angles (>60°). The reason for this discrepancy is still not clear. It should be stressed that for these surface parameters, the s-s and p-p scattering cross-sections do not appear to be particularly material dependent.

One dimensional surfaces - experimental results for dielectric surfaces

Dielectric surfaces scatter less than reflecting ones, and therefore on simple grounds would not be expected to show multiple scattering effects strongly. We have been able to make dielectric

replicas of our surfaces and therefore compare the scattering cross-sections of identical surfaces in different materials (gold and silicone rubber). The results are reported in [R3] and [R8]: perhaps the most significant feature of the scattering cross-sections are that the s-s and p-p sections are quite different and very recently we have been able to show that these curves can be explained essentially of the grounds of single scattering[14]. As with the gold-coated surfaces, the agreement between theory and experiment is fair, but there is still significant disagreement at large scattering angles.

If the rough dielectric surface is above a reflecting plane, then analytical and numerical [R8] studies predict a sharp enhanced backscatter peak. With careful sample preparation (for details, see Appendix), it was possible to make a very thin dielectric sample, rough on one side and coated with gold on the other. The experimental results are reported in [R8] and compared to numerical predictions, with good agreement.

Nieto-Vesperinas and Sanchez-Gil predicted numerically an unusual result for the light *transmitted* by a rough dielectric film: the mean angle of refraction roughly equals the angle of incidence (rather than Snell's law being obeyed). This can also be explained on a single scattering argument. We verified their prediction experimentally [R4].

Multiple scattering Kirchhoff approximation

The Kirchhoff approximation, or tangent plane approximation, assumes that the surface is locally flat, i.e. that the local radius of curvature is everywhere much larger than the wavelength. It is almost invariably applied in a single scattering way but there is no reason why it cannot be extended to the multiple scattering case. This was done, for a perfect conductor in [R5] and [R8], and for the more general case in Ref 14. The point of applying the Kirchhoff approximation is to give more physical insight to the problem than the "rigorous" calculation, by separating single, double, triple.... scattering terms.

The interesting result is that the enhanced backscatter does *not* occur for the single scatter case, i.e. it is associated with multiple scattering.

Dynamics of volume scattering

A small amount of work was carried out on the temporal behaviour of the enhanced backscattering peak produced by dense volume media [R1]. In this case, time scale probes path length of scattering in the media (the longer the path, the shorter the time scale).

References

1 A R McGurn, A A Maradudin and V Celli, "Localisation effects in the scattering of light from a randomly rough grating", Phys Rev B, **31**, 4866-4871 (1985)

2 Z-H Gu, R S Dummer, A A Maradudin and A R McGurn, "Experimental study of the opposition effect in the scattering of light from a randomly rough surface", Appl. Opt, **28**, 537-543 (1989)

3 P Beckmann and A Spizzichino, *The Scattering of Electromagnetic Waves from Rough Surfaces*, Pergamon, 1963.

4 Y Kuga and A Ishimaru, "Retroreflectance from a dense distribution of spherical particles", J Opt Soc Am A, **1**, 831-835 (1984)

5 M P van Albada and A Lagendijk, "Observation of weal localisation of light in a random medium", Phys Rev Lett, **55**, 2692-2695 (1985)

6 P E Wolf and G Maret, "Weak localisation and coherent backscattering of photons in disordered media", Phys Rev Lett, **55**, 2696-2699z (1985)

7 E R Méndez and K A O'Donnell, "Observation of depolarisation and backscatter enhancement in light scattering from gaussian rough surfaces", Opt Commun, **61**, 91-95 (1987)

8 K A O'Donnell and E R Méndez, "Experimental study of scattering from characterised random surfaces", J Opt Soc Am A, **4**, 1194-1205 (1987)

9 M Nieto-Vesperinas and J-M Soto-Crespo, "Monte Carlo simulations for scattering of electromagnetic waves from perfectly conducting random rough surfaces", Opt Lett, **12**, 979-981

10 J-M Soto-Crespo and M Nieto-Vesperinas, "Electromagnetic scattering from very rough random surfaces and deep reflection gratings", J Opt Soc Am A, **6**, 367-384 (1989)

11 A A Maradudin, E R Méndez and T Michel, "Backscattering effects in the elastic scattering of p-polarised light from a large amplitude random metallic grating", Opt Lett, **14**, 151-153 (1989)

12 A A Maradudin, T Michel, A R McGurn and E R Méndez, "Enhanced backscattering of light from a random grating", Ann Phys, **203**, 255-307 (1990)

13 M Saillard and D Maystre, "Scattering from metallic and rough dielectric surfaces", J Opt Soc Am A, **7**, 982-990 (1990)

14 N C Bruce and J C Dainty, "Multiple scattering from rough dielectric and metal surfaces using the Kirchhoff approximation", J Mod Optics, **38**, 1471-1481 (1991)

Refereed Publications

R1 D N Qu and J C Dainty, 'Polarisation dependence of dynamic light scattering by disordered media', Opt Lett, **13**, 1066-1068 (1988)

R2 A J Sant, J C Dainty and M J Kim, 'Comparison of surface scattering between identical, randomly rough metal and dielectric diffusers', Opt Lett, **14**, 1183-1185 (1989)

R3 M J Kim, J C Dainty, A T Friberg and A J Sant, 'Experimental study of enhanced backscattering from one and two dimensional random rough surfaces', JOSA A, **7**, 569-577 (1990)

R4 M Nieto-Vesperinas, J A Sanchez-Gil, A J Sant and J C Dainty, 'Light transmission from a randomly rough dielctric diffuser: theoretical and experimental results', Opt Lett, **15**, 1261-1263 (1990)

R5 N C Bruce and J C Dainty, 'Multiple scattering from random surfaces using the Kirchhoff approximation', J Mod Opt, **38**, 579-590 (1990)

R6 J C Dainty, 'The opposition effect in volume and surface scattering', in *International Trends in Optics*, edited by J W Goodman, Academic Press, 1991.

R7 A A Maradudin, J Q Lu, T Michel, Z-H Gu, J C Dainty, A J Sant, E R Mendez and M Nieto-Vesperinas, 'Enhanced backscattering and transmission of light from random surfaces on semi-infinite substrates and thin films', Waves in Rand Media, **1**, S129-S142 (1991)

R8 J C Dainty, N C Bruce and A J Sant, 'Measurements of light scattering by a characterised rough surface', Waves in Rand Media, **1**, S29-S39 (1991)

Conference Publications & Summaries

C1 A S Harley, M-J Kim and J C Dainty, 'Measurements of light scattering by randomly rough surfaces of known statistics', ICO General Assembly, Quebec 24-28 August 1987.

C2 J C Dainty, A T Friberg and M-J Kim, 'Light scattering by gaussian rough surfaces', OSA Annual Conference, Rochester, 18-23 October 1987 (JOSA A 4, P104 (1987))

C3 D N Qu and J C Dainty, 'Polarisation dependence of dynamic light scattering by latex spheres', Optics-ECOOSA '88, Birmingham, UK 22-25 March 1988

C4 J C Dainty, D N Qu and S Xu, 'Statistical properties of enhanced backscattering produced by dense collections of latex spheres', SPIE San Diego Conference, 14-19 August 1988, (Proc SPIE, **976**, 178-184)

C5 J C Dainty, M J Kim and A J Sant, 'Measurements of angular scattering by randomly rough metal and dielectric surfaces ', in *Scattering in Volumes and Surfaces*, Elsevier Press, Amsterdam, 1989, pp143-155.

C6 N Bruce and J C Dainty, 'Multiple scatter from rough surfaces using the Kirchhoff approximation', ICO—15, Garmisch-Partenkirchen, FRG, 5–10 August 1990 (Conference Summaries, paper 2B3.5)

C7 J C Dainty, N C Bruce and A J Sant, 'Enhanced backscattering and coherent cooperative effects in optical scattering from random rough surfaces', Localisation '90, London, UK, 13–15 August 1990 (Conference Summaries).

C8 A J Sant and J C Dainty, 'Experimental observation of enhanced backscatter from a rough dielectric film on a reflecting substrate', Applied Optics and Opto-Electronics, Nottingham, UK, 17–20 September 1990 (Conference Digest)

Reprinted from Optics Letters, Vol. 13, page 1066, December 1988.

Polarization dependence of dynamic light scattering by dense disordered media

D. N. Qu and J. C. Dainty

Blackett Laboratory, Imperial College, London SW7 2BZ, UK

Received July 14, 1988; accepted September 21, 1988

Photon correlation studies of light scattered by a dense disordered medium at and around the backscatter direction reveal a polarization dependence of the correlation function. This is related to the polarization dependence of the mean intensity of the enhanced backscatter associated with coherent cooperative effects in such media.

There has been considerable interest recently in the phenomenon of enhanced backscattering of light from disordered random media,[1-17] rough surfaces,[18-20] and atmospheric turbulence.[21,22] The phenomenon itself is of general interest and has practical consequences in, e.g., remote sensing, but much of the motivation for studies in this area comes from the possibility of observing the localization of light.[23]

Figure 1 shows the basic experimental layout for measurements of enhanced backscatter. Figure 2(a) shows the average scattered intensity as a function of angle for a scatterer consisting of a 10% concentration of 0.46-μm-diameter latex spheres in water for linearly polarized incident light of 514-nm wavelength. The average intensity of the copolarized and cross-polarized scattered light is different, with the copolarized intensity at the backscatter typically being of the order of 1.7 times that of the intensity off backscatter (e.g., at 20–30 mrad). Figure 2(b) shows a photograph taken in the backscatter direction for copolarized light. It is now established[4-6] that the enhancement is due to the fact that the scattered wave due to the n scattering events associated with the wave vectors $\mathbf{k}_i$, $\mathbf{k}_1, \mathbf{k}_2, \ldots \mathbf{k}_f$ (where $\mathbf{k}_i$ and $\mathbf{k}_f$ are the incident and final wave vectors) is identical to the reverse path in the backscatter (i.e., $\mathbf{k}_f = -\mathbf{k}_i$) for the copolarized component. Since forward and reverse amplitudes are identical for the copolarized case, the waves interfere, and an enhancement of up to a factor of 2 is possible in the backscatter direction. In practice, the enhancement is less than two for the copolarized case because of the contribution of single scattering and multiple scattering involving the same scatterer. For the cross-polarized component, the forward and reverse paths are partially coherent, with the degree of coherence decreasing as the order of scattering increases—in effect, only the shortest paths give any enhancement. The enhancement factor for this case is typically $\approx$1.3 in the above experimental arrangement.

The half-width at half-height of the enhanced backscatter peak is governed by diffraction and is of the order of λ/l^*, where l^* is the effective transport mean free path length. The observed backscatter half-width of the order of 3 mrad in Fig. 2(a) implies an average transport path length $l^* \approx 170\ \mu$m; since the scattering mean free path at this concentration is only a few micrometers, it is clear that the average order of multiple scattering is very high. Because of diffraction effects, all path lengths make a contribution to the copolarized return in the exact backscatter direction, whereas only the shorter paths make a contribution as the angle increases away from backscatter, since the diffraction cones associated with shorter paths are relatively broader.

The dynamic time behavior at and near the backscatter was investigated by Maret and Wolf.[24] The correlation function is strongly nonexponential. Since different angles of observation near the backscatter involve different total transport path lengths, L, each of which has a different time scale, the temporal correlation of the scattered light is a function of the angle. The field correlation is given by[24]

$$\langle E(0)E^*(t)\rangle \approx \int_0^\infty I(L)\exp[-Lt/(4l^*\tau)]\mathrm{d}L,$$

where $I(L)$ is the intensity contribution of transport paths of length L and τ is a single scattering relaxation time. Measurements of the intensity correlation,

$$C(t) = \langle \Delta I(0)\Delta I(t)\rangle,$$

are given in Ref. 24 for the copolarized case and are supported by the above reasoning.

In this Letter we report measurements of the temporal correlation of both the copolarized and cross-polarized components as a function of the angle near backscatter. Correlation times are extracted as a descriptive parameter of the curves, and the variation of the correlation time with the angle close to backscatter

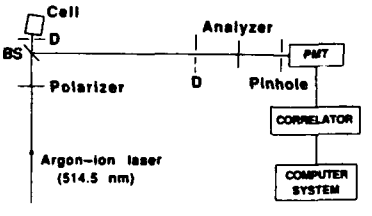

Fig. 1. Experimental setup for measuring the intensity of enhanced backscattering and its dynamic properties. BS, beam splitter; D, diaphragm; PMT, photomultiplier tube.

0146-9592/88/121066-03$2.00/0

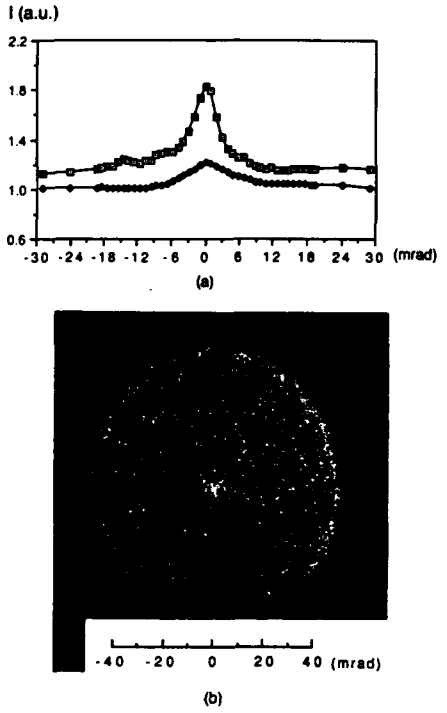

Fig. 2. (a) Measured intensity (in arbitrary units) as a function of the angle around backscatter. Squares, copolarized detection; filled diamonds, cross-polarized detection. (b) Photograph of the scattered intensity around the backscatter in the copolarized case.

turns out to be different in the copolarized and cross-polarized cases.

In our experiments, a 10% concentration of 0.46-μm-diameter latex spheres in water was used with an argon-ion laser at $\lambda = 514$ nm. The sampling pinhole diameter of approximately 30 μrad was much smaller than the speckle size ($\approx$250 μrad), and the sampling time of 2 μsec was much smaller than the typical correlation time of 100 μsec. A polarizer and an analyzer were used to define the direction of linear polarization of the illumination and detected beams. Standard photon correlation techniques were used to estimate the intensity autocorrelation function of the scattered light; the correlator used was a Langley-Ford 128-channel instrument. Typical detected photon rates were $\approx$0.5–1.0 per sample time, and a typical experiment time was 50 sec (i.e., $\approx 2.5 \times 10^7$ samples).

Figure 3 shows a typical measured correlation function (for the copolarized case at an angle $\theta = 3$ mrad). The general form of the curve is nonexponential, in agreement with the measurements of Maret and Wolf.[24] The observed contrast $\sigma^2/\langle I\rangle^2$ of $\approx$0.84 is less than the Gaussian speckle value of unity owing to spatial integration and dead-time effects; corrected for these effects, the normalized contrast is approximately unity.

Figure 4 summarizes the measured correlation data for the copolarized and cross-polarized cases at angles of 0, 1, 3, 7, and 9 mrad from backscatter; the vertical axis is the logarithm of the *ratio* of the measured correlation function in each case to that of the copolarized case at a large angle ($\approx$40 mrad). For the copolarized case, this ratio starts at approximately unity for $\theta = 0$, increases to a maximum at $\theta \approx 3$ mrad, and then falls to unity again at high angles, again in agreement with previous results.[24] However, for the cross-polarized case, the ratio starts at unity at $\theta = 0$ and decreases smoothly as the angle increases.

To compare the differing behavior of the copolarized and cross-polarized cases, a correlation time, defined by

$$\tau_c = \int_0^\infty \frac{\langle \Delta I(0)\Delta I(t)\rangle}{\langle \Delta I^2\rangle}\,dt,$$

was calculated for each case at approximately 40 measurement angles from -18 to 18 mrad. The results are

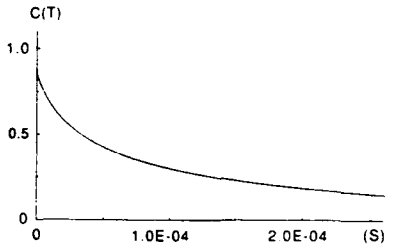

Fig. 3. Temporal correlation function of the intensity fluctuation measured at $\theta = 3$ mrad for the copolarized case, with a sampling time of 2 μsec and $\approx$0.6 detected photons per sample. The speckle contrast $\sigma^2/\langle I\rangle^2 \approx 0.84$.

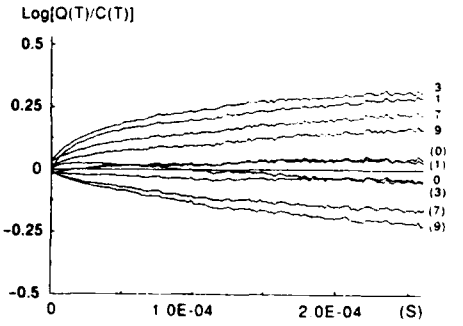

Fig. 4. Correlation function ratio as a function of correlation time for different scattering angles. The numbers at the right are the different measurement angles in milliradians (numbers without parentheses are for the copolarized case; numbers with parentheses are for the cross-polarized case). $C(T)$ is the temporal correlation for $\theta = 40$ mrad in the copolarized case.

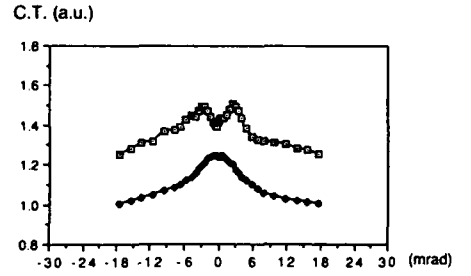

Fig. 5. Measured correlation time (C.T.) in arbitrary units as a function of the scattering angle for the copolarized (squares) and cross-polarized (filled diamonds) cases.

plotted in Fig. 5. The difference in behavior of the correlation time with angle for the two cases is now clear, with the copolarized case showing a double peak and the cross-polarized case showing a gradual decrease of correlation time as one moves from exact backscatter.

A qualitative explanation of the observed dependence of correlation time on angle and polarization is now given, and it is based on the fact that *longer* scattering paths give rise to *shorter* correlation times.[24] The correlation function of scattered light consists of two contributions, one from the incoherent intensity and the other from the coherent intensity (i.e., that responsible for the intensity enhancement at backscatter). The incoherent contribution is approximately independent of angle for the small angles of observation around backscatter in our experiment, whereas the coherent component varies with the angle and polarization, as explained below. At large angles (i.e., a few tens of milliradians), where only the incoherent contribution is present, the time scale is shorter for the cross-polarized case since its average scattering path length is longer.

For the coherent contribution, two effects give rise to the observed behavior of the correlation time. First, by diffraction, each transport path length contributes an enhancement peak whose width is inversely proportional to the path length; therefore, observations at $\theta = 0$ include coherent contributions from all path lengths, whereas observations at larger angles include coherent contributions only from shorter paths. Second, the overall magnitude of the coherent contribution decreases away from the backscatter, and at large angles the time scale observed is that of the incoherent component.

For the copolarized case, it has been established that the forward and the reverse scattering paths are always coherent, regardless of the transport mean free path.[4-6] All transport path lengths contribute at $\theta = 0$ and at large θ, giving similar correlation times in these two cases. However, as θ increases from zero, only shorter transport paths contribute to the coherent component of the intensity, and thus the correlation time begins to increase. But as one increases θ, the relative contribution of the coherent component to the total intensity decreases and ultimately, at large angles, the correlation time must decrease again to that determined by the incoherent intensity. The maximum correlation time for the copolarized case is observed at approximately the half-angle of the enhancement peak.

For the cross-polarized case, only the shortest forward and reverse paths are coherent,[4-6] and so the dominant effect on the correlation time is simply the relative contribution of the coherent component to the total intensity, which gradually decreases from a maximum to zero. The path-length effect is negligible, as large paths never contribute to the coherent component.

In conclusion, we have shown that dynamic light scattering by a dense disordered medium has a strong polarization dependence that can be explained qualitatively in terms of the proposed mechanism of intensity enhancement shown by such systems.

This research was supported by the UK Science and Engineering Research Council and the U.S. Army European Research Office.

References

1. A. A. Golubentsev, Sov. Phys. JETP **59**, 26 (1984).
2. Y. Kuga and A. Ishimaru, J. Opt. Soc. Am. A **1**, 831 (1984).
3. L. Tsang and A. Ishimaru, J. Opt. Soc. Am. A **1**, 836 (1984).
4. M. P. van Albada and A. Lagendijk, Phys. Rev. Lett. **55**, 2692 (1985).
5. P.-E. Wolf and G. Maret, Phys. Rev. Lett. **55**, 2696 (1985).
6. E. Akkermanns, P. E. Wolf, and R. Maynard, Phys. Rev. Lett. **56**, 1471 (1986).
7. M. J. Stephen, Phys. Rev. Lett. **56**, 1809 (1986).
8. S. Etemad, R. Thompson, and M. J. Andrejco, Phys. Rev. Lett. **57**, 575 (1986).
9. M. J. Stephen and G. Cwilich, Phys. Rev. B **34**, 7564 (1986).
10. M. P. van Albada, M. B. van der Mark, and A. Lagendijk, Phys. Rev. Lett. **58**, 361 (1987).
11. M. J. Stephen and G. Cwilich, Phys. Rev. Lett. **59**, 285 (1987).
12. M. P. van Albada and A. Lagendijk, Phys. Rev. B **36**, 2353 (1987).
13. S. Etemad, R. Thompson, M. J. Andrejco, S. John, and F. C. MacKintosh, Phys. Rev. Lett. **59**, 1420 (1987).
14. R. Berkovits and M. Kaveh, Phys. Rev. B **36**, 9322 (1987).
15. A. Ishimaru and L. Tsang, J. Opt. Soc. Am. A **5**, 228 (1988).
16. P. E. Wolf, G. Maret, E. Akkermans, and R. Maynard, J. Phys. (Paris) **49**, 63 (1988).
17. E. Akkermans, P. E. Wolf, R. Maynard, and G. Maret, J. Phys. (Paris) **49**, 77 (1988).
18. E. R. Mendez and K. A. O'Donnell, Opt. Commun. **61**, 91 (1987).
19. K. A. O'Donnell and E. R. Mendez, J. Opt. Soc. Am. A **4**, 1194 (1987).
20. E. Bahar and M. A. Fitzwater, Opt. Commun. **63**, 355 (1987).
21. Yu. A. Kravtsov and A. I. Saichev, Sov. Phys. Usp. **25**, 494 (1982).
22. E. Jakeman, J. Opt. Soc. Am. A **5**, 1638 (1988).
23. A. Lagendijk, M. P. van Albada, and M. B. van der Mark, Physica **140A**, 183 (1986).
24. G. Maret and P. E. Wolf, Z. Phys. B **65**, 409 (1987).

Comparison of surface scattering between identical, randomly rough metal and dielectric diffusers

A. J. Sant, J. C. Dainty, and M.-J. Kim

Blackett Laboratory, Imperial College, London SW7 2BZ, UK

Received June 9, 1989; accepted August 8, 1989

A method of replicating randomly rough surfaces fabricated in photoresist has been developed, enabling comparisons of the scattered light to be made between identical diffusers made from different materials. Experimental measurements on one-dimensional metal (gold) and dielectric surfaces are presented, and some initial comparisons with numerical calculations are made.

Recent observations by Mendez and O'Donnell[1,2] of enhanced backscatter and strong depolarization from two-dimensional, randomly rough surfaces has encouraged critical discussion[3–8] of light-scattering mechanisms. In the development and validation of scattering phenomena the provision of such experimental data has an important part to play. In this Letter we report on observations of light scattering from one-dimensional randomly rough surfaces at a wavelength of 0.633 μm, comparing a metal-coated surface with a dielectric scatterer having identical surface characteristics; some preliminary numerical comparisons based on the Kirchhoff–Helmholtz integral equation[7] are made for normal incidence. Few experimental results have been reported for light scattering from dielectric surfaces,[9,10] least of all any that compare the surface scattering properties between different materials.[11]

The requirement for producing one-dimensional surfaces, or random gratings, arose for two reasons: (1) the need to accommodate one-dimensional scattering theories and (2) the computing time and memory involved in running numerical codes for two-dimensional problems.

The surfaces are produced by using photoresist technology similar to that employed by Mendez and O'Donnell[1,2] but using a thick film resist (Shipley S1400-37) to give a film thickness of ~12 μm. The coated substrates are exposed to eight uncorrelated, one-dimensional speckle patterns formed by focusing a Gaussian beam, using a large-aperture cylindrical lens onto a ground-glass diffuser. The resultant speckles are elongated in one direction; correlation lengths of the order of micrometers across the speckles and of millimeters along them are typically achieved. Once the plates are rinsed in a developer whose etching properties are linear with exposure time, the one-dimensional, randomly rough surface is completed.

In order to make accurate comparisons between the scattering properties of different materials it is preferable that the materials have identical surface characteristics. By using the etched photoresist plate as a master it is possible to reproduce the surface in certain materials by a method of replication. Two copies of plate #39 (rms height 1.18 ± 0.13 μm, 1/e correlation length 2.97 ± 0.05 μm) were formed in clear silicone rubber (Dow Corning Sylgard 182) directly from the gold-coated master (the gold coating was applied with evaporation techniques and has a thickness of ~90 nm). The first copy was used to obtain scattering measurements, whereas the second copy was used to form a mold from which an epoxy resin replica of the original was cast (Araldite MY778 and hardener HY956). The resin copy thus forms a positive replica of the original surface. In order to determine how successfully the master had been replicated, we coated the resin copy with gold, and its diffuse scattering envelopes were measured and compared with those of the original surface.

The scattering equipment and geometry used are

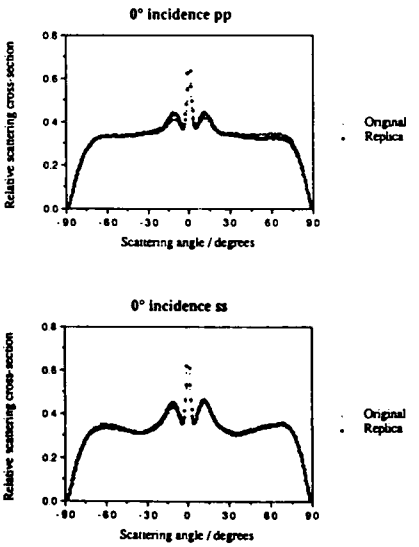

Fig. 1. Comparisons of light scattered by original and epoxy resin replica of plate #39 at a wavelength of 0.633 μm. 1/e correlation length 2.97 ± 0.05 μm, rms height 1.18 ± 0.13 μm; both surfaces are gold coated.

0146-9592/89/211183-03$2.00/0

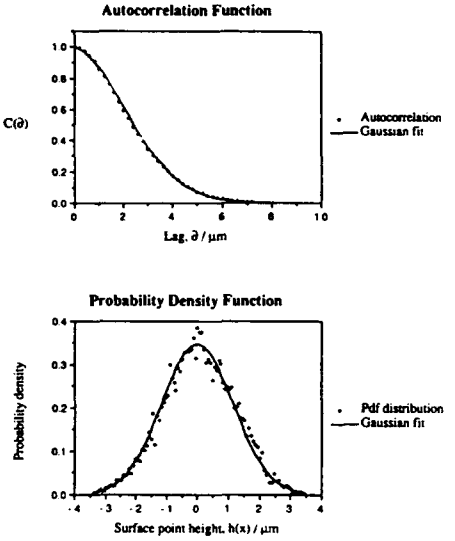

Fig. 2. Autocorrelation function $C(\partial) = \langle h(x)h(x+\partial)\rangle / \langle h^2(x)\rangle$ (where $\langle \ldots \rangle$ represents an ensemble average) and probability-density function of the height fluctuation of an epoxy resin replica of plate #39. $1/e$ correlation length 2.97 ± 0.05 μm, rms height 1.18 ± 0.13 μm.

essentially identical with those described in Ref. 2. For all scattering experiments the incident light was linearly polarized, the electric vector being either parallel (s or TE) or perpendicular (p or TM) to the grooves. The results are shown in Fig. 1 for normal incidence only, although measurements at angles as great as 60 deg have been carried out. The scattered-light envelopes exhibit the phenomenon of enhanced backscatter at 0 deg. Each measurement was normalized assuming perfect conductivity of the gold coating, integrating the total scattered radiation to unity. No depolarization, either sp or ps, of the incident radiation was observed, as expected for surface roughness in one dimension only. The scattering properties of the replica show excellent agreement with those of the original surface. The slight discrepancies can be attributed to misalignment of the scattering and detection planes and possible fine-scale resolution limitations ($\ll 1$ μm) in either the silicone rubber or the epoxy resin.

Autocorrelation and height probability-density functions were obtained from Talystep measurements of the gold-coated replica, examples of which are shown in Fig. 2. Each trace consists of 9000 data points taken every 0.2 μm at a scan speed of 2.5 μm sec^{-1}. Six uncorrelated traces displaced across the surface (i.e., across the grooves) were averaged to arrive at the quoted characteristics. The results in Fig. 2 show good agreement with Gaussian distributions for the height probability and autocorrelation functions. From Fig. 1 the exactness of the agreement between replica and original indicates that the initial copy in silicone rubber is also a faithful reproduction. Since the surface statistics are, to a good approximation, Gaussian, the fact that the silicone copy is a negative of the original should not affect its scattering properties.

One of the main problems involved with measuring the light scattered from the surface of a clear dielectric medium is the light reflected from the dielectric–air interface at the back of the sample. The unwanted transmitted light was absorbed with a neutral-density filter of density 4.0 optically coupled with a matching oil (refractive index 1.47) to the back face of the replica. The filter was angled at ~5° to the vertical to prevent any light reflected from its surface from entering the detector. The diffuse scattering envelopes measured for the dielectric surface are shown in Fig. 3 and should be compared with the relevant graphs in Figs. 1 and 4 of the perfect-conductor measurements. Each measurement shows the diffuse scattering envelope for the same incident power, but the measurements have not been normalized, and the intensity

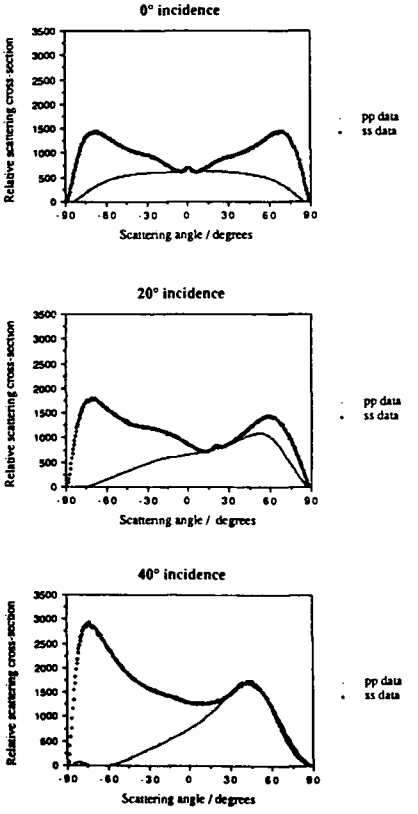

Fig. 3. Measurements of diffuse scattering envelopes of a dielectric surface illuminated at a wavelength of 0.633 μm. $1/e$ correlation length 2.97 ± 0.05 μm, rms height 1.18 ± 0.13 μm. Backscatter occurs to the right-hand sides of the graphs.

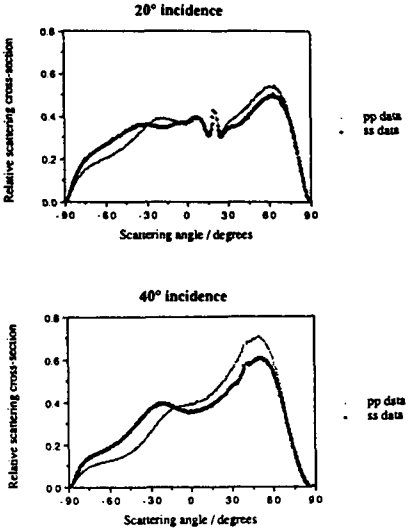

Fig. 4. Measurements of diffuse scattering envelopes of a gold-coated surface illuminated at a wavelength of 0.633 μm. 1/e correlation length 2.97 ± 0.05 μm, rms height 1.18 ± 0.13 μm. Backscatter occurs to the right-hand sides of the graphs.

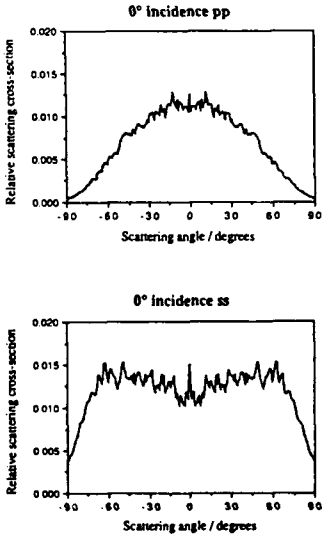

Fig. 5. Numerical calculations of diffuse scattering envelopes for a dielectric surface of refractive index 1.43 illuminated at normal incidence at a wavelength of 0.633 μm; 200 realizations. 1/e correlation length 2.97 μm, rms height 1.18 μm.

scale is therefore somewhat arbitrary. The first thing to note about the results is the lack of any significant backscatter enhancement for the dielectric surface, in contrast to observations for the gold-coated surface. Both *ss* and *pp* data have similar backscattered intensities, but in all the measurements the *ss* data show a greater reflectance for all angles than the *pp* data. A simple explanation may be found by considering Fresnel's reflection formulas: reflection of *p*-incident radiation from a plane dielectric surface momentarily falls to zero at the Brewster angle, whereas reflection of *s*-incident radiation rises at an increasing rate with angle of incidence and is always greater than for *p*-incident radiation. For the gold-coated surface (perfect-conductor case) away from normal incidence the *ss* and *pp* data of Fig. 4 show only slight differences, whereas the corresponding measurements for the dielectric case are quite different from each other. On comparing *pp* data for the two cases (metal and dielectric), one can see certain similarities, but for the *ss* data away from normal incidence one measurement is almost a reflection of the other about 0°.

Figure 5 shows the result of a Monte Carlo numerical calculation[7] for a perfect dielectric of refractive index 1.43, rms surface height 1.18 μm, and correlation length 2.97 μm; 200 realizations, each with 300 sampling points along a length of 25.31 μm (40 wavelengths), were used in the calculation. Comparison of Fig. 5 with the upper graph in Fig. 3 shows broad agreement.

The authors acknowledge the guidance given by Mike Hutley of the National Physical Laboratory, Teddington, UK, in developing the technique used for replicating rough surfaces. This research was supported by the UK Science and Engineering Research Council (GR/E 40910) and the U.S. Army Research Office (DAJA45-87-C-0039).

References

1. E. R. Mendez and K. A. O'Donnell, Opt. Commun. **61**, 91 (1987).
2. K. A. O'Donnell and E. R. Mendez, J. Opt. Soc. Am. A **4**, 1194 (1987).
3. E. Bahar and M. A. Fitzwater, Opt. Commun. **63**, 355 (1987).
4. M. Nieto-Vesperinas and J. M. Soto-Crespo, Opt. Lett. **12**, 979 (1987).
5. E. Bahar and M. A. Fitzwater, J. Opt. Soc. Am. A **6**, 33 (1989).
6. Z.-H. Gu, R. S. Dummer, A. A. Maradudin, and A. R. McGurn, Appl. Opt. **28**, 537 (1989).
7. A. A. Maradudin, E. R. Mendez, and T. Michel, Opt. Lett. **14**, 151 (1989).
8. J. M. Soto-Crespo and M. Nieto-Vesperinas, Opt. Commun. **69**, 185 (1989).
9. W. W. Montgomery and R. H. Kohl, Opt. Lett. **5**, 546 (1980).
10. J. Renau, P. K. Cheo, and H. G. Cooper, J. Opt. Soc. Am. **57**, 459 (1967).
11. P. T. Gough and W.-M. Boerner, J. Opt. Soc. Am. **69**, 1212 (1979).

Experimental study of enhanced backscattering from one- and two-dimensional random rough surfaces

M.-J. Kim, J. C. Dainty, A. T. Friberg, and A. J. Sant

Applied Optics Section, Blackett Laboratory, Imperial College of Science, Technology and Medicine, London SW7 2AZ, UK

Received June 27, 1989; accepted November 16, 1989

An experimental study of backscatter enhancement from rough surfaces is presented. The Stokes parameters of the average scattered light from two-dimensional rough surfaces show the presence of an unpolarized component, which lends support to the multiply scattering ray model. Experimental data from one-dimensional rough surfaces are compared with numerical calculation.

INTRODUCTION

The phenomenon of light scattering from rough surfaces (random or otherwise) has attracted much attention, both experimentally and theoretically. This subject is of particular importance in areas that involve using a wave, either acoustic or electromagnetic, as a probe to observe material and surface properties, e.g., interpretation of radar returns (from the surface of the Earth as well as from other planetary bodies) and noncontact surface characterization.

Recently the enhancement of scattered light intensity in the backscatter direction from metallic rough surfaces was reported by Mendez and O'Donnell.[1,2] This backscatter peak from other random rough surfaces had been previously observed; a sudden increase in the brightness of the Moon when it approached its fullness was reported as far back as 1924 by Markov,[3] while Oetking[4] reported this effect to be present when scattered light from rocks, as well as certain reference samples, was observed. This backscatter peak, also called the opposition effect in the literature, has been reported by several other authors[5,6]; the peaks usually have a small angular width (typically 2 to 3 deg) and result when the scattering of light occurs in the volume as well as on the surface. The phenomenon of backscatter enhancement as observed by Mendez and O'Donnell differed from what the other authors reported in that they used metallic, high-sloped, single-scale, Gaussian, random rough surfaces, whose standard deviation of surface height was much larger than the incident wavelength. The key property was that the scattering of light was confined to the surface owing to its metallic nature. This effect was normally accompanied by a large cross-polarized component.

The high-sloped nature of the surface meant that multiple scattering was a significant contribution to the scattered light. The methods that can be used to explain this phenomenon analytically are limited because of the restrictions imposed on the available scattering theories. Physical optics[7] cannot be used since it accounts only for single scattering and only when the surface structures are much larger than the incident wavelength. Analytical multiple-scattering theories[8-10] utilizing the extended boundary condition are expressed in a perturbation series, and, owing to the difficulty in calculating high-order terms and the slowness or complete lack of convergence, they have been limited to the case of low-sloped surfaces. The full-wave solution[11] may account for the enhanced backscatter peak while single scattering only is used.

The technique of numerical calculation of the scattered light has been available for some time.[12-14] This method is computationally highly intensive, and hence the application of this method was quite limited until recently. Perfectly conducting surfaces were normally considered, and the intent was largely to establish the range of validity of the available scattering theories such as the physical-optics solution[15,16] and the full-wave theory.[17] The technique has also been used to calculate the scattered light from high-sloped surfaces, and enhanced backscatter peaks were observed in the calculated values[15]; such effects were also observed when real metallic surfaces were considered.[18] The major flaw of this procedure is that it gives little physical insight into the scattering process; all effects such as shadowing, multiple scattering, and light–surface interaction are mixed inseparably together.

Mendez and O'Donnell proposed a simple model involving multiple scattering of rays from surface facets; it was an analog of that used in the volume-scattering case.[19] Jakeman[20] used a model consisting of a deep random phase screen with a mirror placed just behind it. However, although these models explained qualitatively the presence of enhanced backscatter peaks, they leave much to be desired, e.g., they do not take into account the polarization of the scattered light or predict the detailed shape of the scatter envelope.

The research reported here is an extension of that presented by Mendez and O'Donnell. The normalization method used to scale the experimental data will be discussed briefly. The polarization behavior of the scattered light from two-dimensional random rough surfaces that exhibit enhanced backscatter peaks is discussed. Interpretation of Stokes parameters leads to an alternative way of mapping the scattered light; instead of the usual copolarized and cross-polarized intensity one can plot the polarized and unpolarized components. In this context, unpolarized means that there is no preferred direction of polarization over the solid angle

0740-3232/90/040569-09$02.00

of measurement (which encompasses many speckles). Finally, an experimental study of approximately one-dimensional random rough surfaces is presented, and the experimental data are compared with numerically calculated values where possible.

SCATTEROMETER RESPONSE

The name scatterometer designates the equipment[21] that was used to perform experiments involving the measurement of scattered light as a function of the angle of incidence θ_i and the scattering angle θ.

Figure 1 is a schematic diagram of the scatterometer viewed from above. Two laser light sources were available: He–Ne (Spectra-Physics 105-1 laser, wavelength $\lambda = 0.633$ μm) and CO_2 (Edinburgh Instruments WL-4, $\lambda = 10.6$ μm). The spot size at the sample was approximately 10 mm in diameter, and the incident beam was collimated. The sample mount held the rough surface such that the mean surface normal was horizontal, although it was possible to tilt the surface normal slightly off the horizontal plane. The sample mount and the rotating arm were movable, both having the same rotational axis, each controlled by an individual stepper motor. The values of angles were such that θ_i was measured clockwise from the surface normal and θ anticlockwise from the surface normal, ensuring that $\theta = \theta_i$ in the specular direction. The detectors used were a Hamamatsu R647 photomultiplier for the visible light and a Plessey PLT222 pyroelectric detector for the far-infrared radiation. When performing experiments in the far infrared, we used a chopper in conjunction with a phase lock-in amplifier (Stanford Research SR530) to eliminate the background noise, the incident beam being chopped at typically 80 Hz. A microscope objective of 5-mm diameter and a CdS lens of 1-cm diameter were used as integrating lenses for the visible and the far infrared, respectively. The distance between the rotational axis and the integrating lens was 62 cm; the angular resolution of the measurement of the scattered light was thus approximately 0.5° for the visible and 1.0° for the infrared.

The light incident upon the rough surfaces was always coherent, and hence a speckle pattern was generated. The detector response R_d is proportional to the spatial integral of speckles in the solid angle of the integrating lens, i.e.,

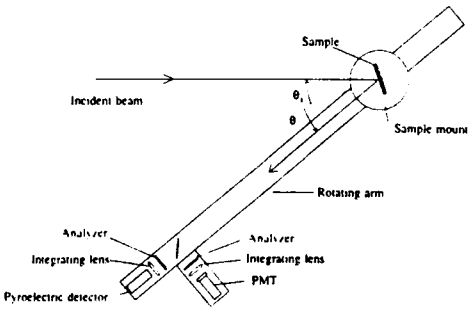

Fig. 1. Schematic diagram of the scatterometer viewed from above. PMT, photomultiplier tube.

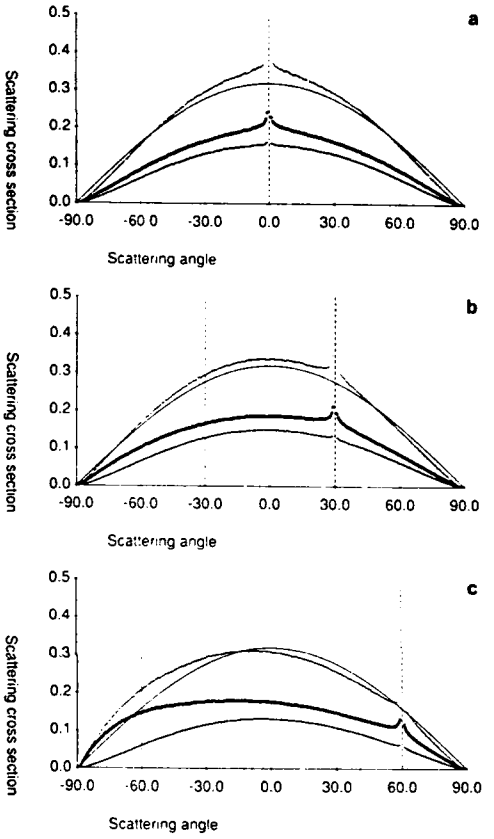

Fig. 2. Scatter envelope from a MgO surface, s incident polarization ($\lambda = 0.633$ μm). Second curves from bottom denote Σ_{ss}, curves immediately below these indicate Σ_{sp}, and topmost curves denote Σ_{tot}. θ_i is a, 0°; b, −30°, and c, −60°. The solid curves denote the case of a perfect Lambertian surface with a perfect scatterometer response.

$$R_d = \mathcal{R} \int_{\Delta\Omega} d\Omega W(\Omega) J(\Omega), \tag{1}$$

where $\Delta\Omega$ is the solid angle of the integrating lens, $W(\Omega)$ a weighting function, $\mathcal{R}$ is the constant of proportionality, and J is the radiant power. Here we make an assumption that the finite spatial average is equal to an ensemble average, i.e.,

$$R_d = \mathcal{R} \Delta\Omega' \langle J \rangle, \tag{2}$$

where $\Delta\Omega'$ is the effective integration angle and does not necessarily stay constant for all θ. $\langle J \rangle$ denotes the average of the radiant intensity for that particular scattering angle, for an ensemble of statistically identical but independent rough surfaces. We introduce a new quantity, the mean normalized differential scattering cross section (DSCS) Σ, defined as

$$\Sigma = \frac{\langle J \rangle}{\Phi_i}, \tag{3}$$

where Φ_i is the incident power. Σ is related to the well-known bidirectional reflection function[22,23] $\langle f_r \rangle$ by a simple expression:

$$\Sigma = \langle f_r \rangle \cos\theta. \tag{4}$$

To denote the polarization property of the incident and scattered light, subscripts are appended to Σ; the first letter of the subscript denotes the polarization state of the incident light, and the second the polarization state of the detected light; e.g., Σ_{sp} is the DSCS for the case when incident light is s polarized and the detected light p polarized.

Hence, by using Eqs. (2) and (3), an accurate value of Σ can be obtained once the angular dependence of $\Delta\Omega'$ is known, and this is usually done by the reference sample method.[21] Normally, a Lambertian scatterer is sought as an ideal reference sample. If the directional reflectance (total scattered power divided by the incident power) is unity, the mean normalized DSCS for a Lambertian diffuser is given by a simple expression:

$$\Sigma(\theta_i, \theta) = \frac{1}{\pi} \cos\theta. \tag{5}$$

The problem with this method is that a perfect Lambertian diffuser is impossible to realize. Historically, a freshly smoked magnesium oxide (MgO) surface was used as an approximation to a Lambertian scatterer, although a barium sulfate ($BaSO_4$) surface as made by the method prescribed by Eastman Kodak has established itself as a standard.[24] To check the response, Σ was initially obtained, for the case of a MgO surface, assuming that $\Delta\Omega'$ remains constant for all θ. The directional reflectance was assumed to be unity.

Figures 2a, 2b, and 2c show the scattering data from a MgO surface for $\theta_i = 0°, -30°$, and $-60°$, respectively. The incident light was s polarized, of wavelength $\lambda = 0.633$ μm. In each figure the copolarized component Σ_{ss} and the cross-polarized component Σ_{sp} are shown together with the sum of both, i.e., Σ_{tot}. Figures 3a, 3b, and 3c show similar data but with the incident polarization being p polarized. The fit with the cosine line is fairly good for both incident polarizations except for the presence of the backscatter peaks (cf. Ref. 6 and references therein). Since our scatterometer gave an approximately cosine response for the case of an approximately Lambertian scatterer, it was decided that the assumption that $\Delta\Omega'$ remains constant for all θ was a reasonable one to take. This approximation is implicit from this point onward. Another important approximation used was that, on normalization, the metallic surfaces were all assumed to be perfect conductors.

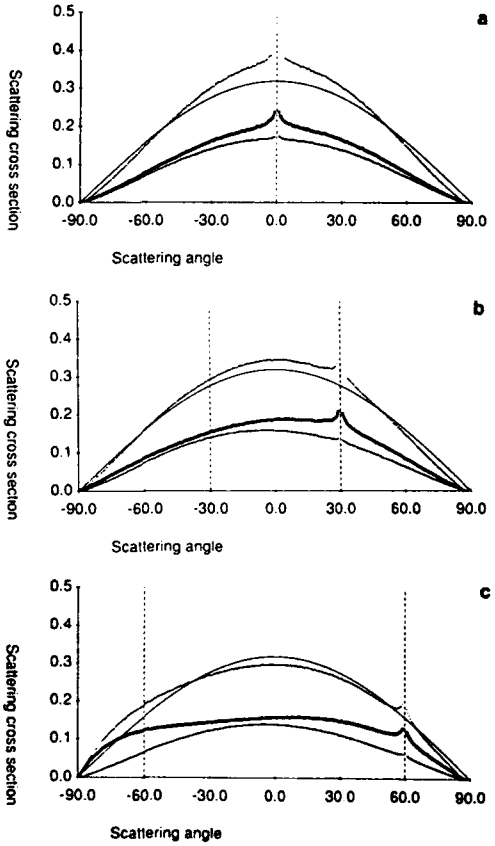

Fig. 3. Scatter envelope from MgO surface, p incident polarization ($\lambda = 0.633$ μm). Second curves from bottom denote Σ_{pp}, curves immediately below these indicate Σ_{ps}, and topmost curves denote Σ_{tot}. θ_i is a, 0°; b, −30°, c, −60°. The solid curves denote the case of a perfect Lambertian surface with a perfect scatterometer response.

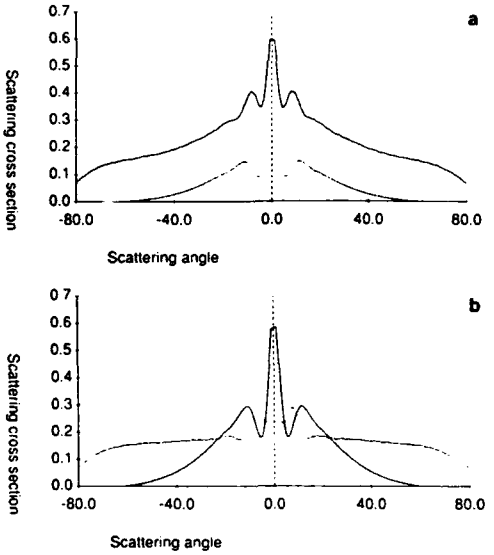

Fig. 4. Plate #313, $\theta_i = 0°$, $\lambda = 0.633$ μm. The copolarized and cross-polarized components Σ_{ss} and Σ_{sp} are shown in a; the equivalent Σ_{pol} and Σ_{unpol} are shown in b. Solid curves denote Σ_{ss} and Σ_{unpol}, and dotted lines denote Σ_{sp} and Σ_{pol}.

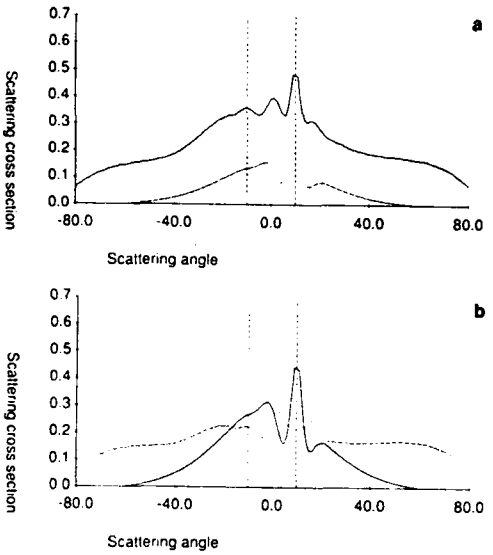

Fig. 5. Plate #313, $\theta_i = -10°$, $\lambda = 0.633\ \mu m$. Labels as in Fig. 4.

STOKES PARAMETERS OF SCATTERED LIGHT

Plate #313 was a gold-coated metallic two-dimensional Gaussian random rough surface. It was made by the method described by Gray,[25] that is, by multiply exposing a photoresist-coated substrate to laser speckle patterns. After extensive analysis of the surface profiles obtained from a Talysurf profilometer with a sufficiently small stylus tip, it was found that plate #313 had a standard deviation of surface height $\sigma_h = 1.0 \pm 0.1\ \mu m$ and a $1/e$ correlation length $\tau = 2.9 \pm 0.2\ \mu m$, i.e., the surface structure was larger than the visible wavelength, but the standard deviation of the surface slope was high, approximately 0.5. This surface showed the enhanced backscatter peak as well as a large cross-polarized component. In fact, the scatter envelope was similar to that obtained from plate #83 in Ref. 2.

Stokes parameters provide a complete description of the polarization state of the scattered light. Ideally, they should have been obtained for all θ and for all angles of incidence. As such, they were calculated for normal incidence and for a few fixed scattering angles θ (one near the backscatter direction). The incident light was linearly polarized. The values of the Stokes parameters showed that for those fixed angles, the scattered light was composed of two components, at least to within the experimental error (5% of the first Stokes parameter): one that is linearly polarized in the direction of the incident light and another that is unpolarized (see below). For scattering of monochromatic light from a single surface realization, light scattered in a single direction will be completely polarized. However, what we are measuring is the scattered light integrated over a detector solid angle, and the measurement indicates is that there is a component of scattered light that, although com-

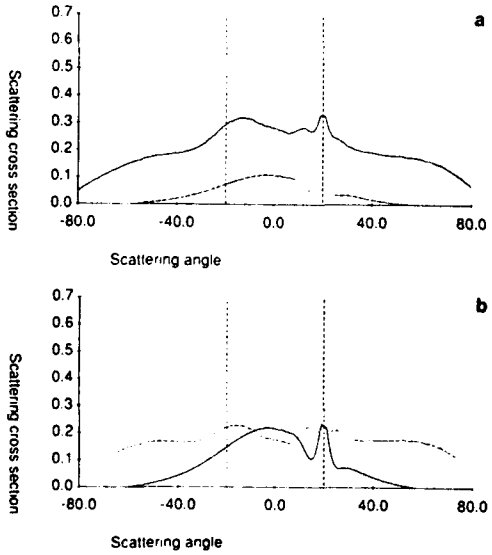

Fig. 6. Plate #313, $\theta_i = -20°$, $\lambda = 0.633\ \mu m$. Labels as in Fig. 4.

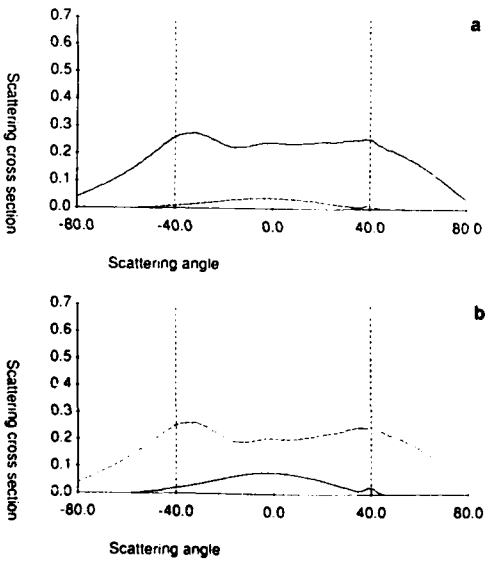

Fig. 7. Plate #313, $\theta_i = -40°$, $\lambda = 0.633\ \mu m$. Labels as in Fig. 4.

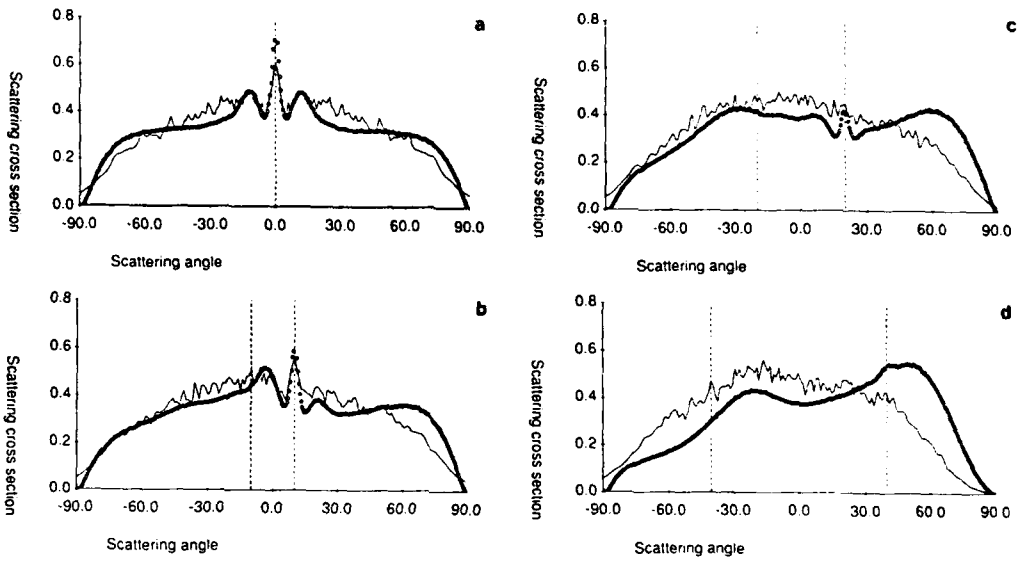

Fig. 8. Plate #440, *s* incident polarization ($\lambda = 0.633\ \mu m$), for θ_i = a, 0°; b, −10°; c, −20°; d, −40°. The thicker curves denote experimental Σ_{ss}; the thinner curves show the numerically calculated values. The measured cross-polarized component, denoted by the line almost coincident with the *x* axis, is shown only for the case of normal incidence.

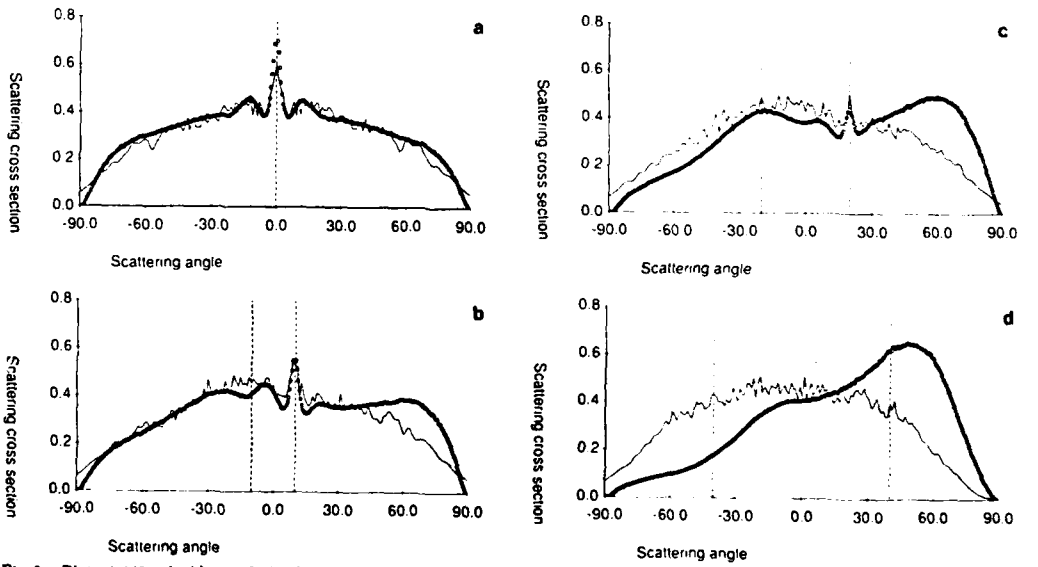

Fig. 9. Plate #440, *p* incident polarization ($\lambda = 0.633\ \mu m$), for θ_i = a, 0°; b, −10°; c, −20°, d, −40°. The thicker curves denote experimental Σ_{pp}; the thinner curves show the numerically calculated values. The measured cross-polarized component, denoted by the line almost coincident with the *x* axis, is shown only for the case of normal incidence.

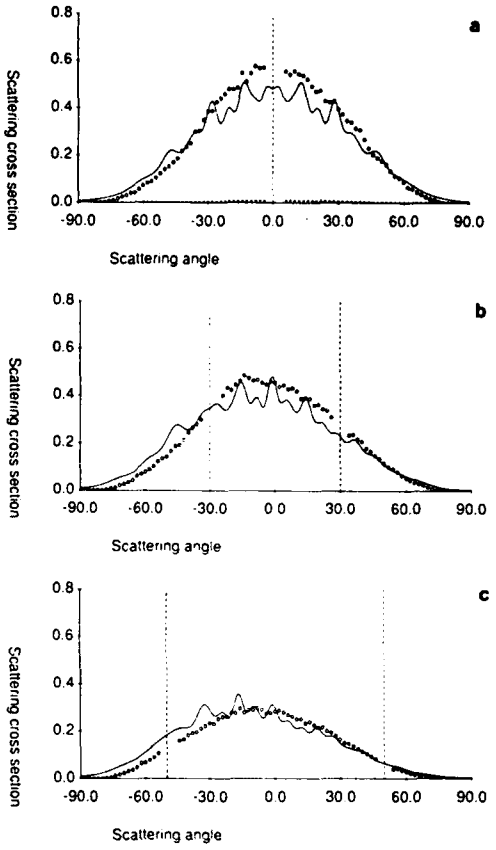

Fig. 10. Plate #440, s incident polarization ($\lambda = 10.6\ \mu m$), for θ_i = a, 0°; b, −30°; c, −50°. Labels as in Fig. 9.

pletely polarized in a single direction, does not have a preferred polarization direction averaged over the detector solid angle, thus giving rise to a measurement that makes it appear to be unpolarized.

The above description gives rise to an interesting conjecture, namely, that the visible scattered light averaged over an ensemble of rough surfaces such as plate #313 is composed of two components only, that is, one component linearly polarized in the direction of the incident polarization and a second component that appears to be unpolarized. Keeping this in mind, it is thus possible to describe the scattered light not in terms of copolarized and cross-polarized components, say Σ_{ss} and Σ_{sp}, but in terms of polarized and unpolarized components, Σ_{pol} and Σ_{unpol}, respectively. The relating expressions are

$$\Sigma_{pol} = \Sigma_{ss} - \Sigma_{sp} \tag{6a}$$

and

$$\Sigma_{unpol} = 2\Sigma_{sp}. \tag{6b}$$

Figure 4a shows the plot of mean normalized DSCS Σ_{ss} and Σ_{sp}, while Fig. 4b shows the plot of mean normalized DSCS converted in the manner given by Eqs. (6), both for the case of plate #313, normal incidence, the incident wavelength's being $\lambda = 0.633\ \mu m$. Figures 5, 6, and 7 show the similar quantities but for angles of incidence of −10°, −20°, and −40°, respectively. It is interesting to note that the enhanced backscatter peak is confined mainly to the unpolarized component.

Multiply scattering rays, according to the model proposed by Mendez and O'Donnell, are the cause of depolarization as well as of enhanced backscatter peaks,[26] i.e., they will not have a preferred polarization direction. Singly scattered rays have a preferred polarization direction. Hence the unpolarized component will contain the enhanced backscatter peak, according to this simple model. This is the case when one studies Figs. 4–7.

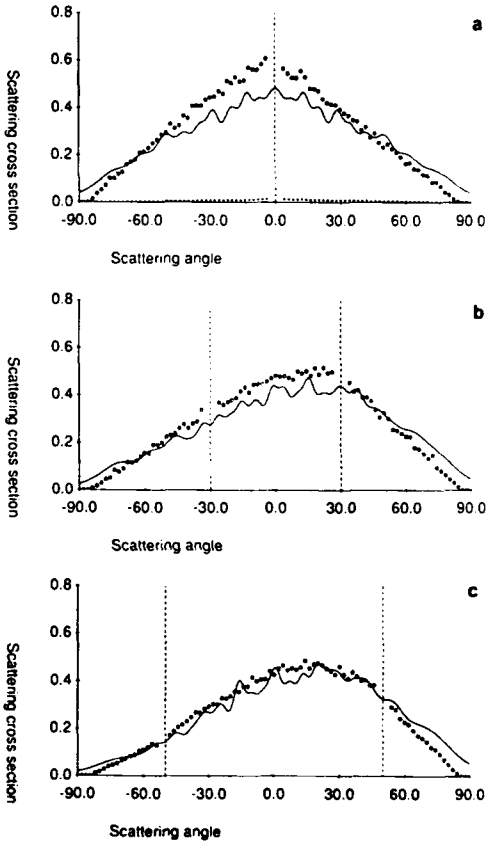

Fig. 11. Plate #440, p incident polarization ($\lambda = 10.6\ \mu m$), for θ_i = a, 0°; b, −30°; c, −50°. Labels as in Fig. 9.

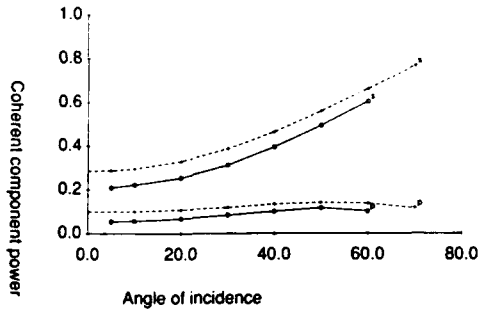

Fig. 12. Plate #440 ($\lambda = 10.6\ \mu m$); plot of the normalized coherent component power for s and p incident polarization obtained from calculation and experiment, shown as crosses and open circles, respectively. The physical-optics solutions for s and p polarizations and a one-dimensional rough surface are shown dashed and dotted.

SCATTERING FROM ONE-DIMENSIONAL SURFACES

Consider a surface whose surface height variation depends on one Cartesian coordinate, i.e., a one-dimensional surface $z = h(x)$. If the incident electromagnetic field has either the electric or the magnetic field lying perpendicular to the incident plane, in this case the xz plane, there is no cross-polarized component, and the scattering problem reduces to a scalar-wave situation. The problem still remains intractable analytically, but it can be solved exactly by numerical calculation, which involves averaging the calculated scattered intensity over an ensemble of surface realizations.

Approximately one-dimensional random surfaces were made by etching a photoresist-coated substrate with a speckle pattern whose correlation length was much longer in one dimension than the orthogonal one. Two surfaces, both gold coated, were considered: plate #440 ($\sigma_h = 1.2 \pm 0.1\ \mu m$, $\tau = 2.9 \pm 0.2\ \mu m$) and plate #436 ($\sigma_h = 1.6 \pm 0.1\ \mu m$, $\tau = 5.2 \pm 0.3\ \mu m$). Surface parameters were obtained by using the traces measured in the x direction.

Following the method described in Refs. 15 and 16, numerical calculations were done for the case of a perfect conductor only. To ensure the accuracy of the solution obtained, the lengths of the discrete surface (40λ) and the sampling distance (0.13λ) were chosen such that the fluctuation of the normalized total scattered energy was less than 3%.

Figures 8a, 8b, 8c, and 8d show Σ_{ss} for $\theta_i = 0°, -10°, -20°$, and $-40°$, respectively, for the case of plate #440, the incident wavelength being $\lambda = 0.633\ \mu m$. Figures 9a–9d show Σ_{pp} for the same angles of incidence. Negligible cross-polarized components were observed. The numerically calculated values, obtained after averaging over 400 surface realizations, are shown as solid curves. Enhanced backscatter peaks are observed, both in the experimental data and in the numerically calculated values. Agreement is good for small θ_i but fails when θ_i becomes large. The reason for this failure is not clear; it may be the fact that the finite conductivity of the real surface has not been taken into account, that the length of the surface in the computer calculation is too short, or that the condition that states that the total scattered power has to equal the incident power is not enough to

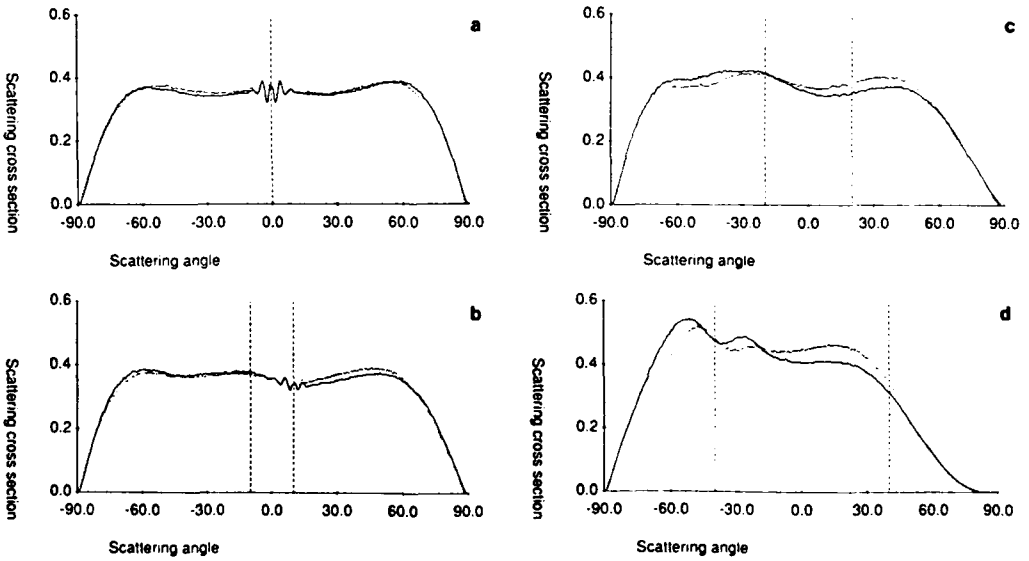

Fig. 13. Plate #436 ($\lambda = 0.633\ \mu m$); plots of Σ_{ss} (solid curves) and Σ_{pp} (dotted curves) for θ_i = a, 0°; b, −10°; c, −20°, d, −40°.

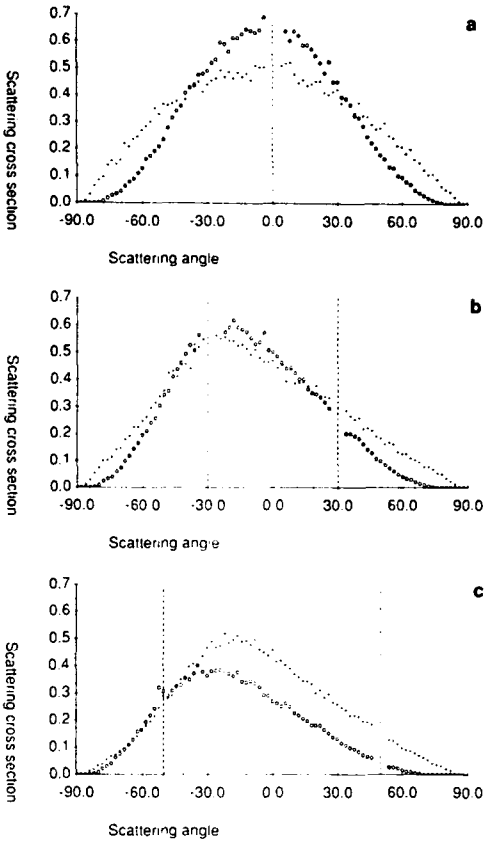

Fig. 14. Plate #436 ($\lambda = 0.633\ \mu m$); plot of Σ_{ss} (open circles) and Σ_{pp} (crosses) for θ_i = a, 0°; b, −30°; and c, −50°.

ensure the accuracy of the solution, as is known from other studies.

Figures 10a, 10b, and 10c show Σ_{ss} for $\theta_i = 0°$, −30°, and −50° respectively, for the same plate but with the incident wavelength now being $\lambda = 10.6\ \mu m$. Figures 11a–11c show Σ_{pp} for the same angles of incidence. We believe that small cross-polarized components shown in Figs. 10a and 11a are due to the intrinsic error in the half-wave plate used in the scatterometer and the imperfect linear polarization state of the output beam from the CO_2 laser. Numerically calculated values are shown for comparison. In both experimental data and numerically calculated values, the coherent component has been removed, but in normalizing the experimental data its power was taken into account. For the numerically calculated values, the coherent component was removed by subtracting from the total intensity the modulus square of the unscattered field.[27] The agreements are good for all θ_i. It is interesting to note that as θ_i increases, the total power of the incoherent component seems to decrease for the case of *s* incident polarization, while for the *p* incident polarization it seems to remain constant. This becomes more evident when one studies Fig. 12, which plots the normalized coherent component power for *s* and *p* polarization, experimental data, and calculated values, over a range of θ_i.

Figures 13a, 13b, 13c, and 13d show Σ_{ss} and Σ_{pp} for plate #436, with $\theta_i = 0°$, −10°, −20°, and −40°, respectively, for $\lambda = 0.633\ \mu m$. Figures 14a, 14b, and 14c show Σ_{ss} and Σ_{pp} for the same plate, with $\theta_i = 0°$, −30°, and −50°, respectively, for $\lambda = 10.6\ \mu m$. Numerical calculations were not possible for the case of plate #436, as the required array sizes were too large to handle. It is interesting to note that, unlike for plate #440, there seems to be little qualitative difference in the scatter envelopes resulting from the different incident polarizations. The key feature to note is the small or nonexistent enhancement in the backscatter direction, presumably a result of the small value of the average of the absolute slope.

CONCLUSION

Stokes parameters of the scatter envelope, which shows an enhanced backscatter peak, have been studied; it was found that the scattered light was composed of polarized and unpolarized light only and that the backscatter peak was confined to the unpolarized component. This result supports the hypothesis claiming that the backscatter peak is due to multiple scattering.

An experimental study of scattering of light from approximately one-dimensional surfaces was presented. Comparison with numerically calculated values was done wherever possible. There are disagreements in some cases, and the reasons are unclear at this stage of investigation. Although numerical calculation gives the numbers with which to compare the experimental data, further work needs be done if we are to understand the physical mechanism behind the scattering of light from high-sloped surfaces. It is hoped that the experimental results presented here will encourage such work.

ACKNOWLEDGMENTS

We are grateful to the UK Science and Engineering Research Council (GR/E/40910) and the U.S. Army (DAJA45-87-C-0039) for the financial support that made it possible to conduct this research.

REFERENCES

1. E. R. Mendez and K. A. O'Donnell, "Observation of depolarization and backscattering enhancement in light scattering from gaussian rough surfaces," Opt. Commun. 61, 91–95 (1987).
2. K. A. O'Donnell and E. R. Mendez, "Experimental study of scattering from characterized random surfaces," J. Opt. Soc. Am. A 4, 1194–1205 (1987).
3. A. V. Markov, "Les particularités dans la réflexion de la lumière par la surface de la lune," Astron. Nachr. 221, 65–78 (1924).
4. P. Oetking, "Photometric studies of diffusely reflecting surfaces with applications to the brightness of the moon," J. Geophys. Res. 71, 2505–2513 (1966).
5. W. G. Egan and T. Hilgeman, "Retroreflectance measurements of photometric standards and coatings," Appl. Opt. 15, 1845–1849 (1976).
6. W. W. Montgomery and R. H. Kohl, "Opposition-effect experimentation," Opt. Lett. 5, 546–548 (1980).
7. P. Beckmann and A. Spizzichino, *The Scattering of Electromagnetic Waves from Rough Surfaces* (Pergamon, New York, 1963).

8. J. Shen and A. A. Maradudin, "Multiple scattering of waves from random rough surfaces," Phys. Rev. B **22**, 4234–4240 (1980).
9. M. Nieto-Vesperinas and N. Garcia, "A detailed study of the scattering of scalar waves from random rough surfaces," Opt. Acta **28**, 1651–1672 (1981).
10. D. P. Winebrenner and A. Ishimaru, "Application of the phase-perturbation technique to randomly rough surfaces," J. Opt. Soc. Am. A **2**, 2285–2294 (1985).
11. E. Bahar and M. A. Fitzwater, "Depolarization and backscatter enhancement in light scattering from random rough surface: comparison of full wave theory with experiment," J. Opt. Soc. Am. A **6**, 33–43 (1989).
12. R. R. Lentz, "A numerical study of electromagnetic scattering from ocean-like surfaces," Radio Sci. **9**, 1139–1146 (1974).
13. R. M. Axline and A. K. Fung, "Numerical calculation of scattering from a perfectly conducting rough surface," IEEE Trans. Antennas Propag. **AP-26**, 482–488 (1978).
14. H. L. Chan and A. K. Fung, "A numerical study of the Kirchhoff approximation in horizontally polarized backscattering from a random surface," Radio Sci. **13**, 811–818 (1978).
15. M. Nieto-Vesperinas and J. M. Soto-Crespo, "Monte Carlo simulations for scattering of electromagnetic waves from perfectly conductive random rough surfaces," Opt. Lett. **12**, 979–981 (1987).
16. J. M. Soto-Crespo and M. Nieto-Vesperinas, "Electromagnetic scattering from very rough random surfaces and deep reflection gratings," J. Opt. Soc. Am. A **6**, 367–384 (1989).
17. E. I. Thorsos, "The validity of the Kirchhoff approximation for rough surface scattering using a Gaussian roughness spectrum," J. Acoust. Soc. Am. **83**, 78–92 (1987).
18. A. A. Maradudin, E. R. Mendez, and T. Michel, "Backscattering effects in the elastic scattering of *p*-polarized light from a large-amplitude random metallic grating," Opt. Lett. **14**, 151–153 (1989).
19. Y. Kuga and A. Ishimaru, "Retroreflectance from a dense distribution of spherical particles," J. Opt. Soc. Am. A **1**, 831–835 (1984).
20. E. Jakeman, "Enhanced backscattering through a deep random phase screen," J. Opt. Soc. Am. A **5**, 1638–1648 (1988).
21. F. O. Bartell, E. L. Dereniak, and W. L. Wolfe, "The theory and measurement of bidirectional reflectance distribution function (BRDF) and bidirectional transmittance distribution function (BRTF)," in *Radiation Scattering in Optical Systems*, G. H. Hunt, ed., Proc. Soc. Photo-Opt. Instrum. Eng. **257**, 154–160 (1980).
22. F. E. Nicodemus, "Directional reflectance and emissivity of an opaque surface," Appl. Opt. **4**, 767–773 (1965).
23. F. E. Nicodemus, "Reflectance nomenclature and directional reflectance and emissivity," Appl. Opt. **9**, 1474–1475 (1970).
24. F. Grum and G. W. Luckey, "Optical sphere paint and a working standard of reflectance," Appl. Opt. **7**, 2289–2294 (1968).
25. P. F. Gray, "A method of forming optical diffusers of simple known statistical properties," Opt. Acta **25**, 765–775 (1978).
26. Ref. 2, Figs. 12–14.
27. Ref. 7, Chap. 6.

Light transmission from a randomly rough dielectric diffuser: theoretical and experimental results

M. Nieto-Vesperinas and J. A. Sánchez-Gil

Instituto de Optica, Consejo Superior de Investigaciones Cientificas, c/Serrano 121, Madrid 28006, Spain

A. J. Sant and J. C. Dainty

Blackett Laboratory, Imperial College, London SW7 2BZ, UK

Received April 4, 1990; accepted June 22, 1990; manuscript in hand July 21, 1990

We report numerical and experimental obeservations of a new transmission effect in rough dielectric interfaces.

Recent experiments with light scattered from highly sloped random rough surfaces[1,2] and the development of new numerical methods of study[3,4] have produced a renewed interest in scattering effects and in the mechanisms that produce them, in both metallic and dielectric surfaces.[5–10]

We report the numerical prediction and experimental demonstration of a new transmission effect in a semi-infinite dielectric material when light is incident from a semi-infinite vacuum upon the rough surface that separates both media.

Because of the limited power of computer calculations in terms of both speed and memory, the surface profiles under study are one dimensional: the random height depends on one transverse coordinate only, being constant along the other coordinate. The experiments have also been performed on specially fabricated one-dimensional surfaces in order to accommodate the observations to the available theory.

Numerical Monte Carlo calculations for the scattered intensities have been carried out from samples with rms deviation σ, normal statistics, and a Gaussian correlation function, with profile correlation length T. The surfaces are generated by means of a procedure identical to that described in Refs. 3 and 7, namely, each sample consists of a portion of a sequence of $\sim 10^5$ random numbers with the desired normal probability density and statistical parameters σ and T. The length L of the samples is typically $L = 40\ \lambda$ (λ being the wavelength); 220 sampling points are taken for each sample. Both the field and its normal derivative are calculated on the surface by using the extinction theorem.[11] The corresponding equations are similar to those already used by Maradudin *et al.* in Refs. 4 and 10, with the sole exception that each sample is assumed to be illuminated by a plane wave instead of a beam (i.e., no tapering is made). Then those boundary values of the fields and their derivatives on the surface are introduced into the far-zone expression of the field so the scattered intensity can be found. Finally these scattered intensities are averaged over 240 samples. At a given angle of incidence and a certain surface record of length L, two sets of scattered intensities are obtained by considering the results for θ_0 and those for $-\theta_0$. This doubles the effective number of samples. Calculations were done on a CDC Cyber 180/855 computer. Unitarity of the normalized reflected and transmitted intensities at the dielectric interface, as well as the convergence of the results when the number of samples is increased, is taken as a criterion of numerical consistency.

The angular distribution of mean intensity in the far zone of light transmitted into the dielectric, after being scattered at the rough surface separating it from vacuum, is plotted in Fig. 1. The dielectric constant is $\Re(\epsilon) = 1.991$ [$\Im(\epsilon) \approx 0$], where $\Re$ and $\Im$ denote real and imaginary parts, respectively, and the surface parameters are $\sigma = 1.86\lambda$ and $T = 4.69\lambda$. The sum of the reflectance R and the transmittance T for each angle of incidence (0°, 20°, 40°, and 60°, respectively) is shown in Fig. 1 (solid curves, p polarization; dashed curves, s polarization). We have marked the direction of refraction that would correspond to a plane interface (dotted vertical lines) and the straight-through direction (small marks at the left of the vertical lines at the tops of the figures). The remarkable effect observed is the deviation from the refraction direction of the mean scattered intensity of light transmitted into the dielectric. A narrow distribution peaked closer to the straight-through direction appears. The roughness makes the angular distribution of light act as though there were no different refractive index on the other side. Moreover, this peak tends to grow and to become narrower as the angle of incidence increases.

We believe that the mechanism that produces this effect can be understood within the diagrammatic approach used by the authors of Refs. 1, 2, 4, 9, and 10. Because of the slope of the surface, the local angle of incidence decreases as the overall angle of incidence increases. On the other hand, since the material is highly transparent, little light is thrown back into vacuum in each scattering event, so double-scattering contributions are negligible in comparison with those of single scattering. These single-scattering contributions tend to broaden the distribution of transmitted light, but the dominant angle of light transmission is observed to be greater than it would be if there were no roughness (Snell's law), and it is close to the straight-

0146-9592/90/221261-03$2.00/0

through direction: this is due to the aforementioned lower local angle of incidence. In the case of nonnegligible multiple-scattering contributions (greater refractive index), since the second hit on the surface would contain almost all local angles of incidence the resulting angular distribution should be expected to spread over a wide solid angle failing to peak clearly in one direction. Calculations made by increasing ϵ have confirmed this point.

The effect reported in this Letter is observed neither on surfaces whose radius of curvature is much larger than λ (this is the general criterion of validity of the Kirchhoff approximation for perfect conductors) nor with very low σ and T (say, one tenth of λ). However, as this effect is essentially due to single scattering, we believe that a calculation based on the Kirchhoff approximation should give a nearly correct solution; recent preliminary computations confirm this belief (this suggests that the range of validity of the Kirchhoff approximation for dielectric surfaces is much broader than accepted for perfect conductors).

In order to verify the findings of the numerical transmission calculations, we fabricated a dielectric diffuser in silicone rubber to produce a slab without a tilt angle. The diffuser considered here is a dielectric replica of the diffuser investigated in reflection by Sant *et al.*[6]

Using an experimental rig essentially identical to that described by O'Donnell and Méndez,[2] with the exception of implementing a transmission geometry, we took transmission data for 0°, 20°, 40°, and 60° incidence for both *s* and *p* polarizations; the results are shown in Fig. 2. The data were converted by Snell's law of refraction (for the plane back face of the sample) to represent light transmission within the medium. The data have not been normalized in an absolute manner, but they are relatively comparable.

For 0° incidence the transmission peak does not appear to have been detected; the precise reason for this is not known but is thought to be misalignment. The refractive index of the silicone rubber at $\lambda = 633$ nm has been more accurately determined to be $n = 1.411$ since it was reported in Ref. 6. One would therefore expect total internal reflection to occur at a plane dielectric interface for angles of incidence beyond $\arcsin(1/1.411) \simeq \pm 45.1°$; this is, in fact, observed for 40° and 60° incidence, where the detected intensity abruptly falls to zero at $\sim -45°$. The dashed curve on each graph of Fig. 2 corresponds to the refraction angle at which the transmitted light would propagate if there were no front-surface roughness.

The agreement between the experimental and numerically calculated results is excellent; particular attention is drawn to the angular position of peak trans-

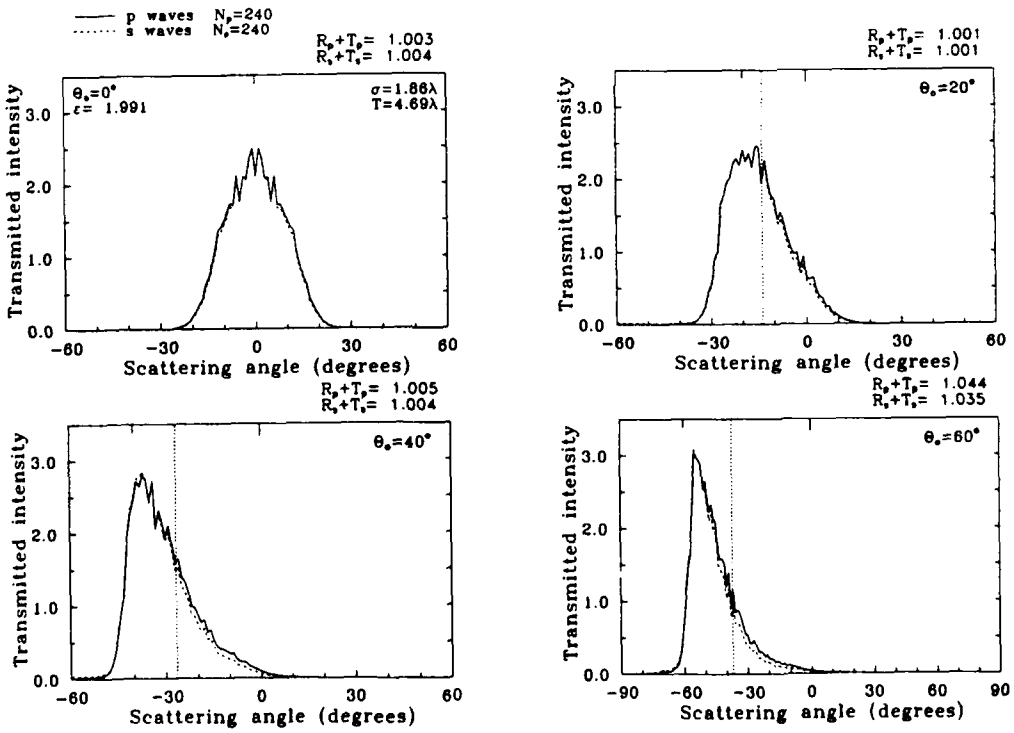

Fig. 1. Numerical calculations of transmitted intensities averaged over 240 surface samples of length $L/\lambda = 40$, correlation length $T/\lambda = 4.69$, rms deviation $\sigma/\lambda = 1.86$, and dielectric constant $\epsilon = 1.991$.

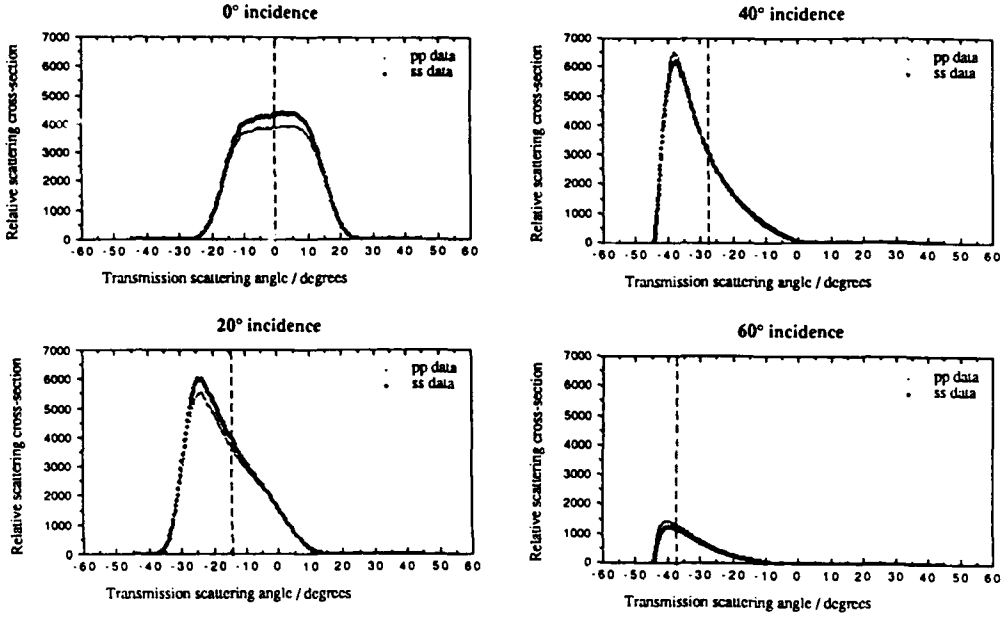

Fig. 2. Measurements of transmission envelopes scattered from a dielectric surface illuminated at a wavelength of 0.633 μm: 1/e correlation length 2.97 ± 0.05 μm, rms height 1.18 ± 0.13 μm, and refractive index 1.411.

mission and angles at which the scattered intensity falls to zero. Although for 60° incidence only a small portion of the transmitted light is detected, agreement is still good.

This research was supported by Comision Interministerial de Ciencia y Tecnologie (Grant PB0278) and the U.S. Army Research Office (DAJA45-87-C-0039). Grants from NATO and the Ministerio de Educación y Ciencia are also acknowledged. The help of J. M. Soto-Crespo is appreciated.

References

1. E. R. Méndez and K. A. O'Donnell, Opt. Commun. **61**, 91 (1987).
2. K. A. O'Donnell and E. R. Méndez, J. Opt. Soc. Am. A **4**, 1194 (1987).
3. M. Nieto-Vesperinas and J. M. Soto-Crespo, Opt. Lett. **12**, 979 (1987).
4. A. A. Maradudin, E. R. Méndez, and T. Michel, Opt. Lett. **14**, 1[illegible] (1989).
5. M. J. Firn, J. C. Dainty, A. T. Friberg, and A. J. Sant, J. Opt. Soc. Am. A **7**, 569 (1990).
6. A. J. Sant, J. C. Dainty, and M. J. Kim, Opt. Lett. **14**, 1183 (1989).
7. J. M. Soto-Crespo and M. Nieto-Vesperinas, J. Opt. Soc. Am. A **6**, 367 (1989).
8. M. Nieto-Vesperinas and J. M. Soto-Crespo, Phys. Rev. B **38**, 7250 (1988); **39**, 8193 (1989).
9. See A. Ishimaru, E. Jakeman, E. R. Méndez, K. O'Donnell, J. C. Dainty, M. J. Kim, A. J. Sant, A. A. Maradudin, T. Michel, M. Nieto-Vesperinas, J. M. Soto-Crespo, D. Maystre, and M. Saillard, in *Scattering in Volumes and Surfaces*, M. Nieto-Vesperinas and J. C. Dainty, eds. (North-Holland/Elsevier, Amsterdam, 1990).
10. A. A. Maradudin, T. Michel, A. R. McGurn, and E. R. Méndez, "Enhanced backscattering from a random grating," Ann. Phys. (to be published).
11. D. N. Pattanayak and E. Wolf, Opt. Commun. **6**, 217 (1972).

JOURNAL OF MODERN OPTICS, 1991, VOL. 38, NO. 3, 579–590

Multiple scattering from random rough surfaces using the Kirchhoff approximation

N. C. BRUCE and J. C. DAINTY
Blackett Laboratory, Imperial College,
London SW7 2BZ, England

(*Received 15 May 1990*)

Abstract. Numerical results for scattering of electromagnetic waves from a rough surface are presented and compared with experimental results. The method uses the Kirchhoff or physical optics approximation to separate the single and double scatter terms in the total scatter pattern. It is shown that enhanced backscatter occurs in the double scatter term as predicted by a simple ray picture of the scattering process.

1. Introduction

The observation of enhanced backscattering by randomly rough surfaces of large root-mean-square (r.m.s.) slope [1–4] has stimulated a re-examination of theoretical approaches to scattering by optically rough surfaces [5–18]. It is now possible, at least for a one-dimensional surface, to solve Helmholtz' equation numerically, realisation-by-realisation, to find the mean scattered intensity and its statistical properties (e.g. variance). This is a powerful method for predicting the angular distribution of the scattered intensity and has been exploited by Maradudin [8–10], Maystre [11], Nieto-Vesperinas [12–14], Thorsos [17] and others. Using this method one can predict the scattered intensity in situations where controlled experiments are difficult or tedious.

The agreement between these exact calculations and experiment, e.g. as reported in [4], is good, but not perfect. The problem with the exact method is that it gives little physical insight into the scattering process. For example, the exact method does not answer the simple question: what is the role of multiple scattering for these high-sloped surfaces? In contrast, the literature on light scattering by dense volume media [19–21], emphasizes the underlying physical processes such as multiple scattering.

The purpose of this paper is to use an approximate theory based on the Kirchhoff approximation to investigate the role of multiple scattering from randomly rough surfaces of large r.m.s. slope. A simple picture of the scattering process [1, 2] leads to the conclusion that the backscatter peak is caused by multiple scatter paths. From figure 1 the scattering paths ABC and CBA give scattered waves with a difference in phase

$$(\mathbf{k}_1+\mathbf{k}_2)\cdot\mathbf{AC}.$$

This term is zero if

$$\mathbf{k}_2=\mathbf{k}_1,$$

which is exactly the case for backscatter. Thus the backscatter terms add coherently to give a factor of two larger intensity in this direction than in other directions which

0950-0340/91 $3·00

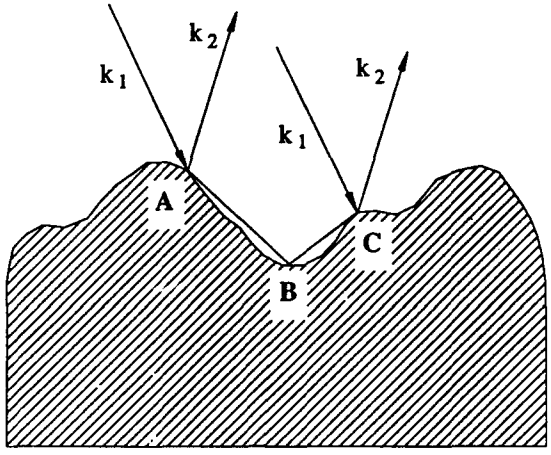

Figure 1. The geometry for the simple ray model of the scattering process showing a possible path ABC and its time reversed partner CBA.

have incoherently added terms. The width of the backscatter peak can also be estimated from this simple model. The coherent term will give no contribution when the scattered waves are π out of phase. The half width of the peak is then found to be

$$\theta_{1/2} \approx \frac{\lambda}{\langle |\mathbf{AC}| \rangle}.$$

To calculate the field scattered by a surface, first the boundary conditions on the field are used to find the field on the surface and then the scattered (usually far field) distribution of this field is found. There are two categories of solution: those based on exact boundary conditions [5, 6, 8–16, 22–28] and those based on approximate boundary conditions [7, 17, 18, 29–33].

When exact boundary conditions are used, the solution has to be found either numerically as in [5, 6, 8–16], or approximately using an appropriate expansion for the scattered field. The problem then is that it is generally very difficult to have a good physical picture of what the equations represent since the expansions of the scattered field tend to be rather complicated. This means that the methods do not give much insight into the physical mechanisms behind the resulting scattered intensity distributions, in particular whether the backscatter intensity is due to single or multiple scattering terms.

The second group of methods, in particular the Kirchhoff or physical optics methods, can however give a clear picture of the physical processes involved in the scattering. In the physical optics method the approximate boundary conditions *at each reflection point* are taken to give, in the two-dimensional case

$$E_t(x, z) = (1 + R)E_i(x, z), \tag{1}$$

$$\frac{\partial E_t(x, z)}{\partial n} = i(1 - R)\mathbf{k}_i \cdot \mathbf{n} E_i(x, z), \tag{2}$$

where $E_t(x, z)$ is the total field at the point (x, z) which is on the surface, R is the planar reflection coefficient at that point which depends on the local incidence angle, $E_i(x, z)$ is the field incident at that point, $\mathbf{k}_i$ is the incident wave-vector and $\mathbf{n}$ is the outward normal to the surface at the point (x, z). This simply states that the total field on the surface is the sum of the incident and reflected field at each point.

The scattered field is usually taken to be given by the two-dimensional Helmholtz integral equation, including the shadowing functions

$$E_s(x,z)=\frac{1}{4i}\int_r S(x',z')S'(x',z')\left(E_t(x',z')\frac{\partial H_0^{(1)}(kr)}{\partial n}-H_0^{(1)}(kr)\frac{\partial E_t(x',z')}{\partial n}\right)ds', \quad (3)$$

where $r=[(x-x')^2+(z-z')^2]^{1/2}$, $H_0^{(1)}(kr)$ is the zeroth order Hankel function of the first kind, ds' is an element of the surface and $S(x', z')$ and $S'(x', z')$ represent the incidence and scatter shadow functions respectively,

$$S(x',z')=\begin{cases}1, & \text{if } (x',z') \text{ is illuminated,}\\ 0, & \text{if } (x',z') \text{ is not illuminated,}\end{cases}$$

$$S'(x',z')=\begin{cases}1, & \text{if } (x',z') \text{ is visible,}\\ 0, & \text{if } (x',z') \text{ is not visible.}\end{cases}$$

It is important to note that these are geometrical shadowing functions and the effects of diffraction are not taken into account. The use of these straight line functions is reasonable if the distance between the blocking edge and the shadowed point is only a few wavelengths, i.e. if the shadowed point is in the Fresnel region of the blocking point, or if the distance between the source point and the blocking point is of the same order. This situation was satisfied in the cases studied with the distances being of the order of the correlation length of the surface which was typically 3λ.

The effects of the shadowing functions were discussed by Brown [33] who deduced that the incidence shadowing function was valid for the case of single scatter whereas the scatter shadow function showed unphysical behaviour. Brown suggested that the scatter shadow function causes the surface field to depend on the position of the observer when it should depend only on the incidence angle and the form of the surface profile. However, $S'(x', z')$ does not change the surface field, it changes the *observed* surface field, or rather it changes the parts of the surface (and hence the surface field distribution) which are visible. This is not unphysical. The main problem with $S'(x', z')$ can be seen from figure 1. The light scattered from point A in the direction $\hat{\mathbf{r}}_{AB}$ is blocked at point B and is re-directed. This means $S'(x', z')=0$ and the contribution from this light is neglected, i.e. the re-directed light is ignored. Therefore $S(x', z')$ in equation (3) is valid for the case of single scatter.

Hence investigations of the validity of equation (3) are therefore investigations of the validity of two separate approximations.

(i) that the total surface field and its normal derivative at each point are given by equations (1) and (2) *at each reflection* and

(ii) that the total scattered field can be approximated by the single scatter term of equation (3).

In this work only the first approximation is used; the second is not required as the second order, double scatter, term is explicitly calculated. This involves using (i) at a scatter point, propagating to another point on the surface taking shadowing into account, using (i) again at the second scatter point and then propagating to the far

zone to give the scattered field. This term is calculated for every pair of points to give the total double scatter contribution.

Obviously this second-order term suffers from the same problem as equation (3), in that there will be a scatter shadow function which will predict that light is blocked and re-directed but then that light will be ignored. However the energy carried by this light is much smaller than that carried by the double scatter term and it is reasonable to expect that any further contribution from this light will be very small. The third-order or triple-scatter has also been calculated for a few cases and is found to be negligibly small.

The surfaces considered in this work have a Gaussian probability density of height and a Gaussian correlation function. Such surfaces are manufactured in our laboratory [3, 4] using the technique of exposing a plate with a layer of photo-resist to many independent speckle patterns and then coating with gold. The experimental results used are normalised to unit area beneath the curves i.e. the material dependence of the total scattering cross-section has been removed.

There remains the question of validity of the solution obtained. Equations (1) and (2) contain the planar reflection coefficients so the solution should be valid for surfaces which are locally quite flat. This requirement is usually interpreted that the radius of curvature of the surface should be very much less than the wavelength of the incident illumination. The radius of curvature is approximately the inverse of the second derivative of the surface height distribution. As the height distribution is gaussian, so is the second derivative, with a standard deviation

$$\sigma_{h''} = 2\sqrt{3}\frac{\sigma_h}{\tau^2},$$

where σ_h is the standard deviation of the surface height distribution and τ is the $1/e$ correlation length. One of the surfaces for which data was available [4] was surface 440 with $\sigma_h \approx 1{\cdot}2\,\mu\text{m}$ and $\tau \approx 2{\cdot}9\,\mu\text{m}$, which gives $\sigma_{h''} \approx 0{\cdot}5\,\mu\text{m}^{-1}$ and thus a radius of curvature of $2\,\mu\text{m}$. Considering illumination with $\lambda = 0{\cdot}633\,\mu\text{m}$ (He–Ne) should give a case where most of the radii of curvature are greater than the wavelength and the approximation (i) is reasonably valid.

2. Theory

The single scatter term is given by equation (3), where the observation point has been taken to be in the far zone. Using the far fields of the Hankel functions

$$\lim_{r\to\infty} H_0^{(1)}(kr) = \left(\frac{2}{\pi kr}\right)^{1/2} \exp\left[\mathrm{i}\left(kR_0 - \frac{\pi}{4} - \mathbf{k}\cdot\mathbf{R}\right)\right], \tag{4}$$

$$\lim_{r\to\infty} \frac{\partial H_0^{(1)}(kr)}{\partial n} = -\left(\frac{2}{\pi kr}\right)^{1/2} \mathrm{i}\mathbf{k}\cdot\mathbf{n} \exp\left[\mathrm{i}\left(kR_0 - \frac{\pi}{4} - \mathbf{k}\cdot\mathbf{R}\right)\right], \tag{5}$$

and equations (1) and (2) gives

$$E_s(x,z) = \left(\frac{2}{\pi kr}\right)^{1/2} \frac{\exp \mathrm{i}\varphi}{4} \int_\Gamma S(x',z')S'(x',z')[(1+R)E_i(x',z')\mathbf{k}\cdot\mathbf{n}\exp(-\mathrm{i}\mathbf{k}\cdot\mathbf{R}) - (1-R)E_i(x',z')\mathbf{k}\cdot\mathbf{n}\exp(-\mathrm{i}\mathbf{k}_i\cdot\mathbf{R})]\,\mathrm{d}s', \tag{6}$$

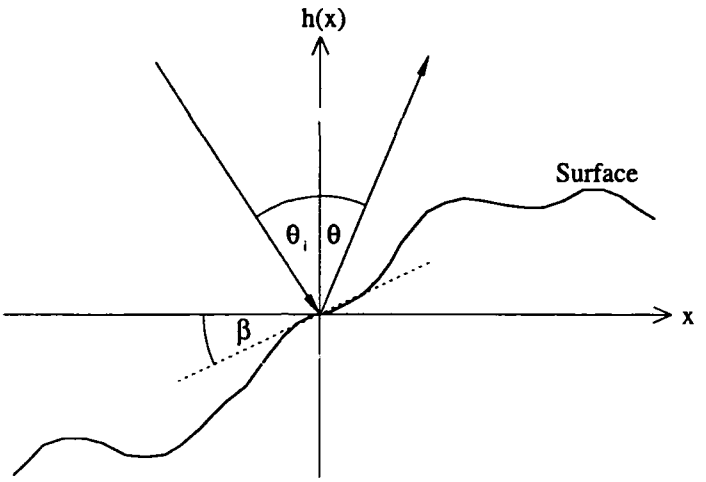

Figure 2. The geometry used for the Kirchhoff approximation. Note that the incident and scattered angles are measured in opposite senses.

where φ is $kR_0 - \pi/4$, $\mathbf{R}_0$ is the vector (x, z) and $\mathbf{R}$ is the vector (x', z'). Also (see figure 2).

$$\mathbf{k}_i = k \sin\theta_i \mathbf{x} - k\cos\theta_i \mathbf{z},$$

$$\mathbf{k} = k\sin\theta\mathbf{x} + k\cos\theta\mathbf{z},$$

$$\mathbf{n} = -\sin\beta\mathbf{x} + \cos\beta\mathbf{z},$$

$$ds = \frac{dx}{\cos\beta}, \quad \tan\beta = \frac{dh(x)}{dx} = m.$$

Then

$$E_s(\theta) = -\left(\frac{2}{\pi kr}\right)^{1/2} \frac{\exp i\varphi}{4} \int_\Gamma S(x', z')S'(x', z')[(1+R)k(m\sin\theta - \cos\theta) + (1-R)k(m\sin\theta_i + \cos\theta_i)]E_i(x', z')\exp(-i\mathbf{k}\cdot\mathbf{R})\,dx'. \quad (7)$$

The incident field is given by a plane wave

$$E_i(x', z') = A_i \exp(i\mathbf{k}_i \cdot \mathbf{R}). \quad (8)$$

Therefore, following Beckmann, equation (7) reduces to

$$E_s(\theta) = -\left(\frac{2}{\pi kr}\right)^{1/2}\left(\frac{\exp i\varphi}{4}\right) 2\left[\frac{1+\cos(\theta+\theta_i)}{\cos\theta + \cos\theta_i}\right] \times \int_\Gamma S(x', z')S'(x', z')RA_i \exp i(\mathbf{k}_i - \mathbf{k})\cdot\mathbf{R}\,dx' + e(\theta), \quad (9)$$

where $e(\theta)$ is an edge effect term which is much smaller than the first term in equation (9) and so shall be neglected.

Now the surface is discretised into N segments to simplify the integration. The phase term inside the integral is taken to be constant over each segment. This is simply a condition on the number of segments along the length of the surface, the length being small enough to neglect the phase term. Taking this and the shadow terms to have the value at the centre of each segment gives

$$E_s(\theta) = -\left(\frac{2}{\pi kr}\right)^{1/2}\left[\frac{\exp(i\varphi)}{4}\right]2\left[\frac{1+\cos(\theta+\theta_i)}{\cos\theta+\cos\theta_i}\right] \times \sum_{j=1}^{N} RS(x_j', z_j')S'(x_j', z_j')\exp[i(\mathbf{k}_i-\mathbf{k})\cdot\mathbf{R}_j]\int_{(j-1)\Delta x}^{j\Delta x} A_i\,dx', \quad (10)$$

with the surface split into N segments of equal x-distance Δx. Assuming a small enough value of surface segment length Δx gives

$$\int_{(j-1)\Delta x}^{j\Delta x} A_i\,dx' = A_i\Delta x.$$

Considering an incident plane wave of unit amplitude, $A_i = 1$, finally gives

$$E_s(\theta) = -\left(\frac{2}{\pi kr}\right)^{1/2}\left[\frac{\exp(i\varphi)}{4}\right]2\left[\frac{1+\cos(\theta+\theta_i)}{\cos\theta+\cos\theta_i}\right] \times \sum_{j=1}^{N} RS(x_j', z_j')S'(x_j', z_j')\exp[i(\mathbf{k}_i-\mathbf{k})\cdot\mathbf{R}_j]\Delta x. \quad (11)$$

This is the usual single scatter term taken to be the solution for the physical optics approximation.

Now consider the double scatter contribution. To find this term the field obtained by scattering the incident field from one point on the surface to another point on the surface must be found, and then this field at any surface point due to light scattered from all the other surface points is

$$E_s(x_2, z_2) = -\frac{1}{4i}\int_\Gamma S(x_1, z_1)S_{12}\left\{(1+R_1)\left[m_1\frac{k(x_2-x_1)}{r_{12}} - \frac{k(z_2-z_1)}{r_{12}}\right]H_1^{(1)}(kr_{12}) - (1-R_1)ik(m_1\sin\theta_i+\cos\theta_i)H_0^{(1)}(kr_{12})\right\}E_i(x_1, z_1)\,dx_1, \quad (12)$$

where the subscript 2 represents the second point and subscript 1 the first point, $r_{12} = [(x_2-x_1)^2+(z_2-z_1)^2]^{1/2}$, the normal derivative of the Hankel function is given by

$$\frac{\partial H_0^{(1)}(kr_{12})}{\partial n} = \left[n_x\frac{k(x_2-x_1)}{r_{12}} + n_z\frac{k(z_2-z_1)}{r_{12}}\right]H_1^{(1)}(kr_{12}), \quad (13)$$

and the shadow function S_{12} is defined as

$$S_{12} = \begin{cases} 1, & \text{if } (x_2, z_2) \text{ is visible from } (x_1, z_1), \\ 0, & \text{if } (x_2, z_2) \text{ is not visible from } (x_1, z_1). \end{cases}$$

The field scattered from all these second points will then be the double scatter term

$$E_s^{[2]}(\theta) = -\left(\frac{2}{\pi kr}\right)^{1/2} \frac{\exp(i\varphi)}{4} \int_\Gamma S'(x_2, z_2) \left[(1+R_2)k(m_2 \sin\theta - \cos\theta) E_s(x_2, z_2) + i(1-R_2) \frac{\partial E_s(x_2, z_2)}{\partial n_2} \right] \exp(i\mathbf{k}\cdot\mathbf{R}_2)\, dx_2. \quad (14)$$

Equations (12) and (14) together form the double-scatter term. The general form of this term can be seen to be rather complicated. However, if p-polarised (TM) light incident on a perfectly conducting rough surface is considered, $R=1$ for both points 1 and 2. Then writing

$$S''_{12} = S(x_1, z_1) S_{12} S'(x_2, z_2),$$

$$E_s^{[2]}(\theta) = -\left(\frac{2}{\pi kr}\right)^{1/2} \frac{\exp(i\varphi)}{4i} \int_\Gamma \int_\Gamma S''_{12} \left[m_1 \frac{k(x_2 - x_1)}{r_{12}} - \frac{k(z_2 - z_1)}{r_{12}} \right] \times H_1^{(1)}(kr_{12}) k(m_2 \sin\theta - \cos\theta) \exp[i(\mathbf{k}_i - \mathbf{k})\cdot\mathbf{R}_2]\, dx_2\, dx_1. \quad (15)$$

For the discretisation in this case if it is assumed that dx is small enough compared to λ that it is possible to simply replace each integral with the sum of the values at the centre point of each segment multiplied by Δx

$$E_s^{[2]}(\theta) = -\left(\frac{2}{\pi kr}\right)^{1/2} \frac{\exp(i\varphi)}{4i} \sum_{j=1}^{N} \sum_{l=1}^{N} S''_{jl} \left[m_j \frac{k(x_l - x_j)}{r_{lj}} - \frac{k(z_l - z_j)}{r_{lj}} \right] \times H_1^{(1)}(kr_{lj}) k(m_l \sin\theta - \cos\theta) \exp[i(\mathbf{k}_i - \mathbf{k})\cdot\mathbf{R}_l]\, \Delta x\, \Delta x. \quad (16)$$

Similarily for s-polarisation (TE), $R=-1$ at both points and the term obtained is

$$E_s^{[2]}(\theta) = -\left(\frac{2}{\pi kr}\right)^{1/2} \frac{\exp(i\varphi)}{4i} \sum_{j=1}^{N} \sum_{l=1}^{N} S''_{jl} \left[m_l \frac{k(x_l - x_j}{r_{lj}} - \frac{k(z_l - z_j)}{r_{lj}} \right] \times H_1^{(1)}(kr_{lj}) k(m_j \sin\theta_i + \cos\theta_i) \exp[i(\mathbf{k}_i - \mathbf{k})\cdot\mathbf{R}_l]\, \Delta x\, \Delta x. \quad (17)$$

To obtain this result the following approximation was used

$$\frac{\partial}{\partial n_l} \int_\Gamma S(x_1, z_1) S_{jl} k(m_j \sin\theta_i + \cos\theta_i) E_i(x_j, z_j) H_0^{(1)}(kr_{lj})\, dx_j \approx \int_\Gamma S(x_1, z_1) S_{jl} k(m_j \sin\theta_i + \cos\theta_i) E_i(x_j, z_j) \frac{\partial H_0^{(1)}(kr_{lj})}{\partial n_l}\, dx_j, \quad (18)$$

i.e. the normal derivative of the shadow function S_{jl} is ignored. The effect of this approximation on the final result is not known.

Once the field as a function of angle is known the power per unit angle at the far field is given by

$$J(\theta) = \lim_{r\to\infty} r|E_s(\theta)|^2. \quad (19)$$

For a perfect conductor $R=1$ for p-polarisation and -1 for s-polarisation, therefore from (11) the modulus of the single scatter term is the same for both polarisations. The double-scatter term, however, is different for the two cases, (16) for p and (17)

for s polarisation. The sum of the single and double contributions, the 'total' power is obtained from

$$J_t(\theta) = \lim_{r\to\infty} r|E_s(\theta) + E_s^{[2]}(\theta)|^2. \tag{20}$$

In this case the sign of the single-scatter term is very important and leads to a difference in the total scattered intensity distribution.

A test of the reliability of any method for calculating the scattered field is the unitarity or the power scattered divided by the incident power. This is given by

$$U(\theta_i) = \frac{\int_\theta J_t(\theta')\,d\theta'}{N\,dx\cos\theta_i}. \tag{21}$$

3. Results

The equations for the single and double-scatter terms for a perfectly conducting rough surface with the parameters given in the introduction were programmed into a computer. To reduce speckle noise on the resulting solutions the angular distribution of intensity was averaged over many (typically 1000) different realisations of the surface profile all with the same statistical properties. The relative amount of energy, the unitarity, in the single, double and single + double terms is shown in the table for both polarisations. From this table it can be seen that, perhaps surprisingly, the double-scatter term decreases with increasing angle of incidence, the single scatter increases and that virtually all of the scattered energy is contained in these terms. It also appears that the rate of decrease of the amount of energy in the second-order term increases with increasing angle, for s-polarisation.

The angular distribution of the scattered light is shown in figures 3 and 4 and the results are compared with experimental curves in figures 5 and 6. Experimental results are represented by the circles. There are a number of features to note about these results. First the double-scatter term has negligible values at high scatter angles (higher than $\pm 60°$) so this is the region where the single scatter dominates, i.e. the usual single scatter physical optics approximation value is closer to the actual scattered field at these higher angles.

	s-polarisation (TE)		
Incidence	Single	Double	Total
0°	0·841	0·139	0·977
10°	0·852	0·142	0·990
20°	0·855	0·135	0·987
40°	0·886	0·088	1·007

	p-polarisation (TM)		
Incidence	Single	Double	Total
0°	0·832	0·156	0·985
10°	0·846	0·141	0·983
20°	0·856	0·123	0·975
40°	0·890	0·098	1·014

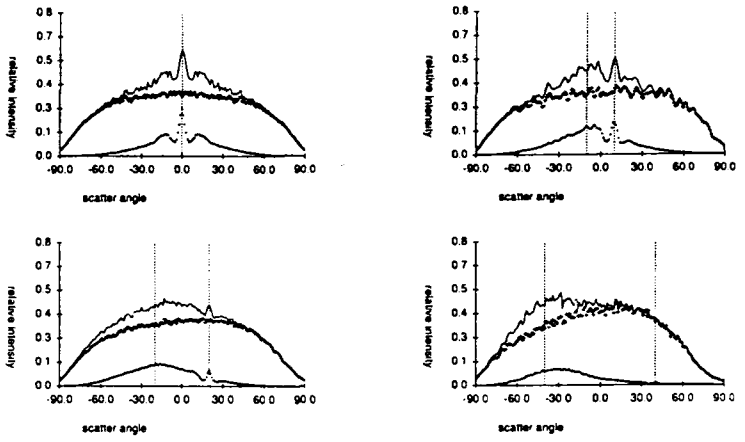

Figure 3. The single (+ + +), double (•••), and single plus double (—) contributions from surface number 440 with s-polarisation incident. The backscatter angles are marked by the dashed lines to the right of the graphs. The number of frames averaged over are (*a*) 2000 at 0°, (*b*) 1000 at 10°, (*c*) 2000 at 20° and (*d*) 1000 at 40°.

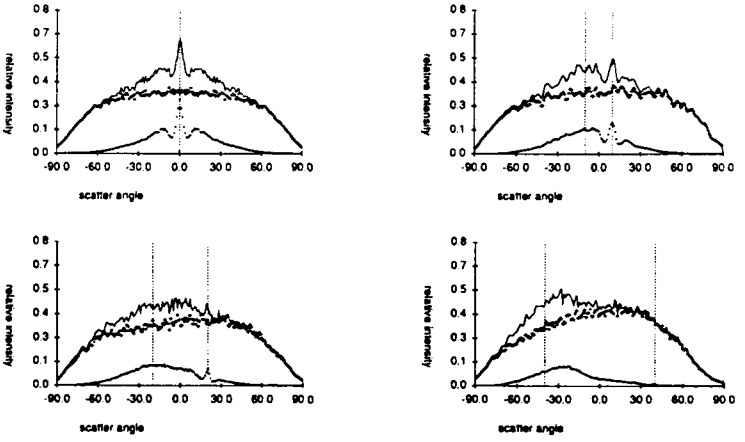

Figure 4. As figure 3 but for p-polarisation incident.

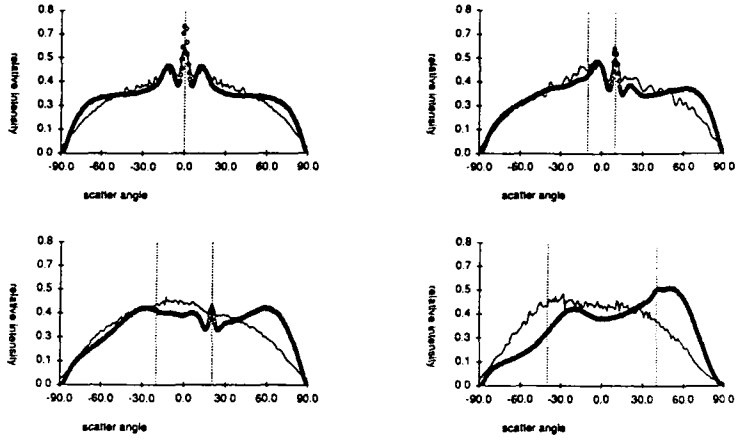

Figure 5. Comparison of single plus double (—) and experimental (○○○) curves for surface number 440 with s-polarisation incident.

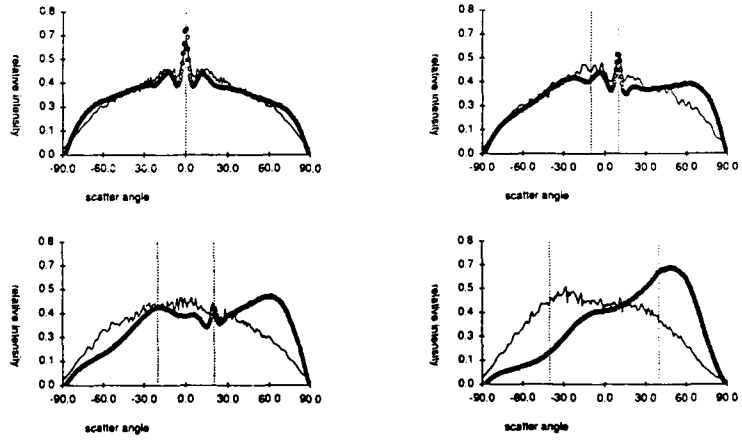

Figure 6. As figure 5 but with p-polarisation incident.

Secondly there is no narrow peak in the single scatter term but there is in the double-scatter one. This peak occurs at the backscatter angle and there are signs of side lobes on either side of this peak. Taking the intensity at the maximum of the peak and dividing by the intensity at the same angle of the curve obtained by simply drawing a smooth line joining the parts of the curve away from the peak gives a factor of roughly two. This is the factor predicted by the simple picture of the scattering process involving the coherent addition of waves in the backscatter direction. It is important to note that the factor of two enhancement is in the double scatter term *not* the total term. Again this is predicted in the simple picture which requires multiple scattering to have coherent interference for the retro-reflected light. Obviously this means that the enhancement factor in the total scatter curve will be less than two in this roughness region ($\tau/\sigma_h \approx 2{\cdot}4$) as the single scatter is not zero at this angle. It may be that the factor in the total scatter term can be used to somehow give a measure of the 'roughness' of a surface since as the roughness is increased there will be less single scatter and more multiple scatter giving a larger enhancement.

Another point which is apparent is that since the amount of double scatter decreases and the double scatter curve has smaller values at the backscatter angle as the incidence angle is increased, the size of the peak and hence the enhancement factor decreases with increasing angles of incidence.

4. Future work

Work is progressing on extending the method to the triple-scatter or third-order term and also to the double-scatter term from dielectric surfaces. The second-order dielectric term is much more complicated than the perfect conductor since light can travel through the material and then scatter away from the surface, i.e. light can travel between grooves which would be hidden from each other considering the usual shadowing term.

Acknowledgments

NCB thanks the UK Science and Engineering Research Council (SERC) for a studentship in collaboration with the Royal Signals and Radar Establishment, Malvern. JCD is an SERC senior research fellow. This research is supported by the US Army Research Office (DAJA45-87-C-0039) and SERC (GR/F 81651).

References

[1] Mendez, E. R., and O'Donnell, K. A., 1987, *Optics Commun.*, **61**, 91.
[2] O'Donnell, K. A., and Mendez, E. R., 1987, *J. opt. Soc. Am.* A, **4**, 1194.
[3] Sant, A. J., Kim, M.-J., and Dainty, J. C., 1989, *Optics Lett.*, **14**, 1183.
[4] Kim, M.-J., Dainty, J. C., Friberg, A. T., and Sant, A. J., 1990, *J. opt. Soc. Am.* A, **7**, 569.
[5] Bahar, E., and Fitzwater, M. A., 1987, *Optics Commun.*, **63**, 355.
[6] Bahar, E., and Fitzwater, M. A., 1989, *J. opt. Soc. Am.* A, **6**, 33.
[7] Jin, Ya-Qiu, 1988, *J. appl. Phys.*, **63**, 1286.
[8] Maradudin, A. A., Mendez, E. R., and Michel, T., 1989, *Optics Lett.*, **14**, 151.
[9] Maradudin, A. A., Michel, T., McGurn, A. R., and Mendez, E. R., 1990, *Ann. Phys.*, **203**, 255.
[10] Lu, Jun Q., Maradudin, A. A., and Michel, T., 1991, *J. opt. Soc. Am.* B, 982.
[11] Saillard, M., and Maystre, D., 1990, *J. opt. Soc. Am.* A, **7**, 982..
[12] Nieto-Vesperinas, M., and Soto-Crespo, J. M., 1987, *Optics Lett.*, **12**, 979.
[13] Soto-Crespo, J. M., and Nieto-Vesperinas, M., 1989, *J. op.. Soc. Am.*, A, **6**, 367.

[14] NIETO-VESPERINAS, M., and SOTO-CRESPO, J. M., 1990, *Optics Commun.*, **75**, 215.
[15] SOTO-CRESPO, J. M., and NIETO-VESPERINAS, M., 1988, *Optics Commun.*, **69**, 185.
[16] NIETO-VESPERINAS, M., and SOTO-CRESPO, J. M., 1988, *Phys. Rev.* B, **39**, 8193.
[17] THOROS, E. I., 1988, *J. acoust. Soc. Am.*, **83**, 78.
[18] THOROS, E. I., and JACKSON, D. R., private communication (informal report presented at a Workshop on Enhanced backscatter, Boston University, 28–29 July, 1989).
[19] TSANG, L., and ISHIMARU, A., 1984, *J. opt. Soc. Am.* A, **1**, 836.
[20] WOLF, P. E., AKKERMANS, E., MAYNARD, R., and MARET, G., 1988, *J. Phys.*, Paris, **49**, 63.
[21] JOHN, S., 1988, *Comments Cond. Mat. Phys.*, **14**, 193.
[22] NIETO-VESPERINAS, M., and GARCIA, N., 1981, *Optica Acta*, **28**, 1651.
[23] BROWN, G. S., 1984, *I.E.E.E. Trans. Antennas Propag.*, **32**, 1308.
[24] JAKEMAN, E., and HOENDERS, B. J., 1982, *Opt. Acta*, **29**, 1587.
[25] BROWN, G. S., 1982, *I.E.E.E. Trans. Antennas Propag.* **30**, 1135.
[26] RICE, S. O., 1951, *Commun. Pure and Appl. Math.*, **4**, 351.
[27] SCHIFFER, R., 1987, *Appl. Opts.*, **26**, 704.
[28] WINEBRENNER, D., and ISHIMARU, A., 1985, *Radio Sci.*, **20**, 161.
[29] BECKMANN, P., and SPIZZICHINO, A., 1963, *The Scattering of Electro-magnetic Waves from Rough Surfaces* (New York: Pergamon).
[30] WAGNER, R. J., 1966, *J. acoust. Soc. Am.*, **41**, 138.
[31] BROCKELMANN, R. A., and HAGFORS, T., 1966, *I.E.E.E. Trans. Antennas Propag.*, **14**, 621.
[32] SANCER, M. I., 1969, *I.E.E.E. Trans. Antennas Propag.* **17**, 577.
[33] BROWN, G. S., 1984, *Radio Sci.*, **19**, 1461.

CHAPTER 15

The Opposition Effect in Volume and Surface Scattering

J. C. Dainty
Blackett Laboratory
Imperial College
London, UK

1. Introduction

In recent years, there has been renewed interest in the so-called *opposition effect*. This term refers to the enhanced intensity that is observed exactly in the backscatter or retro-reflection direction when certain volume and surface scatterers are illuminated with parallel light; it also is referred to sometimes as *enhanced backscattering*. There are many media that exhibit the opposition effect, such as paper, white paint, and even the surface of the moon. (The moon really *is* brighter when it is full [1,2].) Materials used for diffuse reflectance standards, such as barium sulphate, also show the opposition effect. A similar phenomenon can be seen from scattering by clouds (the "glory" or "spectre of the Brocken" [3]), although the mechanism in this case is not the same as that for the examples discussed in this chapter. Figure 1 shows the effect for the case of scattering of a linearly polarised beam by a dense suspension (about 10% by volume) of latex spheres in water. The upper half shows a photograph taken in the backscatter direction and the lower half shows the co- and cross-polarised intensity as a function of scattering angle. The peak intensity in the backscatter direction in this case is up to twice that of the local background.

Observation of the effect is well-documented [4], but it is only recently that the mechanisms have begun to be understood. In this chapter, we

ISBN 0-12-289690-4

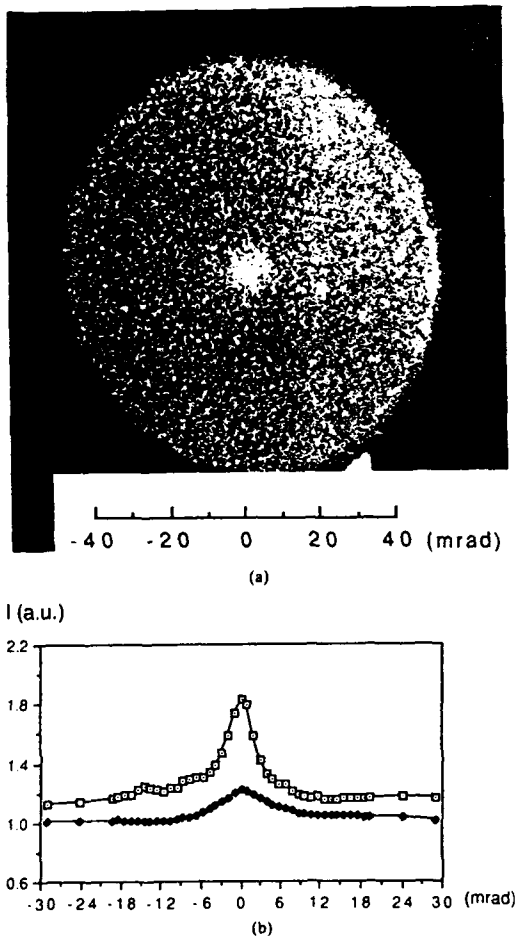

FIG. 1. Enhanced backscattering (opposition effect) by a dense suspension of latex spheres in water (Fig. 2 of *D N Qu* and J. C. Dainty, *Opt. Lett.* 13, 1066–1068, 19[illegible]). The upper photograph is taken in the backscatter direction (co-polarised component) and the lower half shows the co- and cross-polarised intensities as a function of the scattering angle.

concentrate on one particular mechanism, the coherent co-operative effect of multiple scattering. This probably is the dominant mechanism for dense scatterers like white paint, but in other cases, there are geometrical optics effects, such as focussing, that also can give enhancement. To give some structure to the chapter, I shall discuss the cases of dense volume media, randomly rough surfaces, and double passage through a random screen in separate sections; the key unifying feature in all three cases is the occurrence of *multiple scattering*.

2. Scattering by Dense Volume Media

The scattering by many *surfaces* such as paper and paint is, in fact, predominantly a volume effect. To understand the scattering process, experiments often are carried out using controlled concentrations of monosized latex spheres suspended in water [5]. Although the opposition effect has been documented since early this century, in recent times the experiments of three groups [6–8] have resulted in a renaissance of the subject. (See [9] and [10] as a starting point for the literature.) The reason for this is not so much the importance of the opposition effect itself, but that the cause of it—multiple scattering— has other fascinating effects—in particular, the possibility of the localisation of photons in a disordered medium.

The basic mechanism for enhanced backscattering is illustrated in Fig. 2. If a linearly polarised plane wave is incident on a random medium, then a *ray* undergoing multiple scattering with particles $1, 2, 3 \ldots N$ has precisely the same complex amplitude as one interacting with $N \ldots 3, 2, 1$; the two *rays* are coherent and thus interfere constructively, giving an intensity up to twice that of the local background, where there are no such coherent effects. A more rigorous description defines each scattering event by a

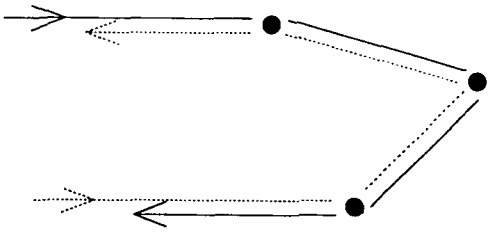

FIG. 2. Basic multiple-scattering explanation of the opposition effect forward and reverse *rays* interfere constructively in the backscatter direction.

matrix equation, in which an incident polarisation vector is multiplied by the scattering matrix to yield the polarisation vector of the scattered light. Using this approach, one can show that the co-polarised multiple-scattered light is enhanced by a factor of two, but the cross-polarised forward and reverse paths only are partially coherent and give an enhancement factor less than two: in fact, as the degree of multiple scattering increases, the enhancement factor tends to unity for the cross-polarised case.

The width of the enhancement peak is related to the mean transport length of photons in the medium. Long paths give a contribution to the enhancement at very small angles, whereas shorter paths contribute over a wider range of angles. Thus, the shape of the enhancement peak gives information on the length of light paths in the medium. The path lengths also are contained in the polarisation behaviour, since, for the cross-polarised case, the degree of correlation between the forward and reverse paths decreases with increased order of scattering. The path lengths also can be probed directly using femtosecond pulses and observing their broadening after scattering.

The energy in the backscatter peak is very small indeed compared to the total scattered energy in all other directions, so, from an applied point of view, one could reasonably ask: Why is there all this fuss (over 100 publications in the past five years, symposia and workshops, etc.) over such a small effect? The reason probably is the following: The opposition effect is the result of scattering mechanisms that hitherto have been ignored almost completely and that could have profound influence on our understanding of the interaction of classical waves with disordered matter. Electrons can be *localised* in a medium if there is a certain degree of disorder and, in particular, if the mean free path of the electron is less than $\lambda/2\pi$, where λ is the electron wavelength. If one could make such a medium for visible electromagnetic waves, light inside would be *trapped*, and from the outside, such a medium would be a perfect reflector. It is still not clear whether, in fact, such a medium can exist for electromagnetic waves, but the first step, that of weak localisation, has been observed in the manifestation of the opposition effect.

3. Scattering by Randomly Rough Surfaces

There is an enormous amount of literature on the elastic scattering of electromagnetic radiation by randomly rough surfaces. Because an exact general solution of Maxwell's equations cannot be found for this problem, the theoretical treatments have tended to focus on approximate solutions, mainly using perturbation theory or the Kirchhoff boundary condition. For surfaces that are rough compared to the wavelength, virtually all theoretical work, until recently, has assumed single scattering. Experimental work

on rough surface scattering has suffered from the fact that the detailed surface statistics frequently are unknown and thus, the measurements are only of empirical value; measurements made on poorly defined surfaces are of no value for checking the validity of approximate theories.

In 1987, E. R. Mendez and K. A. O'Donnell carried out some of the first optical scattering measurements on well-defined surfaces with relatively simple statistical properties [11, 12]. These surfaces were made by exposing photoresist to laser-produced speckle patterns whose statistics are well understood [13]; the surfaces can be coated with metal, typically gold, or replicated to form dielectric or metallised copies [14]. Using this technique, surfaces with a Gaussian probability density of surface height and a Gaussian auto-correlation function can be produced so that, for the first time, surface scattering experiments directly relevant to theory can be performed.

Some of the first experiments conducted by Mendez and O'Donnell were on surfaces of root-mean-square (rms) surface height equal to approximately two wavelengths and correlation length five wavelengths, i.e., surfaces with fairly large rms slope that should exhibit multiple scattering. Figure 3 shows one set of angular scattering curves for a one-dimensional version of such a surface [15] Note the opposition-effect peak in the backscatter direction. This has the same origin precisely as the peak produced by scattering from dense random media; forward and reverse ray paths are coherent and thus interfere.

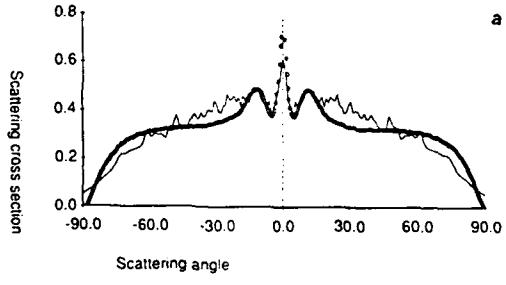

FIG. 3. Angular scattering of light from a one-dimensional gold-coated randomly rough surface of root-mean-square height fluctuation $\sigma = 1.2 \pm 0.1\mu m$ and Gaussian correlation function of 1/e length $2.9 \pm 0.2\mu m$ (Fig 8 of [15]). The angles of incidence are (a) 0°, (b) -10°, (c) -20°, and (d) -40°, and the incident light is s-polarised (TE) The circles are experimental measurements and the jagged line the result of an *exact* calculation for a perfect conductor based on direct numerical solution of the Helmholtz equation. Note the enhanced backscatter peak (opposition effect) in the backscatter half-plane on the right hand side of each graph.

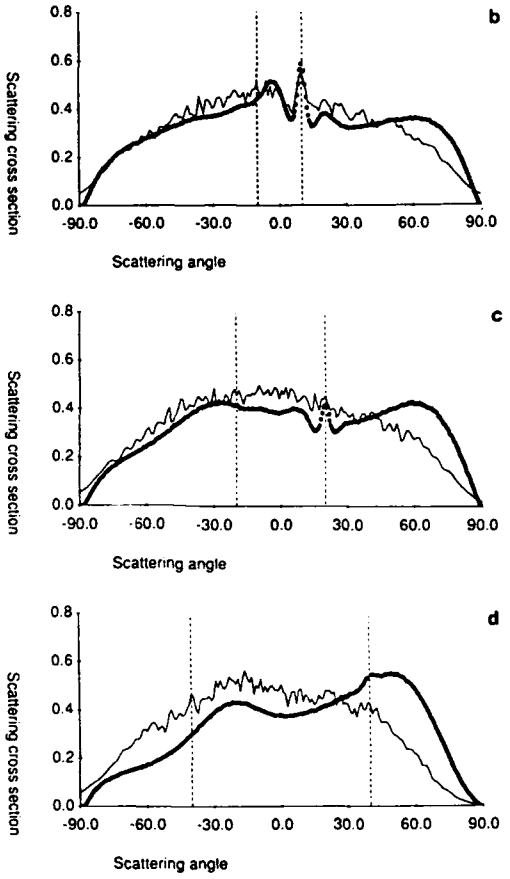

FIG. 3. (*Continued*)

Prior to the experimental work of Mendez and O'Donnell, the opposition effect was unknown in true surface scattering. (Here, we ignore the penetration depth of the wave in a metal, which is on the order of 80Å for visible light and a gold surface.) Their work has stimulated a large number of groups to search for a more "rigorous" explanation of the enhanced backscatter peak; electromagnetic theorists are not very fond of rays! Unfortunately, no analytical solution exists and thus one has to resort to — or exploit—numerical techniques. These give quite good agreement with the measurements [15–18], but otherwise give little physical insight to the nature of the scattering. Figure 3 shows the result of an "exact" numerical calculation for a perfect conductor based on the Helmholtz equation. The agreement is fair, although there is a significant discrepancy at higher angles. (This almost certainly is *not* due to the fact that the calculations are for a perfect conductor, whereas the experiments were done on gold-coated surfaces.)

An alternative approach is to adapt a theory based on approximate boundary conditions, such as the Kirchhoff or *physical optics* theory, to multiple scattering. Figure 4 shows the result of such a calculation carried

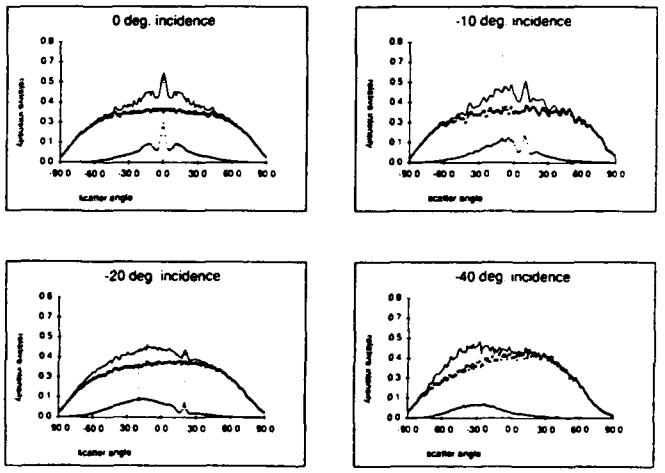

FIG. 4. The single (+++), double (***) and single+double (----) contributions to the angular distribution of scattered light for *s*-polarisation incident, for the same surface parameters as those in Fig. 3, calculated using a double-scattering version of the Kirchhoff approximation.

(a)

(b)

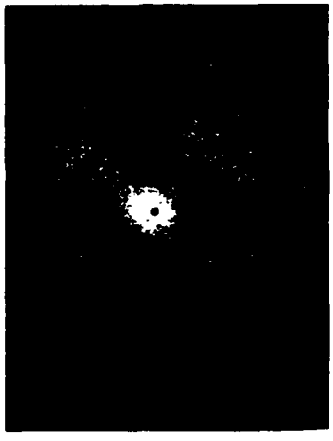

(c)

FIG. 5. Photographs of the backscattered intensity from a two-dimensional randomly rough surface taken (a) with no analyser, (b) through an analyser parallel to the incident polarisation, and (c) with the analyser perpendicular to the incident polarisation (courtesy of E. R. Mendez and K. A. O'Donnell).

out to a double-scattering approximation (including shadowing) for a perfectly conducting surface of the same parameters as that in Fig. 3, illuminated by *s*-polarised (TE) light of wavelength 0.63 μm at normal incidence. The enhanced backscatter peak shows only in the double-scatter term, providing strong support of the ray theory that emphasises the crucial role of multiple scattering.

One important difference between the surface and volume scattering cases is that, in the surface case, only low-order multiple scattering occurs, mainly just second order. This means that the co- and cross-polarised contributions to the enhanced backscatter peak are equally large. For two-dimensional rough surfaces, there are strong polarisation effects. Figure 5 shows photographs of the backscattered light for a surface illuminated by linearly polarised light and viewed (a) with no analyser, (b) with the analyser parallel to the incident electric vector, and (c) with it perpendicular to the incident electric vector. The effect is very striking when observed: as the analyser is rotated through 90°, the scattering pattern appears to rotate 45°. Again, a simple ray argument seems to explain the observations [12].

As with the case of scattering by dense volume media, it is not the opposition effect itself that is particularly important— although it is a fascinating and unusual phenomenon—but, more significantly, the fact that it encourages us to question the *accepted* treatments of a subject. For example, one hears reference to Lambertian scattering surfaces, but it seems certain now that such a thing simply is a figment of the imagination and not realisable by any real surface, because of multiple scattering. Likewise, the angular scattering curves of Fig. 3 are quite remarkable, even ignoring the enhanced backscatter peak; for example, the existence of a large component of light scattered in the backscatter half-space at angles greater than the incident angle is unexpected and counterintuitive.

4. Double Passage through a Random Screen

There is an extensive amount of literature on the double passage of light through turbulence. (See [19] for a partial list.) By analogy with the above cases of surface and volume scattering, one expects to observe the opposition effect, and this has been reported [20, 21]. A practical consequence of this is that diffraction-limited information is present in the average image of a deterministic object that is illuminated and viewed through the same distorting medium. As an example of this, we consider the simplest case, that of a Michelson or two-slit interferometer illuminating and viewing an object through a random (phase) screen, as in Fig. 6.

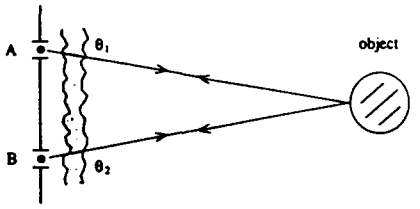

FIG. 6. Double-passage imaging with a Michelson interferometer.

Again, we consider a simple ray approach to explain why diffraction-limited information is present in the image of a point object. Consider light transmitted through slit A towards the object. It accumulates a random phase θ_1 on its passage through the random screen and then is scattered in all directions by the point object. That portion of the light that returns through slit A has a random phase $2\theta_1$ and does not contribute to the diffraction-limited process. However, another portion of the light travels to slit B, accumulating a total random phase of $\theta_1 + \theta_2$. Now consider light that is emitted from slit B. This also will accumulate a total random phase of $\theta_1 + \theta_2$ by the time it arrives at slit A and thus, constructive interference will occur between the forward (A to B) and reverse (B to A) waves. This constructive interference is superimposed on a background level caused by the other paths A to A and B to B.

Figure 7 shows a computer simulation of the fringes in a Michelson interferometer viewing a point source for (a) no random screen, (b) double passage through different random screens (2,000 realisations), and (c) double passage through the same random screen; (d), (e), and (f) show the Fourier transforms of (a), (b), and (c), respectively. Note the high contrast fringes formed in (c) and corresponding side-bands in (f), of magnitude one-half that of the no-random-screen case.

This technique can be generalised to non-redundant and filled imaging pupils [19, 22], with corresponding reductions in fringe visibility.

5. Discussion

The increased understanding of the opposition effect over the past five years has had an impact in at least three areas of physics. First, the importance of multiple scattering has been exposed: this has a profound importance for the behaviour of light in dense scattering media, and may lead to the phenomenon of photon localisation in disordered structures. Dense random media are a new type of scattering that may, in fact, be the

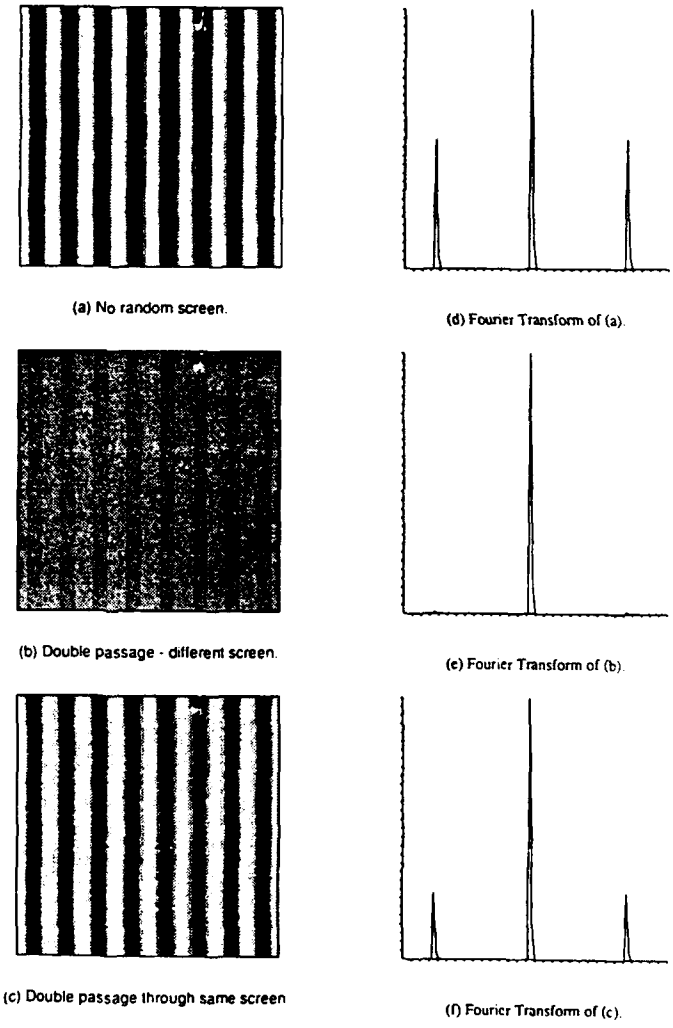

FIG. 7. Computer simulation of the fringes formed in a double-passage Michelson interferometer.

first *natural* random structure to show the unusual spectral shifts predicted by E. Wolf [23, 24].

Secondly, the opposition effect from well-defined surfaces has led to renewed theoretical studies, mainly using numerical techniques. Considering that this effect for true surface scattering was not predicted prior to its experimental discovery in 1987, it is quite amusing to observe that almost every study of light scattering is now considered incomplete without a discussion of it! Thirdly, it is becoming clear that the opposition effect—or more precisely, multiple scattering—has applications in areas other than scattering in volumes and surfaces. The example of the double passage of light through a random screen is one illustration of this, and doubtless there will be others in the future.

Acknowledgments

I am very grateful to my former and current research students, A. S. Harley, M. J. Kim, A. J. Sant, and N. Bruce, and international colleagues A. A. Maradudin, D. Maystre, E. R. Mendez, M. Nieto-Vesperinas, and K. A. O'Donnell for their contributions to this area of my research over the past few years.

References

1. N. Barabascheff, "Bestimmung der Erdalbedo und des Reflexionsgesetzes für die Oberflache der Mondmeere: Theorie der Rillen," *Astron Nachr* **217**, 445–452 (1922).
2. P. Oetking, "Photometric Studies of Diffusely Reflecting Surfaces with applications to the Brightness of the Moon," *J Geophy Res* **71**, 2505–2513 (1966).
3. M. Minnaert, *The Nature of Light and Colour in the Open Air*, Dover Press, 1954.
4. W. W. Montgomery and R. H. Kohl, "Opposition-effect experimentation," *Opt Lett* **5**, 546–548 (1980).
5. Obtainable from, for example, Sigma Chemical Company, Fancy Road, Poole, Dorset BH17 7NH, UK as Product Number LB-5.
6. Y. Kuga and A. Ishimaru, "Retro-Reflectance from a Dense Distribution of Spherical Particles," *J Opt Soc Am A* **1**, 831–835 (1984).
7. M. P. van Albada and A. Lagendijk, "Observation of Weak Localisation of Light in a Random Medium," *Phys Rev Lett* **55**, 2692–2695 (1985).
8. P. E. Wolf and G. Maret, "Weak Localisation and Coherent Backscattering of Photons in Disordered Media," *Phys Rev Lett* **55**, 2696–2699 (1985).
9. P. E. Wolf, G. Maret, E. Akkermans, and R. Maynard, "Optical Coherent Backscattering by Random Media," *J Phys* (Paris) **49**, 63–75 (1988).
10. P. Sheng (editor), "Scattering and Localisation of Classical Waves in Random Media, World Scientific Press (Singapore), 1990.
11. E. R. Mendez and K. A. O'Donnell, "Observation of Depolarisation and Backscattering Enhancement in Light Scattering from Gaussian Rough Surfaces," *Opt Common* **61**, 91–95 (1987).
12. K. A. O'Donnell and E. R. Mendez, "Experimental Study of Scattering from Characterised Rough Surfaces," *J Opt Soc Am A* **4**, 1194–1205 (1987).
13. J. W. Goodman, *Statistical Optics*, Wiley, 1985.

14. A. J. Sant, M.-J. Kim, and J. C. Dainty, "Comparison of Surface Scattering between Identical, Randomly Rough Metal and Dielectric Diffusers," *Opt. Lett.* **14**, 1183–1185 (1989).
15. M.-J. Kim, J. C. Dainty, A. T. Friberg, and A. J. Sant, "Experimental Study of Enhanced Backscattering from One- and Two-Dimensional Random Rough Surfaces," *J. Opt. Soc. Am. A*, **7**, 569–577 (1990).
16. J. M. Soto-Crespo and M. Nieto-Vesperinas, "Electromagnetic Scattering from Very Rough Random Surfaces and Deep Reflection Gratings," *J. Opt. Soc. Am. A* **6**, 367–384 (1989).
17. A. A. Maradudin, T. Michel, A. R. McGurn, and E. R. Mendez, "Enhanced Backscattering by a Random Grating," *Ann. Phys.* **203**, 255–307 (1990).
18. M. Saillard and D. Maystre, "Scattering from Metallic and Dielectric Rough Surfaces," *J. Opt. Soc. Am. A* **7**, 982–990 (1990).
19. T. Mavroidis and J. C. Dainty, "Imaging after Double Passage Through a Random Screen," *Op. Lett.* **15**, 857–859 (1990).
20. Yu. A. Kratsov and A. I. Saichev, "Effects of Double Passage of Waves in Randomly Inhomogeneous Media," *Sov. Phys. Usp.* **25**, 494–508 (1982).
21. P. R. Tapster, A. R. Weeks, and E. Jakeman, "Observation of Backscattering Enhancement through Atmospheric Phase Screens," *J. Opt. Soc. Am. A* **6**, 517–522 (1989).
22. T. Mavroidis, C. J. Solomon, and J. C. Dainty, "Imaging a Coherently Illuminated Object after Double Passage through a Phase Screen," *J. Opt. Soc. Am.* (in press).
23. A. Lagendijk (private communication).
24. J. T. Foley and E. Wolf, "Frequency Shifts of Spectral Lines Generated by Scattering from Space-Time Fluctuations," *Phys. Rev. A* **40**, 588–598 (1989). See also this volume, Chapter 16

Waves in Random Media 3 (1991) S129–S141. Printed in the UK

Enhanced backscattering and transmission of light from random surfaces on semi-infinite substrates and thin films

A A Maradudin†, Jun Q Lu†, T Michel†, Zu-Han Gü‡, J C Dainty§, A J Sant§, E R Méndez‖ and M Nieto-Vesperinas¶

† Department of Physics and Institute for Surface and Interface Science, University of California, Irvine, CA 92717, USA
‡ Surface Optics Corporation, PO Box 261602, San Diego, CA 92126, USA
§ Applied Optics Section, Blackett Laboratory, Imperial College of Science, Technology and Medicine, London, SW7 2AZ, UK
‖ Division de Fisica Aplicada, CICESE, Apdo. Postal 2732, Ensenada, Baja California, Mexico
¶ Instituto de Optica, CSIC, Serrano 121, Madrid 28006, Spain

Received 9 November 1990, in final form 5 February 1991

Abstract. The enhanced backscattering of light from a random surface is manifested by a well defined peak in the retro-reflection direction in the angular distribution of the intensity of the incoherent component of the light scattered from such a surface. In this paper we present several new theoretical and experimental results bearing on the conditions under which enhanced backscattering occurs, and the way in which this phenomenon depends on the nature of the random surface roughness, both in the case that the random surface bounds a semi-infinite scattering medium and in the case that it bounds a film, either free-standing or on a reflecting substrate. In addition, we present new results on the transmission of light through thin metallic films bounded by random surfaces, which display the phenomenon of enhanced transmission, namely a well defined peak in the antispecular direction in the angular distribution of the intensity of the incoherent component of the light transmitted through such films.

1. Introduction

Enhanced backscattering in the scattering of light from a random surface is manifested by a well defined peak in the retro-reflection direction in the angular dependence of the intensity of the incoherent component of the light scattered from such a surface. It has now been studied intensively theoretically [1–15] and experimentally [16–20]. On the basis of these studies it is now believed that the enhanced backscattering of light from a moderately rough, reflecting, random surface results primarily from the coherent interference of each doubly reflected optical path with its time-reversed partner. If the scattering surface supports surface electromagnetic waves, enhanced backscattering occurs even for weak corrugations [1–3,6,15]. In this case it is due primarily to the coherent interference of each doubly scattered surface electromagnetic wave path with its time-reversed partner. Such enhanced backscattering phenomena are examples of a broader class of multiple scattering phenomena that go under the name of weak localization, in the present case of light and of surface electromagnetic waves, respectively.

0959-7171/91/03S129-13$03.50

In this paper we present new computer simulation and experimental results that bear on the enhanced backscattering of light from random one-dimensional surfaces on semi-infinite substrates and thin films. The emphasis in the investigations described here is on elucidating the mechanisms responsible for enhanced backscattering, and the way in which this phenomenon depends on the nature of the surface roughness

In addition, we present new computer simulation and experimental results concerning the enhanced transmission of light through thin metal films, one or both of whose surfaces are random one-dimensional surfaces. Enhanced transmission is a well defined peak in the antispecular direction in the angular distribution of the intensity of the incoherent component of the light transmitted through such films. Of interest is the way in which this phenomenon depends on the nature of the surface roughness.

Thus, we will be concerned with the interaction of light with surfaces defined by the equation $x_3 = \zeta(x_1)$, so that their generators are parallel to the x_2-axis. They can therefore be termed random gratings. The region $x_3 > \zeta(x_1)$ is vacuum, while the region $x_3 < \zeta(x_1)$ is either a semi-infinite metal or dielectric, or a metal or dielectric film that is either free-standing or deposited on a substrate. The surface profile function $\zeta(x_1)$ is assumed to be a single-valued, continuous, differentiable function of x_1, and to constitute a stationary, Gaussian, stochastic process. It is defined by the properties $\langle \zeta(x_1) \rangle = 0$ and $\langle \zeta(x_1)\zeta(x_1') \rangle = \delta^2 W(|x_1 - x_1'|)$. The angle brackets here denote an average over the ensemble of realizations of the surface profile. The form of the surface height correlation function $W(|x_1 - x_1'|)$ will be specified below for each of the surfaces considered. The plane of incidence (the x_1x_3 plane) is perpendicular to the generators of these gratings. The computational method used in the calculation of the angular distribution of the intensity of the incoherent component of the light scattered from, or transmitted through, the structures studied here is the one described in [4,7,12], and extensions thereof. Thus, the random grating occupies the segment $(-L/2, L/2)$ of the x_1 axis, which is divided into $N = L/\Delta x$ equal segments, and is illuminated from the vacuum side by a Gaussian beam of half-width w. The half-width of the intercept of this beam with the x_1-axis is then $g = w/\cos\theta_0$ where θ_0 is the angle of incidence. The total differential reflection or transmission coefficient is calculated for each of N_p different realizations of the surface profile function, and the results are averaged over this number of surfaces. Finally, the coherent contribution is subtracted to yield the incoherent contribution to the mean differential reflection or transmission coefficient.

2. Enhanced backscattering from random gratings of even and odd symmetry

If enhanced backscattering from moderately rough, reflecting surfaces is due primarily to the coherent interference of each doubly reflected optical path with its time-reversed partner, we should expect to see it from any random surface that can multiply scatter light. The earliest computer simulation studies of enhanced backscattering [4,7,11] were carried out for reflecting surfaces with large RMS slopes defined by a surface profile function $\zeta(x_1)$ that was a single-valued function of x_1 and constituted a stationary, Gaussian process, characterized by a Gaussian surface height correlation function $W(|x_1 - x_1'|) = \langle \zeta(x_1)\zeta(x_1') \rangle / \langle \zeta^2(x_1) \rangle = \exp(-(x_1 - x_1')^2/a^2)$, where a is the transverse correlation length of the roughness. In subsequent work it was shown that enhanced backscattering is obtained from reflecting surfaces with large RMS slopes when the surface profile function $\zeta(x_1)$ is no longer a Gaussian-distributed random variable [8]. It has also been shown that enhanced backscattering occurs for forms of the surface height

correlation functions $W(|x_1 - x_1'|)$ other than the Gaussian one used in the first studies, when $\zeta(x_1)$ is a Gaussian-distributed random variable [14].

Continuing our investigations of the kinds of random surfaces that give rise to enhanced backscattering, we explore here the consequences of relaxing the common assumption that the surface profile function is a *stationary* stochastic process. We do this by studying the scattering of p- and s-polarized light from random metallic gratings with large RMS slopes characterized by profile functions that are even and odd functions of x_1. The study of the enhanced backscattering of light from random surfaces characterized by even profile functions also allows us to investigate the enhanced scattering in the specular direction observed in the angular distribution of the intensity of the incoherent component of the scattered light in earlier work on perfectly conducting surfaces by Nieto-Vesperinas and Soto-Crespo [9].

The random gratings we studied were constructed in the following way. We first constructed a random surface profile function $\zeta(x_1)$, obeying Gaussian statistics defined by the properties $\langle \zeta(x_1) \rangle = 0$ and $\langle \zeta(x_1)\zeta(x_1') \rangle = \delta^2 \exp(-(x_1 - x_1')^2/a^2)$, by the method described in appendix A of [12], for x_1 in the interval $(-L/2, L/2)$. The surface profile functions of even and odd symmetry in this interval were then constructed according to $\zeta_{e,o}(x_1) = [\zeta(x_1) \pm \zeta(-x_1)]/2$, respectively. We see immediately that the surface profiles $\zeta_{e,o}(x_1)$ defined in this way are no longer stationary random processes, because the point $x_1 = 0$ is a distinguished point.

We have calculated the contribution to the mean differential reflection coefficient (DRC) from the incoherent component of the scattered light, as a function of the scattering angle θ_s, for light of both p- and s-polarization incident on a silver surface whose surface is a random grating of even and odd symmetry. In figure 1 we present our results for scattering from gratings of even symmetry. For each polarization a well defined peak is observed in $\langle \partial R_{p,s}/\partial\theta_s \rangle_{incoh}$ in the retro-reflection direction, $\theta_s = -20°$. In addition, a second well defined peak is observed in the specular direction, $\theta_s = 20°$. This is the peak we call the specular enhancement peak. We emphasize that this is a peak in the angular dependence of the intensity of the *incoherent* component of the scattered light. It is already present in the Kirchhoff approximation, i.e. in a single-scattering approximation. This is seen in the results presented in figure 2, in which we display the

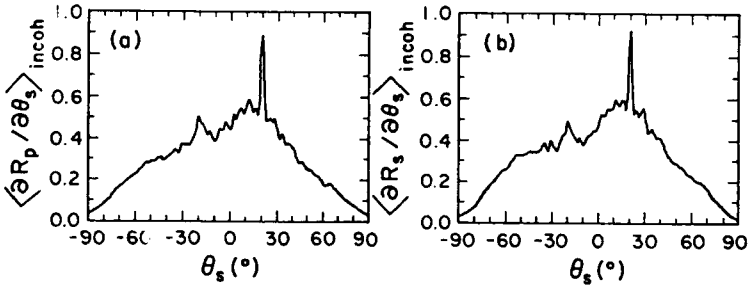

Figure 1. The incoherent contribution to the mean DRC for the scattering of a beam of light from a random grating of even symmetry on a silver surface. $\theta_0 = 20°$; $\lambda = 0.6127\,\mu m$; $\varepsilon(\omega) = -17.2 + i0.498$; $\delta = 1.4142\,\mu m$; $a = 2\,\mu m$; $L = 25.6\,\mu m$; $g = 6.4\,\mu m$; $N = 300$; $N_p = 1000$. (*a*) p-polarization; (*b*) s-polarization.

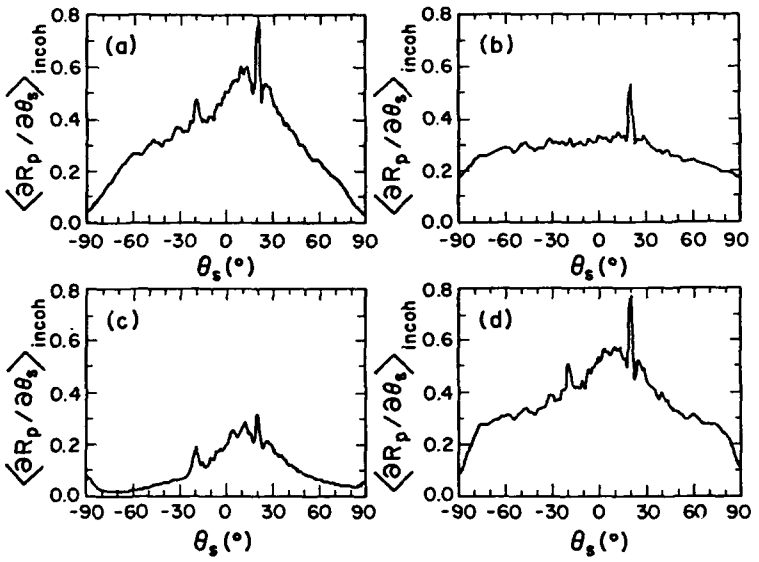

Figure 2. The incoherent contribution to the mean DRC for the scattering of a p-polarized beam of light from a random grating of even symmetry on a perfect conductor. The parameters used in obtaining these results are those used in obtaining figure 1. (*a*) the total incoherent contribution to the DRC; (*b*) the contribution from the single-scattering processes; (*c*) the contribution from the pure double-scattering processes; (*d*) the contribution from the single- and double-scattering processes, including the interference terms.

contribution to the mean differential reflection coefficient of p-polarized light incident on the same surfaces used in obtaining figure 1 but ruled on a perfect conductor, for which such calculations are much simpler than for a metal. No evidence of enhanced backscattering is seen in the single scattering contribution plotted in figure 2(*b*), while a well defined specular enhancement peak is present. The pure double-scattering contribution plotted in figure 2(*c*) shows an enhanced backscattering peak, as well as a weak specular enhancement peak. These results are consistent with the picture of enhanced backscattering as a multiple-scattering phenomenon, and of specular enhancement as a predominantly single-scattering effect. In figure 3 we present our results for the scattering of light of p- and s-polarization from random gratings of odd symmetry on a silver surface. The experimental conditions and roughness parameters are the same in this case as were assumed in obtaining figures 1 and 2. For each polarization a well defined peak is observed in $\langle \partial R_{p,s}/\partial \theta_s \rangle_{incoh}$ in the retro-reflection direction, $\theta_s = -20°$, but there is no peak in the specular direction, $\theta_s = 20°$.

These results can be understood qualitatively with the following arguments. If we consider only single-scattering contributions in the scattering of light from an arbitrary random grating, the amplitude components interfering in the specular direction arise from the so-called specular points. These are points on the surface at which its slope is

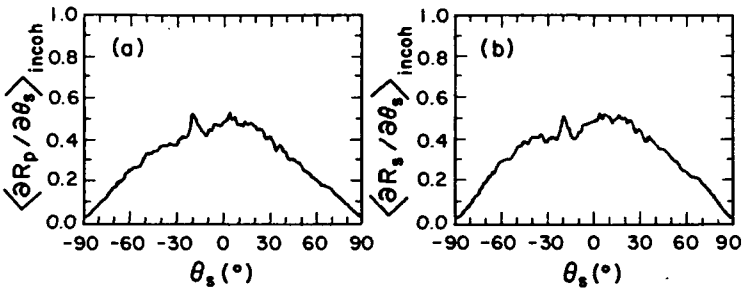

Figure 3. The same as figure 1 but for a random grating of odd symmetry.

zero. For optically rough surfaces the random heights of the specular points have large fluctuations (compared with the wavelength λ of the incident light), and the relative phase of the far-field contributions is completely random, i.e. uniformly distributed in the interval $(-\pi, \pi)$. This destroys the coherent (or specular) component of the scattered light. The situation is the same for random gratings with an odd profile. However, for random gratings with an even profile, there are pairs of contributions, arising from

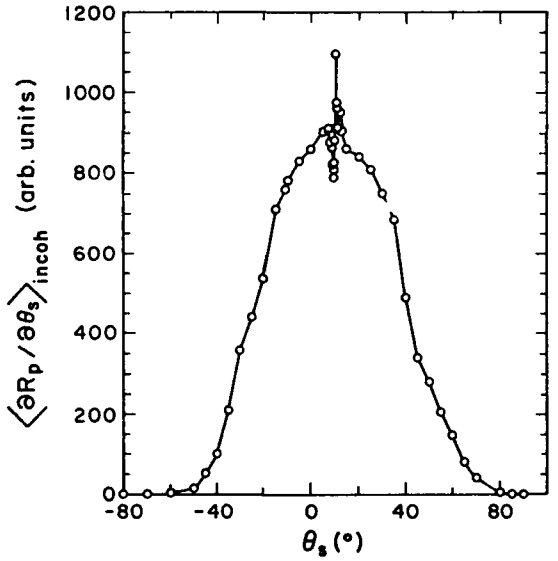

Figure 4. An experimental result for the incoherent contribution to the mean DRC for the scattering of a p-polarized beam of light from a random grating of even symmetry on a gold-coated (d_{Au} = 500 Å) photoresist film of mean thickness d_{ph} = 10 μm deposited on a glass substrate of thickness d_{gl} = 5 mm. θ_0 = 10°; λ = 0.6328 μm; n_{ph} = 1.64; n_{gl} = 1.51; δ = 2.3 μm; a = 9.5 μm.

symmetric specular points at the same height, at x_1 and $-x_1$, which interfere constructively with a fixed, non-random, phase difference. This increases the intensity of the scattered light in the specular direction by a factor of two over that of the background.

Specular enhancement has been observed experimentally. In figure 4 we present the mean DRC for the scattering of p-polarized light from a random grating on a gold-coated photoresist film deposited on a glass substrate. The surface is sufficiently rough that the coherent component of the scattered light is negligible. The surface consists of 150 different, contiguous segments, each of which is 200 μm long, and each of which is an even function of x_1, measured from its midpoint. The width of the incident beam is 3 cm, so that the DRC plotted is equivalent to the result of averaging over 150 different realizations of a random surface. A well defined peak is observed in the specular direction, $\theta_s = 10°$. However, no enhanced backscattering peak is observed in this figure, because the roughness parameters are such that the overwhelming contribution to the DRC is due to single-scattering processes, i.e. the Kirchhoff approximation is valid.

3. Enhanced backscattering from a dielectric film

In the earliest numerical simulation studies of the scattering of p-polarized light from a random grating on a semi-infinite dielectric medium ($BaSO_4$) no enhanced backscattering was observed [11]. In the same work it was also shown that if the index of refraction of the dielectric medium was artificially doubled then enhanced backscattering was observed in this polarization [11]. Subsequent calculations of the scattering of s-polarized light from the same surfaces predicted enhanced backscattering [12]. It was later found that a more modest increase in the refractive index, namely by a factor of about 1.4–1.5, was sufficient to induce enhanced backscattering in p-polarization [12].

It is interesting, then, to ask whether there are other ways to induce enhanced backscattering in the scattering of p-polarized light from a random grating on a dielectric medium. In this section we describe a way of doing so, which relies on the dielectric medium being in the form of a thin film rather than semi-infinite.

We consider the case in which a film of a nearly transparent dielectric of average thickness d is deposited on a perfectly conducting substrate. The interface $x_3 = -d$ between the film and the interface is assumed to be planar. The interface between the film and the vacuum above it is a random grating defined by a surface profile function $\zeta(x_1)$, that is a Gaussianly distributed random variable with the properties $\langle \zeta(x_1) \rangle = 0$, $\langle \zeta(x_1)\zeta(x_1') \rangle = \delta^2 \exp(-(x_1 - x_1')^2/a^2)$. This structure was suggested by recent work of Jakeman and his colleagues who showed in a series of papers that light scattered from a deep random phase screen placed in front of a mirror displays a strong increase in its intensity in the backscattering direction [21–23]. The random surface in our case plays the role of the deep random phase screen, while the perfect conductor is the mirror.

We have carried out numerical simulations of the scattering of light of p-polarization from this structure [13]. In figure 5(*a*) we present our results for the angular distribution of the intensity of p-polarized light scattered incoherently from a dielectric film of mean thickness $d = 4.8$ μm. In these calculations a value of the mean film thickness d was used that was four times the value of the RMS height of the surface roughness δ. This was because for such large values of the film thickness the probability of obtaining values of $|\zeta(x_1)|$ larger than d, which would produce 'holes' in the film, is reduced to a negligible level. A sharp peak is seen in $\langle \partial R_p/\partial\theta_s \rangle_{incoh}$ in the retro-reflection direction

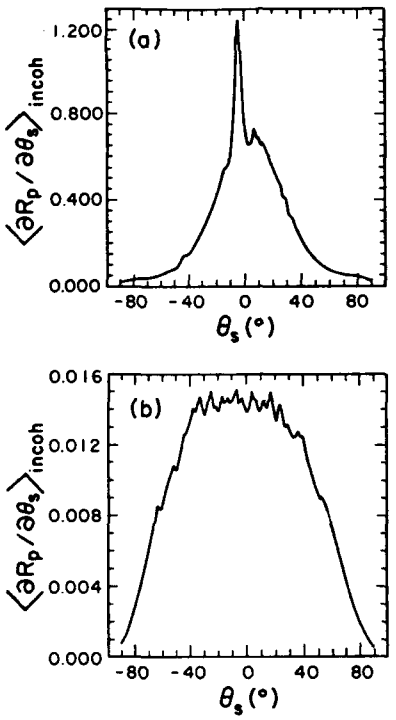

Figure 5. (*a*) The incoherent contribution to the mean DRC for the scattering of a p-polarized beam of light from a random grating on the surface of a film of $BaSO_4$ deposited on a planar, perfectly conducting substrate. $\theta_0 = 5°$; $\lambda = 0.6328\ \mu m$; $n_d = 1.628 + i0.0003$; $d = 4.8\ \mu m$; $\delta = 1.2\ \mu m$; $a = 2\ \mu m$; $L = 25.6\ \mu m$; $g = 6.4\ \mu m$; $N = 300$; $N_p = 1000$. (*b*) The same as in (*a*) except that the random grating is on a semi-infinite $BaSO_4$ substrate.

$\theta_s = -5°$. For comparison, we present in figure 5(*b*) the result for $\langle \partial R_p / \partial \theta_s \rangle_{incoh}$ obtained for exactly the same experimental conditions and roughness parameters except that the dielectric is now semi-infinite. No enhanced backscattering is seen in this case.

We believe that the enhanced backscattering we observe in figure 5(*a*) can be explained by a modification of an argument given by Jakeman [21] to explain the enhanced backscattering of light from a deep random phase screen placed in front of a plane mirror. When the perfect conductor is placed well beyond the focusing plane of the random surface, as is the case for the results presented here, the coherent addition of the contribution from a given light path that interacts with the random surface at two different points due to its reflection from the perfect conductor, and its time-reversed partner leads to an enhancement of up to a factor of two in the intensity of light scattered into the backward direction. The angular width of this peak is determined by a transverse scattering length, which is the characteristic distance between the points on the random

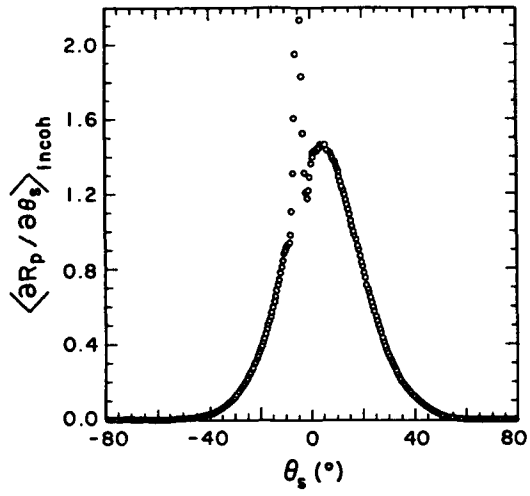

Figure 6. An experimental result for the incoherent contribution to the mean DRC for the scattering of a p-polarized beam of light from a random grating on the surface of a dielectric film deposited on a planar gold substrate. $\theta_0 = 5°$; $\lambda = 0.6328\ \mu m$; $n_d = 1.41$; $d = 8.5\ \mu m$; $\delta = 1.08\ \mu m$; $a = 3.06\ \mu m$.

surface through which the light paths from the source pass and repass in being scattered into the retro-reflection direction.

The effect described in this section has been observed experimentally. In figure 6 we present experimental results for the mean differential reflection coefficient for the scattering of p-polarized light from a dielectric film on a gold substrate. Although gold is not a perfect conductor under the conditions of the experiment, it is highly reflecting, and the consequence of this is that a well defined peak in the retro-reflection direction, $\theta_s = -5°$, is seen in the angular dependence of the intensity of the incoherent component of the scattered light. Despite the differences between the parameters defining the theoretical and experimental results, a comparison of the differential reflection coefficients presented in figures 5(*a*) and 6 shows them to be qualitatively very similar, and even quantitatively close.

4. Enhanced transmission through thin films

Not all of the interesting manifestations of weak localization in the interaction of light with random gratings are observed in reflection. It was shown recently [24] that the angular distribution of the intensity of the incoherent component of p-polarized light transmitted through a thin metal film surrounded by vacuum, whose illuminated surface is randomly rough while the back surface is planar, displays a well defined peak in the direction of transmission that is directly opposite to the direction of specular reflection of the incident light (the antispecular direction). It is believed that the physical origin of this effect is the scattering, by the surface roughness, of the surface polaritons in the

film excited, through the roughness, by the incident light. The coherent interference of a doubly scattered light/surface polariton path with its time-reversed partner gives the dominant contribution to this *enhanced transmission*.

The original, perturbation-theoretic calculation of this effect was extended in two directions in subsequent numerical simulation calculations [14]. Rougher surfaces were studied, and calculations were carried out for metal films on semi-infinite dielectric substrates. In addition, the phenomenon of enhanced transmission was observed experimentally [14].

If we relax the assumption that only the illuminated surface of the film is a random grating, and allow the back surface to be a random grating as well, the enhanced transmission of light through the resulting structure can be amplified with respect to what it is when only the illuminated surface is rough. In figure 7(*a*) we present results for the incoherent contribution to the mean differential transmission coefficient (DTC) for the transmission of p-polarized light through a thin silver film, whose illuminated surface is defined by $x_3 = \zeta(x_1)$, while its back surface is given by $x_3 = -d + \zeta(x_1)$. Thus, the thickness of the film is the same for each value of x_1. The surface profile function $\zeta(x_1)$ is a stationary, Gaussian process defined by $\langle \zeta(x_1) \rangle = 0$ and $\langle \zeta(x_1)\zeta(x_1') \rangle = \delta^2 \exp(-(x_1 - x_1')^2/a^2)$. A narrow, high peak in the antispecular direction, $\theta_t = -20°$, is observed in the angular distribution of the intensity of the incoherent component of the light transmitted through the film. This result should be compared with the one displayed in figure 7(*b*), which presents the corresponding result for a film whose back surface, at $x_3 = -d$, is planar. Although the overall transmitted intensity is higher in this case than in the case of a film with both surfaces rough, the enhanced transmission peak is broader and lower compared with the background at its position that it is in the latter case.

In section 2 we have discussed the scattering at light from random gratings on metal surfaces when the surface profile function $\zeta(x_1)$ of the random grating is an even or odd function of x_1. It was found that the angular dependence of the intensity of the

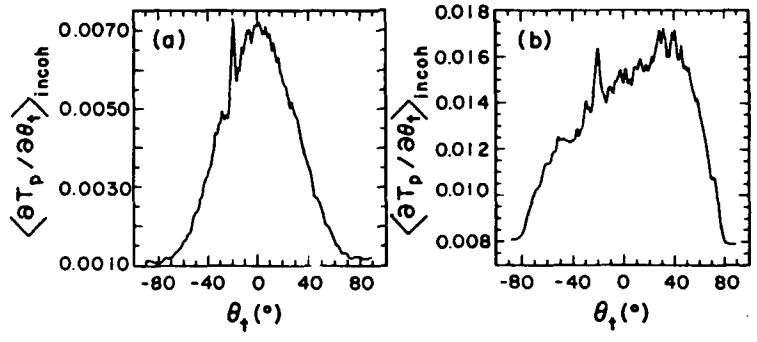

Figure 7. The incoherent contribution to the mean DTC for the transmission of a p-polarized beam of light through a thin silver film with rough surfaces. $\theta_0 = 20°$, $\lambda = 0.4579\,\mu m$; $\varepsilon(\omega) = -7.5 + i0.24$; $d = 800$ Å, $\delta = 282.8$ Å; $a = 1500$ Å; $L = 13.7\,\mu m$; $g = 3.425\,\mu m$; $N = 300$; $N_p = 1000$. (*a*) The illuminated and back surfaces are at $x_3 = \zeta(x_1)$ and $x_3 = -d + \zeta(x_1)$, respectively; (*b*) the illuminated and back surfaces are at $x_3 = \zeta(x_1)$ and $x = -d$, respectively.

incoherent component of the scattered light displayed not only a peak in the retro-reflection direction but also a peak in the specular direction when the scattering occurred from random gratings characterized by even surface profiles. Similar effects occur in the transmission of p-polarized light through a thin metal film whose illuminated face is a random grating of even symmetry, and whose back face is planar. In figure 8 we plot the contribution to the mean DTC from the incoherent component of the transmitted light when light of p-polarization is incident on a silver film whose mean thickness is 700 Å, and whose illuminated surface is a random grating of even symmetry. From figure 8 we see that the transmission of p-polarized light through a metal film whose illuminated surface is a random grating of even symmetry displays a peak in the antispecular direction $\theta_t = -\theta_0$ (enhanced transmission) and a second peak in the forward direction $\theta_t = \theta_0$, which we describe as being due to *enhanced refraction*.

Thus, the imposition of the constraint of evenness of an otherwise random surface, and the consequent removal of its stationarity, does not eliminate the enhanced transmission that occurs in the transmission of p-polarized light through a metal film with a random surface that has no such symmetry property, and gives rise to a new effect—enhanced refraction. The phenomenon of enhanced refraction is believed to be due to the coherent interference of light scattered from correlated pairs of points on the random surface, which already occurs in a single-scattering approximation.

Enhanced refraction has now been observed experimentally. In figure 9 we present the angular distribution of the intensity of the incoherent component of p-polarized light transmitted through a gold-coated photoresist plate of mean thickness $d = 10\,\mu$m deposited on a glass film of 5 mm thickness. It was fabricated in the manner described

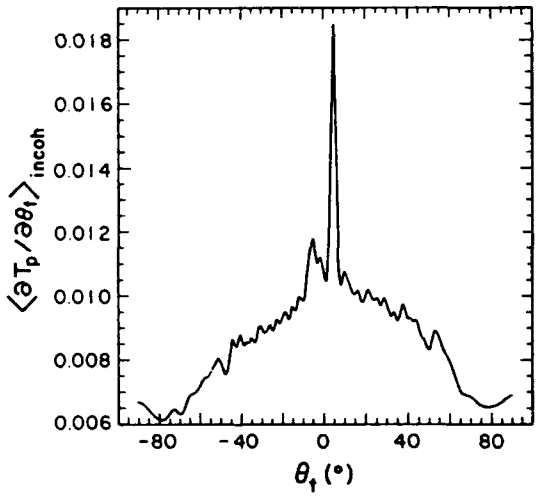

Figure 8. The incoherent contribution to the mean DTC for the transmission of a p-polarized beam of light through a silver film whose illuminated face is a random grating of even symmetry while its back face is planar $\theta_0 = 5^\circ$; $\lambda = 0.4579\,\mu$m; $\varepsilon(\omega) = -7.5 + i0.24$; $d = 700$ Å, $\delta = 282.84$ Å, $a = 1500$ Å; $L = 13.7\,\mu$m; $g = 3.425\,\mu$m; $N = 300$; $N_p = 1500$.

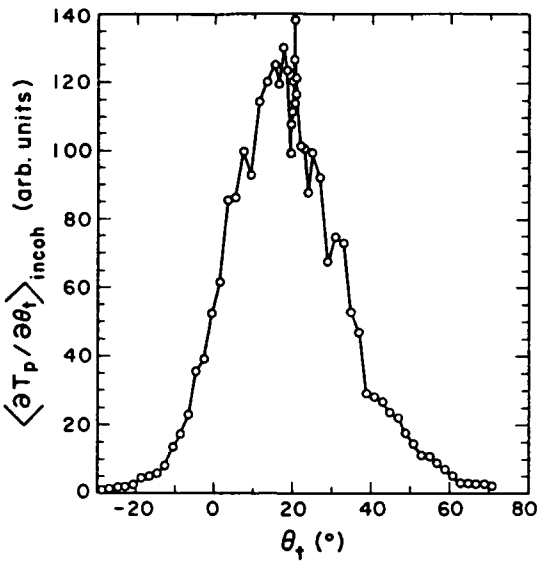

Figure 9. An experimental result for the incoherent contribution to the mean DTC for the transmission of a p-polarized beam of light through a random grating of even symmetry on a gold-coated ($d_{Au} \approx 500$ Å) photoresist film of mean thickness $d_{ph} \approx 10\,\mu$m deposited on a glass substrate of thickness $d_{gl} = 5$ mm. $\theta_0 = 20°$; $\lambda = 0.6328\,\mu$m; $n_{ph} = 1.64$, $n_{gl} = 1.51$; $\delta \approx 1.4\,\mu$m; $a \approx 8.0\,\mu$m.

in section 2. A prominent peak is seen in the angular dependence of the transmitted intensity in the forward direction, i.e. for a scattering angle $\theta_t = 10°$. It is due to enhanced refraction. The absence of enhanced transmission in this case is consistent with results of numerical simulations which show that enhanced transmission is suppressed as δ/a is increased, presumably because the surface polaritons responsible for the effect [24] are strongly damped by the roughness. The subsidiary maxima in the mean DTC are believed to be due to multiple reflections from the two interfaces in the structure studied.

5. Conclusions

The results presented in this paper, taken together with those of earlier investigations [8,14], show that the enhanced backscattering of light from moderately rough, reflecting, random surfaces that scatter light multiply is a remarkably robust phenomenon. Provided that these surfaces scatter light multiply, it is independent of the statistics of the surface profile function; it is independent of the form of the surface height correlation function; and it occurs for surfaces for which the surface profile function is not a stationary stochastic process. These results strongly suggest that the dominant property of a moderately rough, reflecting surface that is responsible for enhanced backscattering is

its ability to scatter the incident light multiply; other properties of such surfaces may affect the form the differential reflection coefficient possesses, but not the existence of enhanced backscattering itself.

In addition, when the random surface profile is constrained to be an even function of x_1, a new scattering effect is observed, specular enhancement, which is absent in general in the scattering from an unconstrained random surface (see, however, [8]). This effect however, is already present in a single-scattering approximation, and thus is not primarily a multiple-scattering effect.

The results presented in section 3 show that a dielectric medium bounded by a moderately rough random grating surface which does not display enhanced backscattering of p-polarized light when it is semi-infinite can be made to do so by depositing the dielectric medium in the form of a thin film, whose interface with vacuum is a random grating of large RMS slope, on the planar surface of a perfect conductor. The observed enhanced backscattering from this structure is believed to be due to the coherent interference of a light path that passes through the random surface twice, due to its reflection from the perfect conductor, and its time-reversed partner. In effect, the presence of the perfect conductor ensures the double-scattering of the incident light from the random surface that is primarily responsible for enhanced backscattering.

Finally, the enhanced transmission of p-polarized light through a thin metal film, whose back surface, as well as its illuminated surface, is a random grating is noticeably stronger than it is when the back face is planar. This conclusion may make this effect easier to observe experimentally. When the back face of such a film is planar, and the illuminated face is a random grating characterized by a surface profile function that is an even function of x_1, the incoherent component of the transmitted light displays enhanced refraction in addition to enhanced transmission. The former effect, however, is primarily a single-scattering effect, in contrast with the multiple-scattering nature of the latter.

Acknowledgments

This research was supported by ARO Grants DAAL-88-K-0067 and DAAL-03-89-C-0036, and by Nato Grant 890528. It was also supported by UC Irvine, through an allocation of computer time.

References

[1] McGurn A R, Maradudin A A and Celli V 1985 *Phys. Rev.* B 31 4866–71
[2] Celli V, Maradudin A A, Marvin A M and McGurn A R 1985 *J. Opt. Soc. Am.* A 2 2225–39
[3] McGurn A R and Maradudin A A 1987 *J. Opt. Soc. Am.* B 4 910–26
[4] Nieto-Vesperinas M and Soto-Crespo J M 1987 *Opt. Lett.* 12 979–981
[5] Bahar E and Fitzwater M A 1987 *Opt. Commun.* 63 355–60
[6] Tran P and Celli V 1988 *J. Opt. Soc. Am.* A 5 1635–7
[7] Maradudin A A, Méndez E R and Michel T 1989 *Opt. Lett.* 14 151–3
[8] Michel T, Maradudin A A and Méndez E R 1989 *J. Opt. Soc. Am.* B 6 2438–46
[9] Nieto-Vesperinas M and Soto-Crespo J M 1989 *Phys. Rev.* B 39 8193–7
[10] Bahar E and Fitzwater M A 1989 *J. Opt. Soc. Am.* A 6 33–43
[11] Maradudin A A, Méndez E R and Michel T 1990 *Scattering in Volumes and Surfaces* ed M Nieto-Vesperinas and J C Dainty (Amsterdam: North-Holland) pp 157–74
[12] Maradudin A A, Michel T, McGurn A R and Méndez E R 1990 *Ann. Phys., NY* 203 255–307
[13] Lu Jun Q, Maradudin A A and Michel T 1991 *J. Opt. Soc. Am.* B 8 311–8

[14] Celli V, Tran P, Maradudin A A, Lu Jun Q, Michel T and Gu Zu-Han 1991 *Laser Optics of Condensed Matter* vol 2, ed E Garmire, A A Maradudin and K K Rebane (New York: Plenum) to appear
[15] McGurn A R, Maradudin A A and Wallis R F 1991 *Waves in Random Media* 1 43–57
[16] Méndez E R and O'Donnell K A 1987 *Opt. Commun.* 61 91–5
[17] O'Donnell K A and Méndez E R 1987 *J. Opt. Soc. Am.* A 4 1194–205
[18] Gu Zu-Han, Dummer R S, Maradudin A A and McGurn A R 1989 *Appl. Opt.* 28 537–43
[19] Dainty J C, Kim M-J and Sant A J 1990 *Scattering in Volumes and Surfaces* ed M Nieto-Vesperinas and J C Dainty (Amsterdam: North-Holland) pp 143–55
[20] Kim M-J, Dainty J C, Friberg A T and Sant A J 1990 *J. Opt. Soc. Am.* A 7 569–77
[21] Jakeman E 1988 *J. Opt. Soc. Am.* A 5 1638–48
[22] Tapster P R, Weeks A R and Jakeman E 1989 *J. Opt. Soc. Am.* A 6 517–22
[23] Jakeman E 1990 *Scattering in Volumes and Surfaces* ed M Nieto-Vesperinas and J C Dainty (Amsterdam: North-Holland) pp 111–23
[24] McGurn A R and Maradudin A A 1987 *Opt. Commun.* 72 279–285

Waves in Random Media 3 (1991) S29–S39. Printed in the UK

Measurements of light scattering by a characterized random rough surface

J C Dainty, N C Bruce and A J Sant
Blackett Laboratory, Imperial College, London SW7 2BZ, UK

Received 26 November 1990

Abstract. Measurements are presented of the angular distribution of four wavelengths of light scattered by a one-dimensional random rough surface, whose probability density function is Gaussian with a standard deviation $\sigma = 1.22 \pm 0.02\,\mu m$ and whose lateral correlation function is also Gaussian with $1/e$ width $\tau = 3.17 \pm 0.07\,\mu m$. The wavelengths used are 0.63, 1.15, 3.39 and 10.6 μm. The surface is used in two forms: coated with gold and as an almost lossless dielectric. The results are compared to those predicted by a double scattering form of the Kirchhoff formulation. Agreement is good at small angles of incidence but less good at larger angles of incidence.

1. Introduction

The experimental observation of enhanced backscattering from random rough surfaces of large root-mean-square slope, first reported by Mendez and O'Donnell [1,2], has stimulated a re-examination of the problem of light scattering in the past few years. The main progress to date has been the development of 'exact' numerical codes for the solution of Maxwell's equations from a one-dimensional surface illuminated with either s (i.e. TE) polarization or p (i.e. TM) polarization [3–7]. With s polarization, the electric vector is parallel to the grooves, whereas with p polarization it is perpendicular to the grooves, as in figure 1 (this figure also shows the sign convention used for the incident and scattering angles). An important feature of the work of Mendez and O'Donnell was that the surfaces were relatively well characterized, with Gaussian statistics for the surface height and a single-scale Gaussian correlation function. Since the statistics of the surface were known, a critical comparison between experiment and theory could be made with confidence.

The shape of the scattering cross section curves with angle of observation for high-sloped surfaces is quite different from that for simple low-sloped ones and early numerical results [3] were encouraging since they were in fairly good agreement with the experimental ones particularly at near-normal incidence. In order to carry out a more critical comparison between real experiments and numerical ones, it is important that the surface is well characterized and also helpful if a range of wavelengths are used. The results presented here are intended to supplement those already reported [8–10] with the aim of providing a reliable body of experimental data for comparison with numerical work and analytical theory. The surface used is one-dimensional, for two reasons: firstly, it can be characterized much more accurately than a two-dimensional one, since a sharp chisel-shaped stylus can be used in a surface profilometer; secondly,

0959-7171/91/03S029-11$03.50

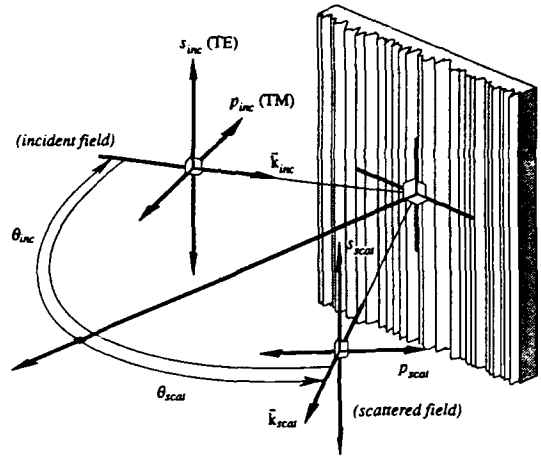

Figure 1. Polarization and angle notation for in-plane scattering from a one-dimensional rough surface.

'exact' numerical calculations of the light scattering are only feasible at the present time for the one-dimensional case.

When comparing experimental measurements of light scattering with numerical computations, it is helpful if the numerical results provide some physical insight to the scattering process. For example, it is believed from the experiments that the mechanism giving rise to the enhanced backscatter peak is multiple scattering; however, numerical calculations based on exact theory do not separate the single and multiple scatter terms, and therefore do not provide the insight that is desirable (however, iterative solutions do separate the single and multiple scatter terms). For this reason, we have written numerical code based on a multiple (double and triple) scattering extension of the Kirchhoff boundary condition, including the effects of shadowing (see [11] for details and further references). In section 3 of this paper we compare the results of this code with the experimental results and 'exact' numerical code.

2. Experimental results

Master surfaces are produced by exposing a thick layer of photoresist ($\approx 12\,\mu$m of Shipley S1400-37) to several statistically independent laser speckle patterns. Two versions of the surface were prepared using a replication technique [8], one being coated with ≈ 1000 Å of gold and the other being an almost lossless dielectric of refractive index $n = 1.41$ (at $\lambda = 0.63\,\mu$m). Figure 2 shows the probability histogram of surface height and surface autocorrelation function, as measured by a Talystep profilometer whose stylus is a pyramid of 70° apex angle truncated by a flat region of $\approx 0.5\,\mu$m. Both are good fits to Gaussian functions, with the root-mean-square height $\sigma = 1.22 \pm 0.02\,\mu$m and $1/e$ correlation length $\tau = 3.17 \pm 0.07\,\mu$m. The angular distribution of the scattered

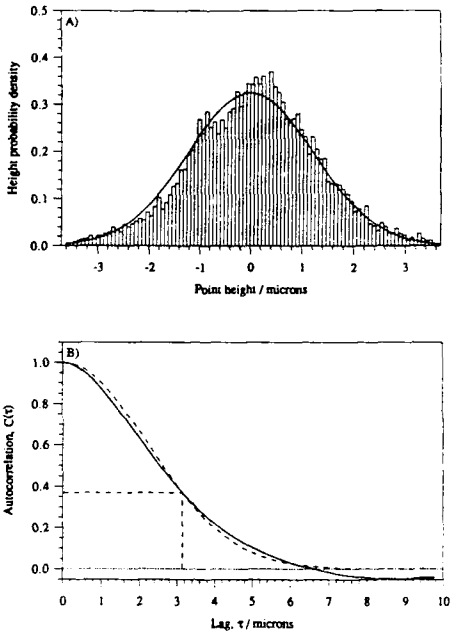

Figure 2. Probability histogram (upper) and autocorrelation function (lower) of the surface height fluctuation as calculated from Talystep measurements for the surface (# 46) used in this paper.

light was measured at four wavelengths (0.63 μm, 1.15 μm, 3.39 μm and 10.6 μm) using the equipment described in [10]. For each angle of incidence, measurements are made with p-polarization incident and p-polarization collected ('p-p' scattering) and s-polarization incident and s-polarization collected ('s-s' scattering); no crossed polarized components were detectable. For a perfect conductor, these measurements give a complete description of the scattering characteristics of the surface, but in general four scattering coefficients are required for materials of finite conductivity; these can be found by measuring the polarization of the scattered light for various input polarizations. Also, the measurements reported here yield the relative scattering cross section, as no absolute calibration is performed.

The relative scattering cross sections for angles of incidence of 0°, $-30°$ and $-60°$ and the four wavelengths are shown in figures 3 and 4 for the gold-coated surface and figures 5 and 6 for the dielectric surface. The enhanced backscatter peak, where present, occurs on the right-hand side of the graphs (i.e. at positive angles, see figure 1 for the sign convention for the angles) and any specular component is on the left-hand side (i.e. negative angles); for the 10.6 μm measurements, the specular peak was very much greater than the diffuse component and is not shown. A few features are of particular note.

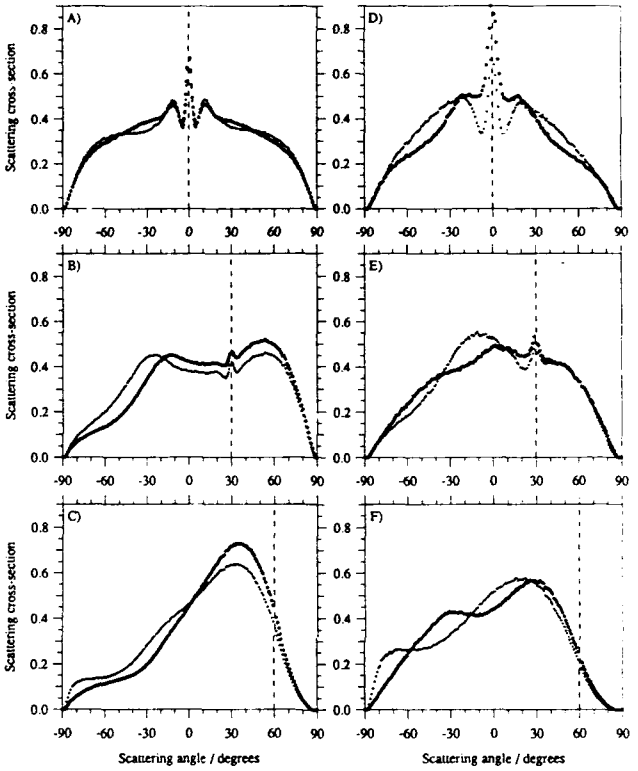

Figure 3. Relative scattering cross section as a function of scattering angle for the gold-coated surface, for angles of incidence of 0°, −30° and −60°, for p-p scattering (open circles) and s-s scattering (crosses). The left-hand column is for a wavelength of 0.63 μm, for which $\sigma/\lambda = 1.93$ and $\tau/\lambda = 5.02$ and the right-hand column for $\lambda = 1.15\ \mu$m, for which $\sigma/\lambda = 1.07$ and $\tau_i/\lambda = 2.76$. The enhanced backscatter peak, where present, occurs at positive angles (right-hand side of each graph).

(1) The enhanced backscatter peak and sidelobe structure are clearly visible for the shorter wavelengths at an angle of incidence less than approximately −30° for the gold-coated surface; the width of the peak is proportional to the wavelength. The peak is not observed for the p-p scattering at 10.6 μm for the gold surface or for scattering from the dielectric.

(2) With the exception of the p-p case at 10.6 μm, the p-p and s-s scattering by the gold surface are very similar; for the dielectric surface, however, the p-p and s-s scattering cross sections are quite different, as one might expect by analogy with reflection from a planar surface. Using a value of $n = 1.41$ for the refractive index of the (almost lossless)

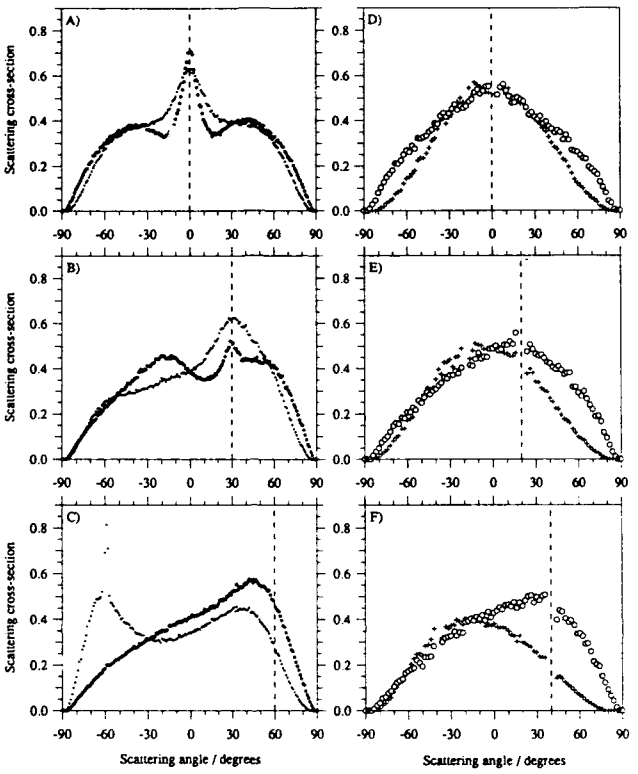

Figure 4. As for figure 3 but wavelengths of 3.39 μm ($\sigma/\lambda = 0.36$, $\tau/\lambda = 0.94$) and 10.6 μm ($\sigma/\lambda = 0.12$, $\tau/\lambda = 0.30$). For the 10.6 μm curves, the angles of incidence were 0°, −20° and −40°. The (strong) specular component in the 10.6 μm curves is not shown.

dielectric gives a Brewster angle of $\approx 55°$. Considering single scattering to be the dominant mechanism and treating this as a reflection from a locally plane surface gives an expected minimum of the p-p scattered intensity at an angle equal to approximately ($-110° -$ incident angle): the angles are roughly in accordance with this simple picture. The s-s and p-p scattered intensities in the backscatter direction appear to be almost equal to each other for all angles of incidence and wavelengths, for the dielectric.

(3) The overall shape of the curves is dramatically different from the Gaussian-type shapes (centred on the specular angle) normally encountered in scattering from low-sloped surfaces.

The principal purpose of figures 3 to 6 is to provide a reliable set of data for comparison with numerical calculations, and analytical theories should any become available.

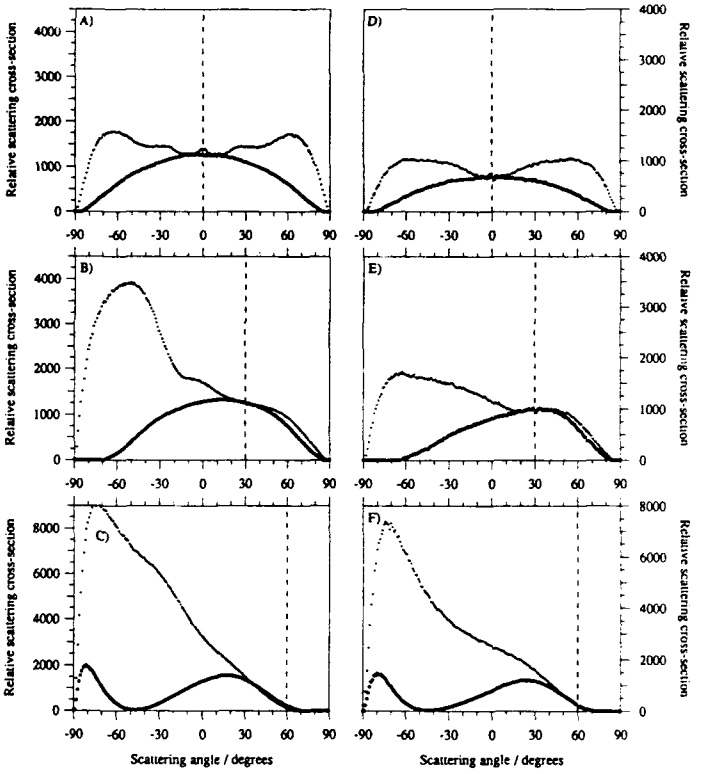

Figure 5. As for figure 3 but for the dielectric surface, $n_{0.63} = 1.41$, $n_{1.15} = 1.40$. The vertical scale is not the same as that used in figure 3 (both are *relative* scattering cross sections).

3. Kirchhoff multiple scatter approximation

One can compare the above experimental results to those of 'exact' numerical calculations based on the extinction theorem and its extensions [3–7], and some comparisons of experiment and calculations for a perfect conductor were given in [10]. Although such comparisons are valuable, one problem with the 'exact' numerical solution is that it gives little physical insight into the problem. We have therefore attempted to extend the Kirchhoff approximation (i.e. tangent plane approximation for each scattering event) to double (and multiple) scattering [11].

The numerical calculations were carried out using the method described in [11] for a perfect conductor; typically the energy conservation (unitarity) held to better than 3% considering just the single and double scatter terms for surface # 46 (except for the

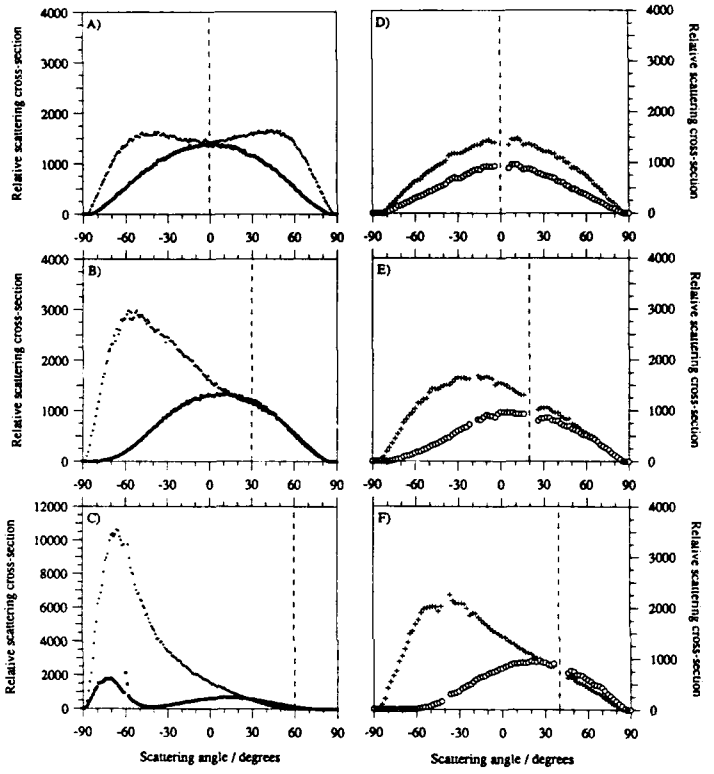

Figure 6. As for figure 4 but for the dielectric surface, $n_{3.39} = n_{10.6} = 1.41$.

$-60°$ results for which the departure from unitarity is $\approx 6\%$) and the results are averaged over approximately 10^3 realizations. Figures 7 and 8 show the results of the calculations for $\lambda = 0.63\ \mu m$ and $1.15\ \mu m$ respectively, for incident angles of $0°$, $-30°$ and $-60°$ and s-s and p-p scattering. Each graph shows the single, double and total scattered intensity. The enhanced backscatter peak occurs *only* in the double scatter component, showing conclusively that the enhancement is a multiple scattering effect. The enhancement is on the order of a factor of two in the double scattered component for all angles of incidence, but the enhancement in the total intensity is much less than two and decreases with increasing angle of incidence due to the fact that the double scattered intensity also decreases with incidence angle.

Figure 9 compares the total scattered intensity for s-s scattering from figures 7 and 8 with the results of 'exact' numerical calculations (based on the extinction theorem method for a perfect conductor [3]) and the experimental results of figure 3, for

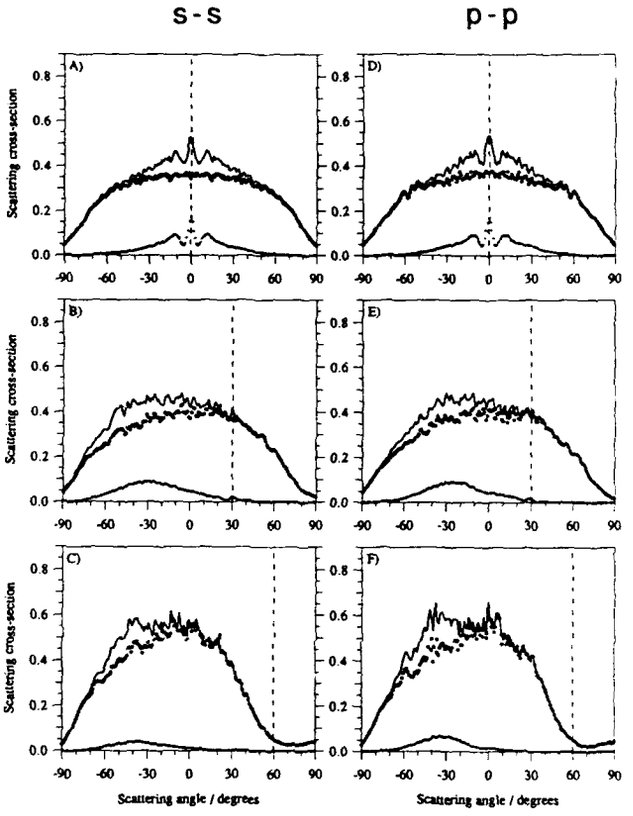

Figure 7. Numerically calculated scattered intensities for a perfect conductor, using the double-scattering Kirchhoff approximation, for angles of incidence of 0°, $-30°$ and $-60°$ and s-s scattering (*left*) and p-p scattering (*right*). The wavelength is 0.63 μm. Each graph shows the doubly scattered intensity (lowest curve), single scattered (middle) and total intensity (coherent sum) (top curve).

$\lambda = 0.63\,\mu$m and $1.15\,\mu$m at three angles of incidence. The two numerical calculations agree well, showing that the Kirchhoff approximation is reasonable for these surface parameters (the average radius of curvature, defined as the inverse of the standard deviation of the surface curvature $2\sqrt{3}\sigma/\tau^2$, is $\approx 2.4\,\mu$m for surface #46) and both agree well with the experimental measurements for zero angle of incidence. However, there is a clear discrepancy between experiment and numerical calculation for the $-30°$ and $-60°$ angles of incidence. (This general behaviour is also shown in the case of *p-p* scattering.)

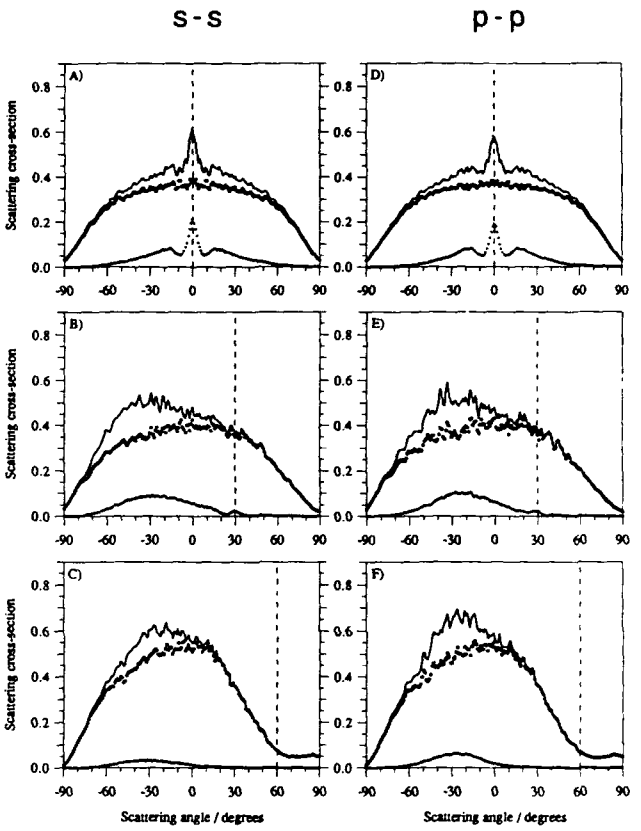

Figure 8. As for figure 7, but wavelength of 1.15 μm.

One possible cause of the discrepancy could be that the calculations are for a perfect conductor, whereas the experiments are for a real metal (gold). However, calculations by ourselves and others [5] show that, for these values of RMS surface height and correlation length, there is very little difference between the results for gold and for a perfect conductor, particularly for s-s scattering. One problem with most methods of calculation, including that used here, is that a very small length of surface is considered, giving rise to the possibility of an 'end-effect' error (e.g. due to long-range surface plasmons); however, the method of calculation of Saillard and Maystre [7] uses an extremely long length of surface with good agreement with the other calculations and poor agreement with the measurements at larger angles of incidence.

It seems, therefore, that there may be some aspect of the experiment that does not correspond to the calculations. Previous results for a Lambertian diffuser have

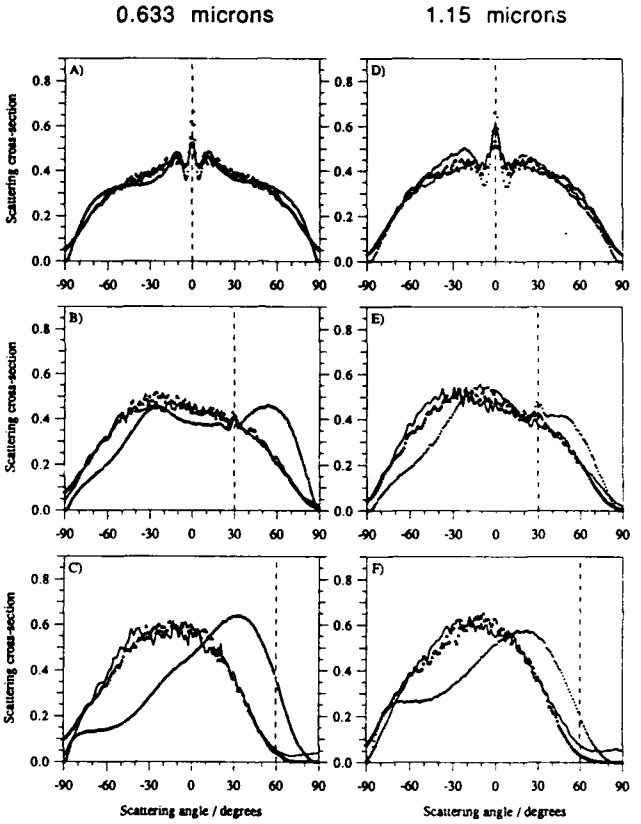

Figure 9. Comparison of Kirchhoff calculation (from figures 7 and 8), 'exact' numerical calculation and experiment (from figure 3), for *s-s* scattering at $\lambda = 0.63\,\mu m$ and $1.15\,\mu m$, and angles of incidence equal to $0°$, $-30°$ and $-60°$. The solid curves are the Kirchhoff calculation, triangles the 'exact' calculation and crosses are the experimental results. Note the good agreement between the two numerical calculations but the departure of the experimental results for larger angles of incidence.

demonstrated that the scatterometer measures the correct quantity [10]. The measurement of surface properties might be in error. If one calculates the scattered intensity for, say, $-60°$ angle of incidence for a surface that has an RMS roughness 50% larger than the measured value, then reasonable agreement is obtained between experiment and numerical calculation. However, (*a*) it is extremely unlikely that such a gross error could occur (stylus tips effects are discussed by Church [12]) and (*b*) the agreement for $0°$ angle of incidence is then very poor indeed, particularly as regards the location of the minima around the backscatter peak. Ishimaru and Chen [13] have shown that

a departure from Gaussianity of the correlation function could be responsible for the discrepancy, and the measured correlation does show a small departure from the Gaussian shape. However, it is notoriously difficult to estimate the correlation function of stylus traces and the departure shown in figure 2 is characteristic of inadequate de-trending of the mean; the method of manufacture of the surfaces strongly encourages a Gaussian correlation of surface height. The cause of this discrepancy for larger angles of incidence is therefore not resolved at the present time.

4. Summary

A set of scattering data for a one-dimensional surface at four wavelengths, three angles of incidence and two materials has been presented for critical comparison with numerical calculations and theoretical studies. A multiple scatter extension of the Kirchhoff approximation has been shown to provide additional physical evidence that the predominant cause of the enhanced backscatter peak is due to multiple scattering. There remains a significant disagreement between experiment and numerical calculations for large angles of incidence the cause of which is still unresolved.

The data presented in figures 3 to 6, together with sample Talystep traces, is available on a PC- or Macintosh-compatible diskette on application to the first author.

Acknowledgments

This work is supported by the UK Science and Engineering Research Council (GR/F81651) and the US Army (DAJA45-90-C-0026). JCD is also grateful to A A Maradudin and M Nieto-Vesperinas for discussions made possible by a Nato Travel Grant (890528).

References

[1] Mendez E R and O'Donnell K A 1987 *Opt. Commun.* **61** 91–5
[2] O'Donnell K A and Mendez E R 1987 *J. Opt. Soc. Am.* A **4** 1194–205
[3] Nieto-Vesperinas M and Soto-Crespo J-M 1987 *Opt. Lett.* **12** 979–81
[4] Maradudin A A, Mendez E R and Michel T 1989 *Opt. Lett.* **14** 151–3
[5] Maradudin A A, Michel T, McGurn A R and Mendez E R 1990 *Ann. Phys.* **203** 255–307
[6] Thorsos E I 1988 *J. Acoust. Soc. Am.* **83** 78–92
[7] Saillard M and Maystre D 1990 *J. Opt. Soc. Am.* A **7**, 982–90
[8] Sant A J, Kim M-J and Dainty J C 1989 *Opt. Lett.* **14** 1183–5
[9] Dainty J C, Kim M-J and Sant A J 1990 *Scattering in Surfaces and Volumes* (Amsterdam: Elsevier) pp 143–55
[10] Kim M-J, Dainty J C, Friberg A T and Sant A J 1990 *J. Opt. Soc Am.* A **7** 569–77
[11] Bruce N C and Dainty J C 1991 *J. Mod. Opt.* **38** 579–90
[12] Church E 1990 *Paper* presented at Conf. on Modern Analysis of Scattering Phenomenon, Marseille, September, 1990
[13] Ishimaru A and Chen J S 1991 *Opt. Lett.* in press